THE PATTERN OF ANATOMICAL CONNECTIONS IN VISUAL AREA V2 OF MACAQUE MONKEY

by

Paul Lawrence Abel

A dissertation submitted in partial fulfillment of
the requirements for the degree of

Doctor of Philosophy

University of Washington

1997

Approved by _____
Chairperson of Supervisory Committee

Program Authorized
to Offer Degree PSYCHOLOGY

Date JUNE 6 1997

Doctoral Dissertation

In presenting this dissertation in partial fulfillment of the requirements for the Doctoral degree at the University of Washington, I agree that the Library shall make its copies freely available for inspection. I further agree that extensive copying of this dissertation is allowable only for scholarly purposes, consistent with "fair use" as prescribed in the U.S. Copyright Law. Requests for copying or reproduction of this dissertation may be referred to University Microfilms, 1490 Eisenhower Place, P.O. Box 975, Ann Arbor, MI 48106, or to the author.

Signature 

Date 6/6/97

University of Washington

Abstract

THE PATTERN OF ANATOMICAL CONNECTIONS IN VISUAL AREA V2 OF MACAQUE MONKEY

by Paul Lawrence Abel

Chairperson of the Supervisory Committee:
Associate Professor Jaime F. Olavarria
Department of Psychology

In visual area V2, cytochrome oxidase (CO) histochemistry reveals a pattern of alternating densely labeled thick and thin stripes separated by lightly labeled interstripe regions. These stripe-like compartments have been related to three separate cortico-cortical pathways, which may be involved with different aspects of visual processing.

In the first experiment, we examined whether the tangential distribution of cells projecting to the superior colliculus bear a relationship with the CO stripes in V2. The cortico-tectal pathway is thought to be functionally specific, extending from magnocellular layers of the lateral geniculate nucleus (LGN). From previous evidence that V2 thick stripes are closely associated with the magnocellular LGN layers, we predicted that V2 neurons projecting to the superior colliculus would preferentially reside in thick stripe regions. Our results bore out this prediction. These data support the idea that the stripe-like compartments in V2 represent separate functional pathways, and extend the notion of segregated cortico-cortical pathways to cortico-subcortical projections.

In the second experiment, we compared the distribution of interhemishperic connections in V2 with the pattern of CO stripes. We found that V2 callosal connections tend to accumulate within a continuous band along the V1/V2 border from which callosal cells cluster within finger-like extensions within thin and thick stripe regions in V2 up to 7-8 mm from the V1 border. Our findings extend the notion of segregated cortico-cortical pathways to interhemispheric connections. In addition, different from the pattern of *intra*cortical connections, our results suggest that few cells within interstripe regions in V2 send connections to V2 or other extrastriate areas in the contralateral hemisphere.

In the third experiment we examined the pattern of callosal linkages in V2. Based on previous data on the visual field map in V2, callosal connections could link representations of the visual field located away from the vertical meridian. We examined whether the pattern of V2 callosal linkages supports this idea. The results demonstrate that callosal connections preferentially link corresponding regions between areas V2. These data support the hypothesis that V2 callosal connections mediate interactions between visual field representations located away from the vertical meridian.

TABLE OF CONTENTS

LIST OF FIGURES

LIST OF TABLES

ACKNOWLEDGMENTS

The author wishes to acknowledge the unlimited advice, patience, persistence, and support of Dr. Jaime Olavarria. These experiments resulted from the collaboration and friendship of Dr. Brendan O'Brien.

Completing the dissertation work and surviving the five years as a graduate student could not have been done without the love and support of my wife Cecile.

DEDICATION

I dedicate this dissertation to my family, who have endured through the years my thoughtful habit of analyzing and solving all of the problems they never new they had.

INTRODUCTION

Visual area V2 is one of over thirty cortical areas, which have been described in visual cortex of macaque monkey. A strip of V2 is located along the dorsal surface of the operculum, although the majority of V2 is found on the medial side of the hemispheres and buried within the lunate and inferior occipital sulci. Along its posterior border, V2 forms a belt around striate cortex in all but the most peripheral portions of V1, where prostriate area has been described (e.g., Van Essen et al., 1982). The anterior border of V2 is less certain due to the absence of clear anatomical distinctions, although as many as 5 extrastriate areas may neighbor V2 along this edge. Based on the pattern of connections with V1, cytochrome oxidase (CO) histochemistry and physiological data, the anterior limit of V2 has been reported to extend about 10-12 mm from the V1 border (Gattass et al., 1981; Weller and Kaas, 1986; Olavarria and Van Essen, 1997). V2 is one of the largest cortical areas, similar in size to area V1. Surface area estimates range from 660 to 920 mm^2 in the macaque (Gattass et al., 1981; Weller and Kaas, 1986).

Area V2 can be divided into three stripe-like compartments. CO histochemistry reveals a pattern of alternating densely labeled thick and thin stripes separated by lightly labeled interstripe regions (Horton and Hubel, 1981; Livingstone and Hubel, 1982, Tootell et al., 1983; Horton, 1984, Livingstone and Hubel, 1984; Wong-Riley and Carroll, 1984; Olavarria and Van Essen, 1997). Extending tangential to the cortical surface, these stripes are most readily observed in layers 3 and 5, although extend throughout the lamina (Tootell et al., 1983; Horton, 1984). The separation between stripes of the same class have been found to be between 3-5 mm (Olavarria et al., 1989; Tootell and Hamilton, 1989; Shipp and Zeki, 1989; Van Essen et al., 1990; Olavarria and Van Essen,

1997). The monoclonal antibody Cat-301 (Hockfield et al., 1983) has been found to preferentially bind to cells located within CO-dense thick stripes (Hendry et al., 1988; DeYoe et al., 1990; Abel et al., 1997; Olavarria and Van Essen, 1997). This independent criterion for distinguishing between the CO-dense stripes is important for these stripes can appear quite similar in width and there are examples in which alternate stripes were found to be of the same class (e.g., Olavarria and Van Essen, 1997).

These stripe-like compartments have been related to three separate cortico-cortical pathways emanating from V1. One pathway originates from layer 4B in V1 and projects to thick stripes in V2, area MT and other areas within the parietal cortex (DeYoe and Van Essen, 1985; Shipp and Zeki, 1985; Livingstone and Hubel, 1987a; Felleman et al., 1988; Shipp and Zeki, 1989a,b). A second pathway connects CO-dense blobs in V1 with thin stripes in V2, and a third pathway connects CO-pale interblobs in V1 with interstripes in V2 (Livingstone and Hubel, 1983, 1984). Thin stripes and interstripes project separately to V4 (DeYoe and Van Essen, 1985; Shipp and Zeki, 1985; Zeki and Shipp, 1989; Van Essen et al., 1990; Nakamura et al., 1993; DeYoe et al., 1994), and from here these pathways project into inferotemporal cortex (Desimone et al., 1980; Nakamura et al., 1993; DeYoe et al., 1994). These findings have led to the idea each pathway is involved with different aspects of visual processing (Ungerleider and Mishkin, 1982; Mishkin et al., 1983; Hubel and Livingstone, 1987; Livingstone and Hubel, 1987b; Maunsell and Newsome, 1987; DeYoe and Van Essen, 1988; Livingstone and Hubel, 1988; Zeki and Shipp, 1988).

However, the relationship between these compartments and cortico-subcortical and interhemispheric pathways has not been thoroughly examined. In the first two experiments these issues were examined using retrograde tracing techniques and quantitative analyses.

In chapter one, we examined whether the tangential distribution of cortico-tectal projections bears a relationship with the pattern of CO stripes. The cortico-tectal projection is believed to be functionally related to the broadband pathway extending through magnocellular layers in the LGN (Schiller et al., 1974; 1979). From previous evidence that V2 thick stripes are closely associated with the magnocellular LGN layers, we predicted that a significant proportion of V2 neurons projecting to the superior colliculus would reside in thick stripes. Our results bore out this prediction.

In chapter two, we compared the tangential distribution of cells projecting to the contralateral hemisphere with the pattern of CO stripes. Previous studies suggested that the callosal patches in macaque V2 overlap regions of high CO activity. However, these data had been analyzed only in the parasagittal plane where the V2 stripes are difficult to appreciate and a large region of V2 was not examined. Our findings demonstrate that V2 callosal connections tend to form a continuous band along the V1/V2 border from which callosal cells accumulate within finger-like extensions up to 7-8 mm from the V1 border. The callosal 'fingers' were found to lie in spatial register with both CO-dense thick and thin stripe regions.

In the final chapter we examined the topography of V2 callosal connections. Based on previous data on the visual field map in V2, callosal connections could link representations of the visual field located away from the vertical meridian. We examined whether the pattern of V2 callosal linkages supports this idea. Do callosal connections randomly link portions of V2 between the hemispheres, or is there an underlying pattern in the organization of these connections. We found that the organization of callosal linkages is not random. The results demonstrate that callosal connections preferentially link corresponding regions between areas V2. These data support the hypothesis

that V2 callosal connections mediate interactions between visual field representations located away from the vertical meridian.

CHAPTER 1: THE DISTRIBUTION OF NEURONS PROJECTING TO THE SUPERIOR COLLICULUS CORRELATES WITH THICK CYTOCHROME OXIDASE STRIPES IN AREA V2

In visual area V2 of macaque monkeys, cytochrome oxidase (CO) histochemistry reveals a pattern of alternating densely-labeled thick and thin stripes, and lightly-labeled interstripes (Horton and Hubel, 1981; Livingstone and Hubel, 1982; Tootell et al., 1983; Horton, 1984; Livingstone and Hubel, 1984; Wong-Riley and Carroll, 1984; Olavarria et al., 1989). These stripe-like compartments have been related to three parallel pathways emanating from subdivisions in V1. One pathway originates from layer 4B in V1 and projects to thick stripes in V2, area MT and other areas within the parietal cortex (DeYoe and Van Essen, 1985; Shipp and Zeki, 1985; Livingstone and Hubel, 1987a; Felleman et al., 1988; Shipp and Zeki, 1989a,b). A second pathway connects CO-dense blobs in V1 with thin stripes in V2, and a third pathway connects CO-pale interblobs in V1 with interstripes in V2 (Livingstone and Hubel, 1983, 1984). Thin stripes and interstripes project separately to V4 (DeYoe and Van Essen, 1985; Shipp and Zeki, 1985; Zeki and Shipp, 1989; Van Essen et al., 1990; Nakamura et al., 1993; DeYoe et al., 1994), and from here these pathways project into inferotemporal cortex (Desimone et al., 1980; Nakamura et al., 1993; DeYoe et al., 1994).

In recent years, several views have emerged regarding the role of these pathways in vision. One of these views is that the pathway passing through thick stripes in V2 (dorsal stream) is mainly involved in visual motion analysis while the pathway passing through thin and interstripes in V2 (ventral stream) is concerned with the analysis of form and color (Ungerleider and Mishkin, 1982; Mishkin et al., 1983; Hubel and Livingstone, 1987; Livingstone and Hubel, 1987b;

Maunsell and Newsome, 1987; DeYoe and Van Essen, 1988; Livingstone and Hubel, 1988; Zeki and Shipp, 1988). This hypothesis has been examined by many anatomical and physiological studies (see reviews by Felleman and Van Essen, 1991; Maunsell, 1992; Merigan and Maunsell, 1993). Some of the data support the idea that CO compartments in V2 are associated with different functional pathways, while other evidence points to a more subtle or complex relationship between modular architecture and specificity of visual functions (e.g., DeYoe and Van Essen, 1985; Martin, 1988; Merigan and Maunsell, 1990; Schiller et al., 1990; Van Essen et al., 1992; Peterhans and von der Heydt, 1993; Ferrera et al., 1994; Levitt et al., 1994a; Bullier and Nowak, 1995; Roe and T'so, 1995; Gegenfurtner et al., 1996).

Additional information about the relationship between CO stripes in V2 and specific functional pathways can come from studying the projections from V2 to subcortical centers that have been associated with functionally specific pathways. For instance, it has been shown in the macaque that visual activity in the superior colliculus can be greatly reduced or abolished by blocking magnocellular layers, but not parvocellular layers of the lateral geniculate nucleus (LGN) (Schiller et al., 1979). Thick stripes in V2 receive significant input from magnocellular LGN layers via layer 4B in V1 (Livingstone and Hubel, 1987a), and project selectively to cortical areas associated with the 'magnocellular' dorsal stream (DeYoe and Van Essen, 1985; Shipp and Zeki, 1985; Felleman et al., 1988; Shipp and Zeki, 1989b). If CO compartments in V2 are associated with different functional pathways, then we would predict that input from V2 to the superior colliculus originates predominantly from cells within thick stripe compartments.

We tested this prediction by comparing the distribution of corticotectal projection neurons in V2 with the pattern of CO stripes. We found

that neurons which project to the superior colliculus accumulated preferentially into band-like clusters which were in alignment with thick CO stripes. These results support the notion that CO compartments in V2 are associated with functionally separate pathways.

MATERIALS AND METHODS

Data in this experiment come from five adult monkeys (*Macaca fascicularis*) weighing 3-7 kg. Surgery was performed aseptically under general anesthesia, which was induced with ketamine (0.10 mg/kg i.m.) and maintained with Halothane (1.5-3.0% in oxygen). Following a midline craniotomy over the central sulcus, the position of the superior colliculus was determined by recording evoked responses to stroboscopic illumination with low impedance (<2M) tungsten electrodes (A-M Systems). The stereotaxic coordinates at which evoked potentials were recorded were used to guide subsequent penetrations with pipettes containing anatomical tracers.

In three monkeys, the superior colliculi were injected bilaterally with horseradish peroxidase (30% HRP Sigma type VI in saline), and in two additional monkeys, the superior colliculus on one side was injected with Fast Blue (10% FB in dH2O) (see Table 1). In each superior colliculus, total volumes of 2.0-3.0 l were delivered in 10-20 pressure-injections distributed evenly across the surface of the nucleus. At each site, the anatomical tracer was injected along tracks that extended about 2 mm below the tectal surface.

After a 3 or 5 day survival period, to allow for retrograde transport of HRP or FB, respectively, animals were deeply anesthetized with pentobarbital (0.40 mg/kg i.v.) and perfused transcardially with 0.9% saline followed by a fixative solution containing 2% paraformaldehyde and 0.25% glutaraldehyde in

0.1 M phosphate buffer. All surgical procedures were performed in accordance with NIH guidelines (NIH publications 85-23 and 91-3207) and according to protocols approved by the U.W. Animal Care Committee (IACUC).

Histochemical Processing

Data were analyzed in cortical sections cut tangential to the surface of the cortex in all but two of the tissue blocks (see Table 1). In the two animals injected with FB, the occipital opercula containing portions of dorsal and ventral V2 were separated from the rest of the brain and flattened between glass slides. In two of three animals injected with HRP, the hemispheres were physically unfolded and flattened according to procedures described previously (Olavarria and Van Sluyters, 1985). In the remaining animal injected with HRP, both ventral opercula were unfolded and flattened, while the dorsal opercula were separated and sectioned perpendicular to the cortical surface. The extent of the injection sites was analyzed in coronal or parasagittal sections through the superior colliculus.

The flattened tissue was kept between glass slides for about 12 h at 4 ^{0}C in 0.1 M phosphate buffer. The glass slides were then removed and the block of tissue was placed in 20% sucrose in fixative for approximately thirty minutes, after which time it was transferred to a solution of 20% sucrose in phosphate buffer at 4 ^{0}C until it sank. The brainstems were kept in 20% sucrose in fixative at 4 ^{0}C until they sank. All tissue blocks were sectioned at 40-60 m on a freezing microtome.

In each of the unfolded and flattened cortical blocks from animals injected with HRP, 4-5 superficial sections were processed for CO according to the protocol of Wong-Riley (1979). The remaining sections were reacted for HRP, with tetramethyl benzidine as the chromogen (Mesulam, 1978). In the

flattened cortical blocks from animals injected with FB, CO histochemistry was performed on alternate sections. The remaining sections were immediately mounted on subbed slides and, after they had been scored for fluorescent FB labeling, they were processed for Cat-301 immunohistochemistry to aid in the identification of CO stripes (Hendry et al., 1988; DeYoe et al., 1990). A series of sections from the dorsal opercula which had been sectioned perpendicular to the cortical surface, as well as a series from each brainstem, were stained for Nissl substance.

Data Acquisition

Histological sections were scored using a microscope equipped with a motorized stage controlled by the graphic system Neurolucida (MicroBrightField). Reconstructions of the distribution of retrogradely labeled cells and Cat-301 positive cells were prepared by superimposing all tangential sections which contained labeled cells. These sections were carefully aligned with each other and with CO-stained sections using blood vessels and tissue contours as landmarks.

Statistical Analysis

To correlate the patterns of labeled cells and CO staining quantitatively, we determined the density of labeled cells and measured the density of CO staining in regions 8.0-16.5 mm long, measured parallel to the V1/V2 border. Each region was subdivided into bins which were either 0.25 or 0.50 mm wide, oriented roughly parallel to the CO stripes. In each bin, tracer-labeled cells and Cat-301 positive cells were counted and the density of CO staining was measured using digitized images of neighboring CO-stained sections. The measurements of CO staining density were done with the public

domain NIH Image program (written by Wayne Rasband, National Institutes of Health).

Time-series analysis was used to quantitatively evaluate the degree of correlation between the distributions of tracer-labeled neurons and CO stripes. To investigate whether neurons projecting to the superior colliculus were distributed randomly, we used spectral analysis to search for frequencies in the distribution of tracer-labeled cells that were significant ($p < 0.05$). We then performed a cross-spectral analysis of coherence and phase to determine whether the distribution of tracer-labeled cells and the CO-density profile were significantly coherent ($p < 0.05$) at these frequencies. Phase values not significantly different from zero ($p > 0.05$) for a particular frequency indicated that the distribution of labeled cells and CO staining were aligned at that frequency. These techniques are specially suited for analyzing cyclic data series and have the advantage that they do not require the delineation of the boundaries of CO stripes, which can be difficult to determine unambiguously. Similar methods were used by Olavarria and Abel (1996) in their analysis of the correlation between callosal connections and CO stripes in V2. Detailed descriptions of the techniques and software used are provided elsewhere (Gottman, 1981; Williams and Gottman, 1982).

RESULTS

In all five monkeys studied, the region infiltrated with HRP or FB extended virtually throughout the superior colliculus. This region included the superficial (I-III) and intermediate (IV-V) layers of the nucleus, where afferents from V2 terminate (Kuypers and Lawrence 1967; Wilson and Toyne, 1970; Lund, 1972; Graham, 1979; Tigges and Tigges, 1981; Cusick, 1988; Lui et al., 1995).

Retrogradely-labeled cells studied in sections cut perpendicular to the cortical surface (blocks 4LD and 4RD) were pyramidal in shape and located in layer 5 (see Fig. 1), in agreement with previous studies (Lund et al., 1981; Fries, 1984; Fries et al., 1985). In sections cut tangential to the cortical surface, we found that labeled cells in V2 were not homogeneously distributed in the tangential plane. Instead, they formed band-like clusters which bore a consistent spatial relationship to the pattern of CO labeling.

ANIMALS INJECTED WITH FAST BLUE

Figure 2 shows the data from the dorsal portion of V2 from an animal injected with FB (block 5LD). In CO stained sections, an alternating sequence of CO-dense thick (T) and thin (t) stripes could be clearly recognized (Fig. 2A,B). In addition, the preferential accumulation of Cat-301 immunopositive cells (black dots in Fig. 2A) in the thick stripes confirmed the identity of the CO stripes derived by their physical appearance (Hendry et al., 1988; DeYoe et al., 1990).

The reconstructed distribution of FB-labeled cells is superimposed with the pattern of CO staining in Figure 2B. Inspection of this figure shows that FB-labeled cells (black dots) form band-like clusters that correlate very closely with the thick CO stripes. This impression was borne out by our quantitative analyses of the area bounded by the segmented lines in Figure 2B. The spectral analysis of the distribution of FB-labeled cells (solid line curve in Fig. 2C) revealed a significant frequency whose period was approximately 5 mm. The cross-spectral analysis showed that the spatial coherence between the distributions of labeled cells and CO staining was significant at this frequency, and that these data series were in phase.

Similar results were obtained from the ventral portion of V2 (block 5LV) in the same animal (Fig. 3A). Large fluctuations in the number of FB-labeled cells occurred at 5 mm intervals. As Figure 3A shows, peaks in cell labeling coincided with alternate increases in CO density, and with increases in the number of Cat-301 positive cells. This result was borne out by our quantitative analyses of these data (see Table 1).

Figure 3B shows data from the dorsal portion of V2 (block 8LD) in the second monkey studied with injections of FB into the superior colliculus. As in the case shown in Figure 3A, fluctuations in the number of FB-labeled cells were in close correspondence with increases in the number of Cat-301 positive cells, and with alternate peaks in CO density. The quantitative analyses of these data indicated that there was a significant spatial correspondence between accumulations of FB-labeled cells and thick CO stripes. The increases in the number of FB-labeled cells occurred approximately every 4 mm.

In the animals injected with FB (Figs. 2, 3) we were able to reveal the distribution of Cat-301 positive cells in the same cortical sections that had been scored for fluorescent labeling. This was not possible in the cortical sections processed for HRP. In order to reconstruct the distributions of HRP-labeled cells and CO staining as completely as possible, we did not stain a separate series of sections for Cat-301 in these tissue blocks.

Animals Injected with Horseradish Peroxidase

Animals injected with HRP yeilded similar results to those described above. Figure 4A,B (block 2RD) shows that HRP-labeled cells in dorsal V2 accumulated preferentially in alternate CO-dense stripes which were identified as thick based on their appearance. Data from ventral V2 in the same animal (block 2RV) are shown in Figure 5A. In both data sets, the spectral

analysis revealed that the distribution of HRP-labeled cells had a significant frequency with a period of approximately 3 mm. At this frequency, the cross-spectral analysis showed that the distributions of labeled cells and CO labeling cohered and were in phase.

In a second monkey studied with HRP, peaks in the numbers of HRP-labeled cells from both dorsal (block 6RD; Fig. 5B) and ventral (block 6RV; Fig. 5C) V2 occurred about every 4 mm. Although the distinction between thick and thin CO stripes was less clear in this animal, the data obtained were consistent with those from the other cases; increases in the number of HRP-labeled cells coincided with alternate CO dense stripes. Finally, in ventral V2 from both hemispheres of animal 4 (block 4LV and 4RV), the labeled regions were restricted to areas representing central visual fields (Gattass et al., 1981). The small size of the labeled regions precluded statistical analyses, but visual inspection of the data showed that two clusters of HRP-labeled cells were present in each block, and these were aligned with increases in the density of CO staining (data not shown).

DISCUSSION

We found that corticotectal neurons in V2 were located preferentially in regions that were in spatial register with thick CO stripes. Our finding is based on the direct correlation of the distributions of labeled corticotectal cells and CO staining, and on the use of spectral analysis techniques to statistically assess the significance of this correlation. The latter techniques were chosen because they circumvent the need to delineate the boundaries of CO stripes, which can be difficult to identify unambiguously. The analyses revealed that periodic increases in the numbers of neurons projecting to the superior colliculus occurred about every 3-5 mm, which is approximately the

distance between two CO stripes of the same class (Olavarria et al., 1989; Shipp and Zeki, 1989b; Tootell and Hamilton, 1989; Van Essen et al., 1990). Because these increases in the number of labeled cells were spatially aligned with alternate peaks in the CO density profile, it could be inferred that periodic increases in the density of superior colliculus projection neurons were in register with one class of CO dense stripes. From analyzing cases in which thick and thin CO stripes were easily identified either by their physical appearance (e.g., Fig. 2, 4A), and/or by their affinity to the Cat-301 monoclonal antibody (Fig. 2A, 3), we concluded that periodic increases in the density of corticotectal cells in V2 were in register with thick CO stripes.

Our results extend previous reports on the distribution of corticotectal cells in macaque V2. Fries (1984) and Fries et al. (1985) analyzed the overall distribution of retrogradely labeled corticotectal cells in horizontally cut sections. Although these authors do not describe the detailed tangential distribution of cells in V2, it is possible to see clusters of labeled cells in V2 in some of their data (see Figs. 3, 6 and 9 in Fries, 1984; and Fig. 2 in Fries et al., 1985).

Methodological Considerations

It is unlikely that periodic distributions of neurons projecting to the superior colliculus resulted from uneven uptake of the tracer in the tectum. In all cases, inspection of histological sections through the tectum indicated that the injections had impregnated virtually the entire nucleus, from the superficial through the deep layers, including all layers receiving projections from V2 (Kuypers and Lawrence 1967; Wilson and Toyne, 1970; Lund, 1972; Graham, 1979; Tigges and Tigges, 1981; Cusick, 1988; Lui et al., 1995). In addition, our results did not depend on the type of tracer used because we obtained the same

results with HRP and the fluorescent tracer FB. Finally, the observation that labeled cells were located in layer 5 indicates that the tracers did not spread to axons of the neighboring interhemispheric pathway because the laminar and tangential distribution of neurons in this pathway is different (Lund et al., 1981; Van Essen et al., 1982; Kennedy et al., 1986; Olavarria and Abel, 1996).

Relationship of CO Architecture and Functional Pathways

It has been hypothesized that CO compartments in V2 identify pathways that are anatomically and functionally segregated (Hubel and Livingstone, 1987; Livingstone and Hubel, 1987b, DeYoe and Van Essen, 1988; Livingstone and Hubel, 1988; Shipp and Zeki, 1988). This hypothesis has been examined in numerous anatomical and physiological studies (see Felleman and Van Essen, 1991; Maunsell, 1992; Merigan and Maunsell, 1993 for review). While some studies support the idea that CO compartments in V2 represent different functional pathways, evidence from other studies is more ambiguous.

Perhaps the most compelling suggestion that V2 stripes are associated with separate functional pathways comes from anatomical studies of cortical afferent projections to V2 and efferent projections from V2. Each stripe compartment has been found to receive segregated input from compartments in V1 (Livingstone and Hubel, 1983, 1984, 1987a), and to project differentially to other cortical areas (DeYoe and Van Essen, 1985; Shipp and Zeki, 1985; Felleman et al., 1988; Shipp and Zeki, 1989b; Zeki and Shipp 1989; Van Essen et al., 1990; Nakamura et al., 1993; DeYoe et al., 1994). Moreover, analysis of the intrinsic connections in V2 reveals that connectivity patterns can reflect the striped architecture of V2, even though interconnections between stripes of different compartments appear to exist (Livingstone and Hubel, 1984; Rockland,

1985; Levitt et al., 1994b; Malach et al., 1994; Olavarria and O'Brien, unpublished observations).

On the other hand, inferences about the functional segregation of V2 stripes based on physiological data have been somewhat mixed. A recent analysis of the fine visual topography in V2 revealed that each class of V2 compartments contain a continuous representation of the visual field (Roe and T'so, 1995). In addition, there is general agreement that neurons with selective responses to some visual attributes, such as color, motion and disparity, tend to cluster in different CO compartments (DeYoe and Van Essen, 1985; Hubel and Livingstone, 1987; Peterhans et al., 1993; Levitt et al., 1994a; Gegenfurtner et al., 1996). However, responses to other visual attributes appear to be more homogeneously distributed in V2, without an obvious relationship to CO architecture (Peterhans et al., 1993; Levitt et al., 1994a; Gegenfurtner et al., 1996). The latter results may in part reflect the mixing of physiological and anatomical pathways that appears to occur as early as striate cortex (Malpeli and Schiller, 1981; Lachica et al., 1992; Nealey and Maunsell, 1994; Yoshioka et al., 1994; Sawatari and Callaway, 1996; see Merigan and Maunsell, 1993; Casagrande and Kaas, 1994 for review).

CORTICOSUBCORTICAL PROJECTIONS: AREA V2

The present study stems from the idea that correlating the distribution of subcortically projecting neurons with the pattern of CO stripes may yield additional information about the relationship of V2 stripes with functional pathways. We studied the corticotectal pathway because superior colliculus neurons have been shown to depend upon "broad-band" input passing through the magnocellular layers of the LGN (Schiller, 1981). Using cooling and ablation procedures, Schiller and colleagues (Schiller et al., 1974; 1979) found that visual

responses of collicular cells located preferentially outside the retino-recipient layers depended on cortical input. Moreover, by inactivating either magnocellular or parvocellular LGN layers, they showed that the responses of this neuronal population depended on the magnocellular, but not the parvocellular, pathway (Schiller et al., 1979). Because V2 thick stripes receive significant input from magnocellular LGN layers through layer 4B in V1 (Livingstone and Hubel, 1987a), we predicted that projections to the superior colliculus from V2 would originate preferentially from cells within thick stripes.

Our findings bear out this prediction, thereby supporting the notion that CO compartments in V2 are associated with functionally separate pathways. Our observation that a small proportion of labeled cells were located in thin and interstripe regions suggests that these compartments are less closely associated with broad-band functions than thick stripes.

It should be noted that V2 thick stripes may not receive only magnocellular input. Parvocellular input can potentially reach thick stripes through intrinsic V2 projections (Livingstone and Hubel, 1984; Rockland, 1985; Levitt et al., 1994b; Malach et al., 1994). In addition, layer 5 cells in V2 can have extensive dendritic trees (Valverde, 1978; Lund et al., 1981), making it possible for dendrites of corticotectal cells in V2 thick stripes to sample information from neighboring stripes. Dendritic sampling across processing streams has been investigated for some cell populations in V1 (H bener and Bolz, 1992; Malach, 1992), but data on this issue are not yet available for corticotectal cells in V2. Finally, the recent report (Sawatari and Callaway, 1996) that layer 4B in striate cortex also receives parvocellular input opens the possibility that this input can be directly relayed to thick CO stripes in V2 (Livingstone and Hubel, 1987a). However, the dependance of collicular cells on magnocellular input shown by Schiller and colleagues (Schiller et al.,1979) implies that even if substantial

parvocellular input reaches V2 thick stripes either from layer 4B or other sources, this input does not appear capable of driving collicular activity during blockade of the magnocellular LGN layers.

If the segregation of V2 corticotectal projections does reflect functional differences between CO compartments, then the analysis of the distribution of corticotectal projections may provide a useful criterion for delineating functional differences among visual areas beyond V2. The potential of this approach is illustrated by recent studies reporting that different cortical regions in parietal and temporal cortices differ in the extent of their projections to the superior colliculus (Lynch et al., 1985; Baizer et al., 1993; Lui et al., 1995).

Corticosubcortical Projections: Area V1

Segregation of corticotectal projection neurons in relation to CO architecture has also been described for V1. In this area, corticotectal cells are distributed preferentially in the interblob compartment in infragranular cortex (Lia and Olavarria, 1996). A similar relationship with the CO architecture has been reported for cytologically-identified Meynert cells in V1 (Fries, 1986; Payne and Peters, 1989), many of which are known to project to both the superior colliculus and area MT (Fries et al., 1985).

It is of interest to point out that segregation of neuronal populations in relation to CO architecture does not appear to be a general rule for all cortical layers. For instance, in contrast to the infragranular corticotectal population, the magnocellular-recipient supragranular layer 4B population projecting to the thick stripes in V2 (Livingstone and Hubel, 1987a) and to MT (Maunsell and Van Essen, 1983; Shipp and Zeki, 1989a) is not segregated in relation to CO architecture (Shipp and Zeki, 1989a). In addition, Fitzpatrick and colleagues (1994) have reported that there are sublaminar differences between the

populations of layer 6 neurons projecting to either the magnocellular or parvocellular LGN layers, but no overt patchiness in the tangential plane has yet been described for this neuronal population (Horton, 1984).

Segregation of Subcortical Loops

In addition to the superior colliculus, another major subcortical target of V2 is the pulvinar complex, and a recent study suggests that this descending projection also correlates with the modular organization of this area. Levitt et al. (1995) reported that the distribution of pulvinar projecting neurons in V2 fluctuates within layer 5A in vertical registration with thick and thin CO stripes. Likewise, pulvinar afferents to V2 have been shown to be segregated into stripe-like domains (Ogren and Hendrickson, 1977; Curcio and Harting, 1978) that are in vertical alignment with thick and thin CO stripes (Livingstone and Hubel, 1982; Levitt et al., 1995). These data open the possibility that the exchange of visual information between V2 and the pulvinar complex flows along functionally segregated loops.

Input from V2 may also reach the pulvinar complex through superior colliculus-pulvinar projections (Benevento and Fallon, 1975; Partlow et al., 1977; Harting et al., 1980; Benevento and Standage, 1983). Tectal-recipient regions in the pulvinar appear to overlap with cortically-projecting regions (Benevento and Rezak, 1976), but the specificity of the tecto-pulvino-fugal projections with respect to thick and thin stripes in V2, and to other visual areas of the dorsal or ventral streams, remains to be determined. Based on physiological data, it has been proposed that tectofugal pathways are associated preferentially with cortical areas of the dorsal stream (Bruce et al., 1986; Girard et al., 1991; Gross, 1991). This proposal raises the intriguing possibility that cortico-tectal projections, including those from thick stripes described in the

present study, may be part of a superior colliculus-pulvinar-cortical loop that preferentially processes broad-band information. Additional studies are necessary to further characterize the various components of such tecto-fugal circuits and the extent to which they relate to specific visual functions.

Table 1: Summary of methods and results

TABLE 1. Summary of Methods and Results.

Monkey	SC	Histology	Blocks	CO Stripes	Period[1]	Fig.
5	Left FB	Operculum flattened.	5LD 5LV	Thick stripes identified in both blocks.[2]	4.7 mm in both blocks	2A-C & 3A
8	Left FB	Operculum flattened.	8LD	Thick stripes identified.[2]	3.6 mm	3B
2	Left and Right HRP	L-hem damaged. R-hem unfolded and flattened.	2RD 2RV	Thick stripes identified in both blocks.	2.8 mm in both blocks	4A,B & 5A
6	Left and Right HRP	L-hem damaged. R-hem unfolded and flattened.	6RD 6RV	Distinction between thick and thin stripes could not be made in either block.	3.8 mm in both blocks	5B,C
4	Left and Right HRP	Ventral blocks unfolded and flattened, opercula flattened in dorsal blocks.	4LV 4RV 4LD 4RD	Distinction between thick and thin stripes could not be made in ventral blocks. Dorsal blocks were analyzed in perpendicularly cut sections.		1A-C

[1] Values indicate the period of those frequencies in the distribution of labeled cells which were significant and coherent with frequencies in the distribution of CO.

[2] The identification of thick and thin stripes in these blocks was facilitated by immunostaining for CAT-301 positive cells, which are found predominantly within CO dense thick stripe regions (Hendry et al., 1988; DeYoe et al., 1990).

HRP, horseradish per oxidase; FB, fast blue.

Figure 1: V2-SC radial distribution (4RD).

A. Nissl-stained section cut perpendicular to the cortical surface of the dorsal operculum (block 4RD). **B**. Adjacent horseradish peroxidase (HRP)-stained section containing three labeled pyramidal cells (arrows) within layer V. **C**. Higher-power view of HRP-labeled cells shown to the left in B. Scale bar = 500 m in A & B, 100 m in C.

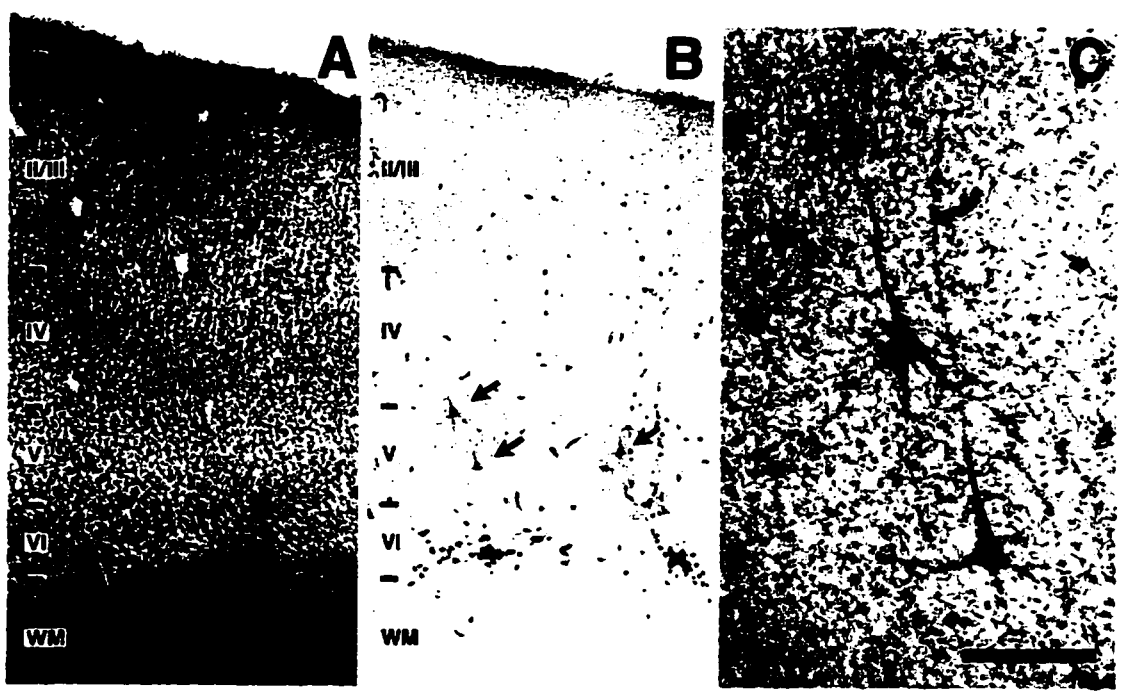
A
II/III
IV
V
VI
WM
B
II/III
IV
V
VI
WM
C

Figure 2: V2-SC tangential distribution (5LD).

A. Distribution of Cat-301 positive cells (black dots) superimposed on the pattern of CO staining in dorsal V2 (block 5LD). Posterior is to the left, dorsal is up. **B.** Distribution of V2 cells (black dots) projecting to the superior colliculus (V2-SC). This population was retrogradely labeled by injections of Fast-Blue (FB) into the tectum. The distribution of FB-labeled cells is shown superimposed on the pattern of CO staining. T: thick stripes; t: thin stripes. These sections come from a flattened operculum which contains portions of V2 on one side and portions of V1 on the other. The apparent superficial location of labeled layer 5 cell at the edge of the reconstruction in B is an artifact resulting from not unfolding the opercular lip prior to flattening the tissue block. The area analyzed quantitatively (bounded by the segmented lines) measured 16.5 mm in the direction parallel to the V1/V2 border. Labeled cells lying on white areas of the section shown in A,B were scored in more superficial sections. **C.** Quantitative analysis of area located between segmented lines in B. The solid curve (V2-SC) represents the distribution of FB-labeled cells and the segmented curve (CO) indicates the density profile for CO staining.

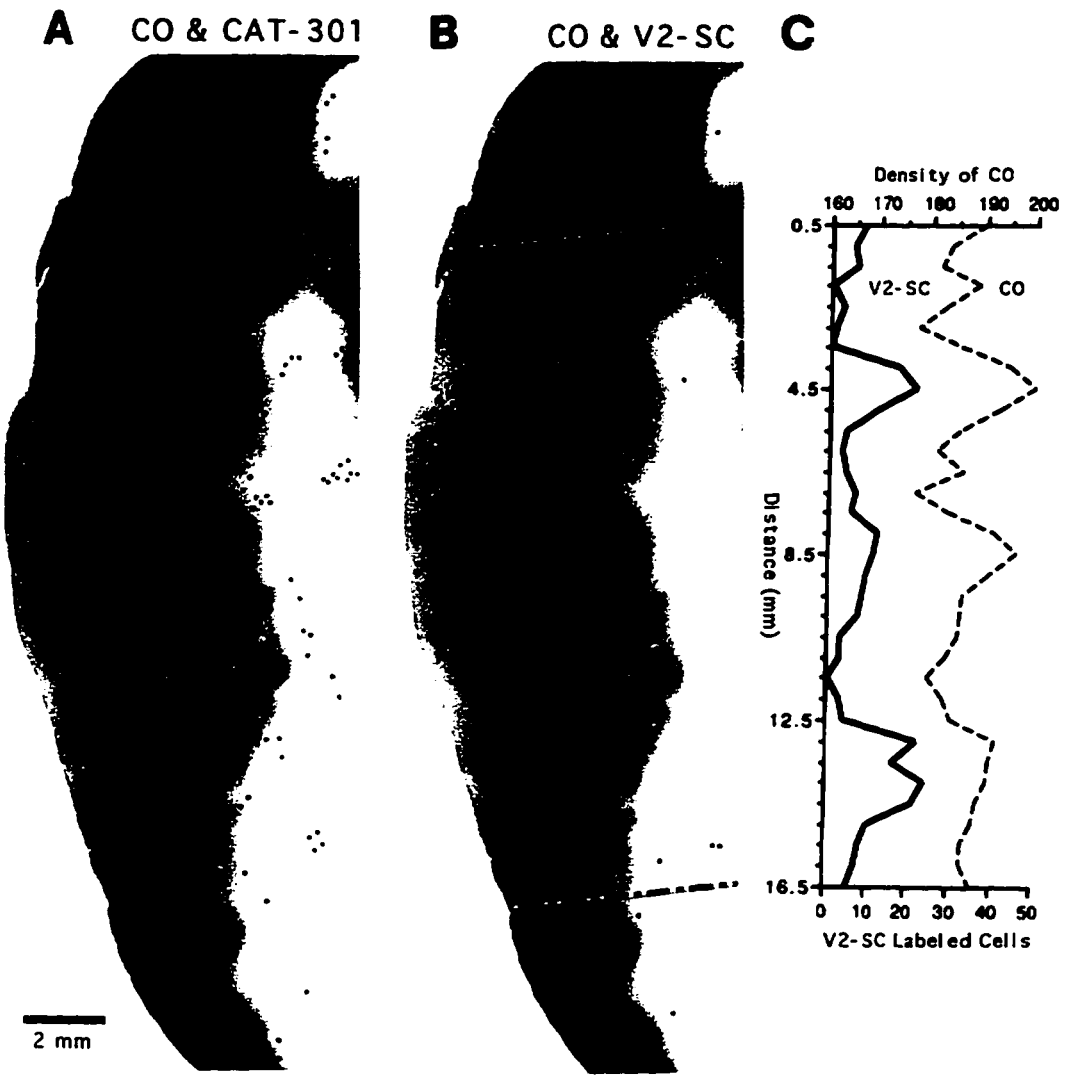
A
CO & CAT-301
B
CO & V2-SC
C
2 mm
Density of CO
160 170 180 190 200
0.5
4.5
8.5
12.5
16.5
V2-SC
CO
Distance (mm)
0 10 20 30 40 50
V2-SC Labeled Cells

Figure 3: V2-SC data (5LV,8LD).

Data from ventral V2 in monkey 5, **A**, and from dorsal V2 in monkey 8, **B**. The solid curves (V2-SC) represent the distribution of FB-labeled cells, the dashed curves (CO) indicate the density profile for CO staining (ordinate scale not shown), and the dotted curves represent the distribution of Cat-301 positive cells. In both graphs, the number of FB-labeled cells peaks in close correspondence with increases in the number of Cat-301 positive cells and alternate CO dense regions (thick stripes).

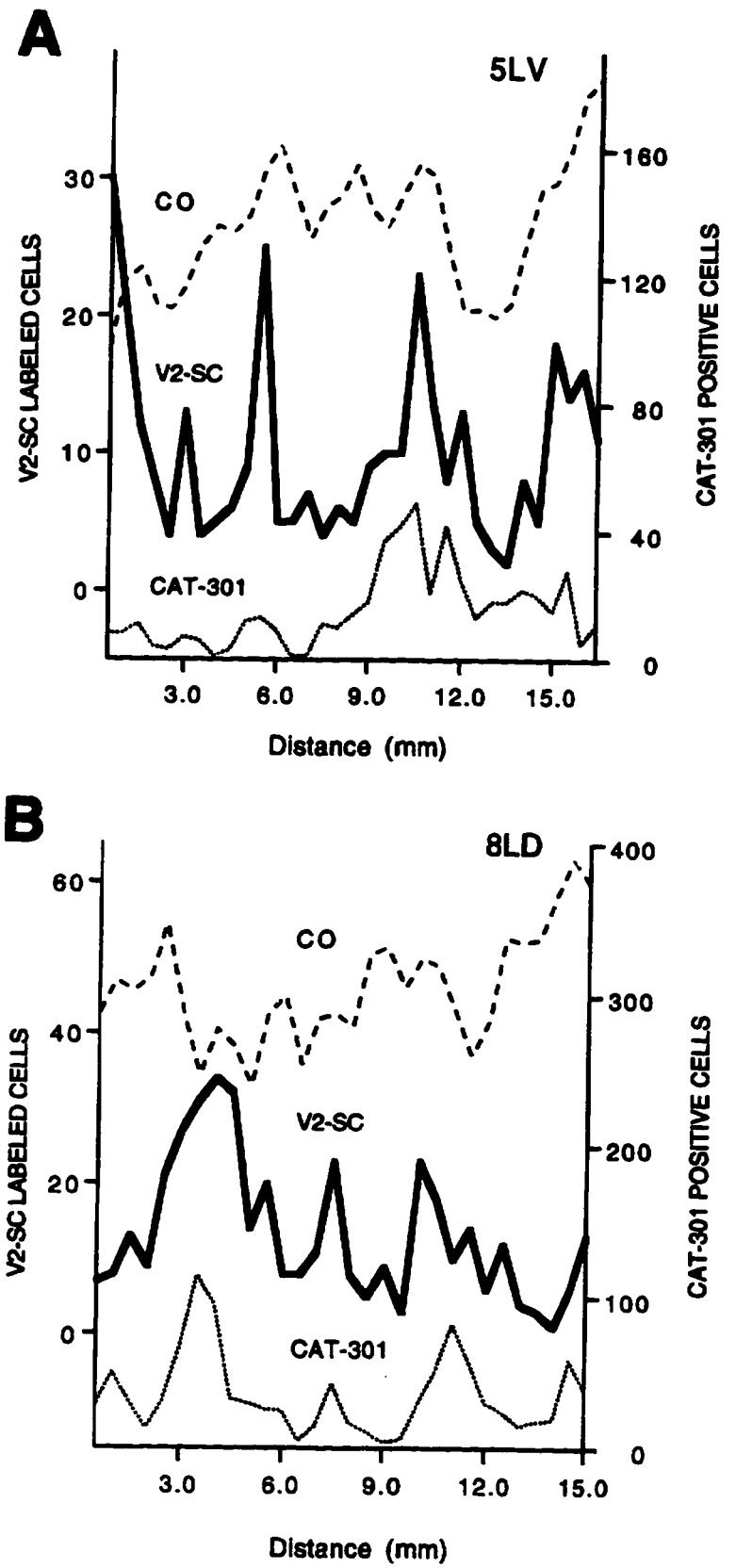
A
5LV
CO
V2-SC
CAT-301
V2-SC LABELED CELLS
CAT-301 POSITIVE CELLS
30
20
10
0
160
120
80
40
0
3.0
6.0
9.0
12.0
15.0
Distance (mm)
B
8LD
CO
V2-SC
CAT-301
V2-SC LABELED CELLS
CAT-301 POSITIVE CELLS
60
40
20
0
400
300
200
100
0
3.0
6.0
9.0
12.0
15.0
Distance (mm)

Figure 4: V2-SC tangential distribution
(2RD).

Data from dorsal V2 in monkey 2 studied with injections of HRP into the tectum. **A.** Distribution of HRP-labeled cells (black dots) superimposed on the pattern of CO staining; T: thick stripes, t: thin stripes. Tangential sections came from unfolded and flattened tissue. Labeled cells lying in the region of tissue discontinuity were scored in deeper sections, which were continuous in this region. Posterior is to the left, dorsal is up. At left, the CO-stained section includes a portion of V1, which can be recognized by the presence of CO blobs. The segmented lines indicate area analyzed quantitatively. **B.** Distribution of HRP-labeled cells (V2-SC) and density profile for CO staining (CO).

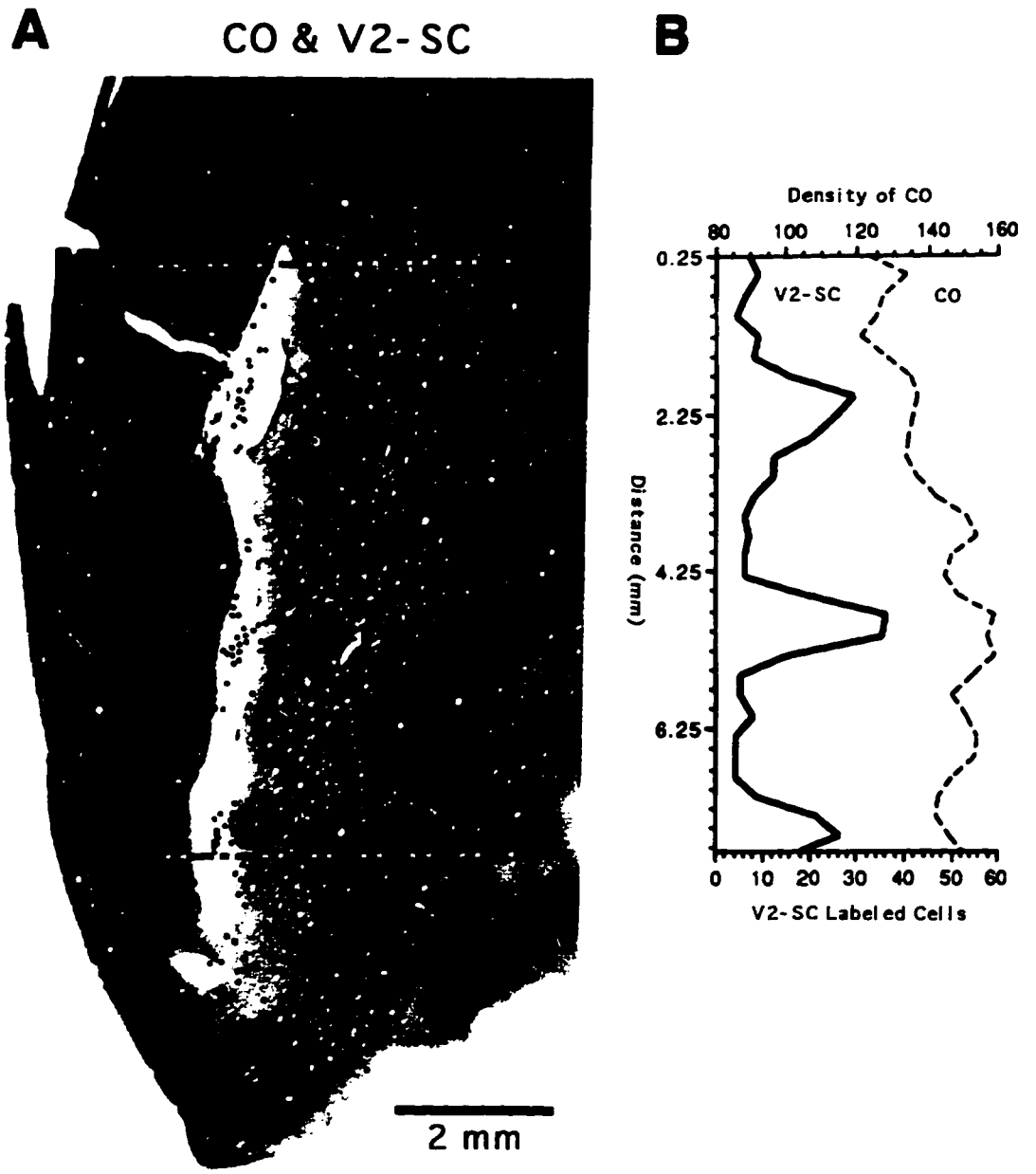
A
CO & V2-SC
2 mm
B
Density of CO
80
100
120
140
160
0.25
2.25
4.25
6.25
V2-SC
CO
Distance (mm)
0
10
20
30
40
50
60
V2-SC Labeled Cells

Figure 5: V2-SC data (2RV, 6RD, 6RV).

Data from ventral V2 in monkey 2, **A**; dorsal V2, **B**, and ventral V2, **C**, from monkey 6. Monkeys 2 and 6 were studied following injections of HRP into the tectum. In each graph, increases in the number of HRP-labeled cells (V2-SC) correspond closely with alternate peaks in the CO density profile (CO).

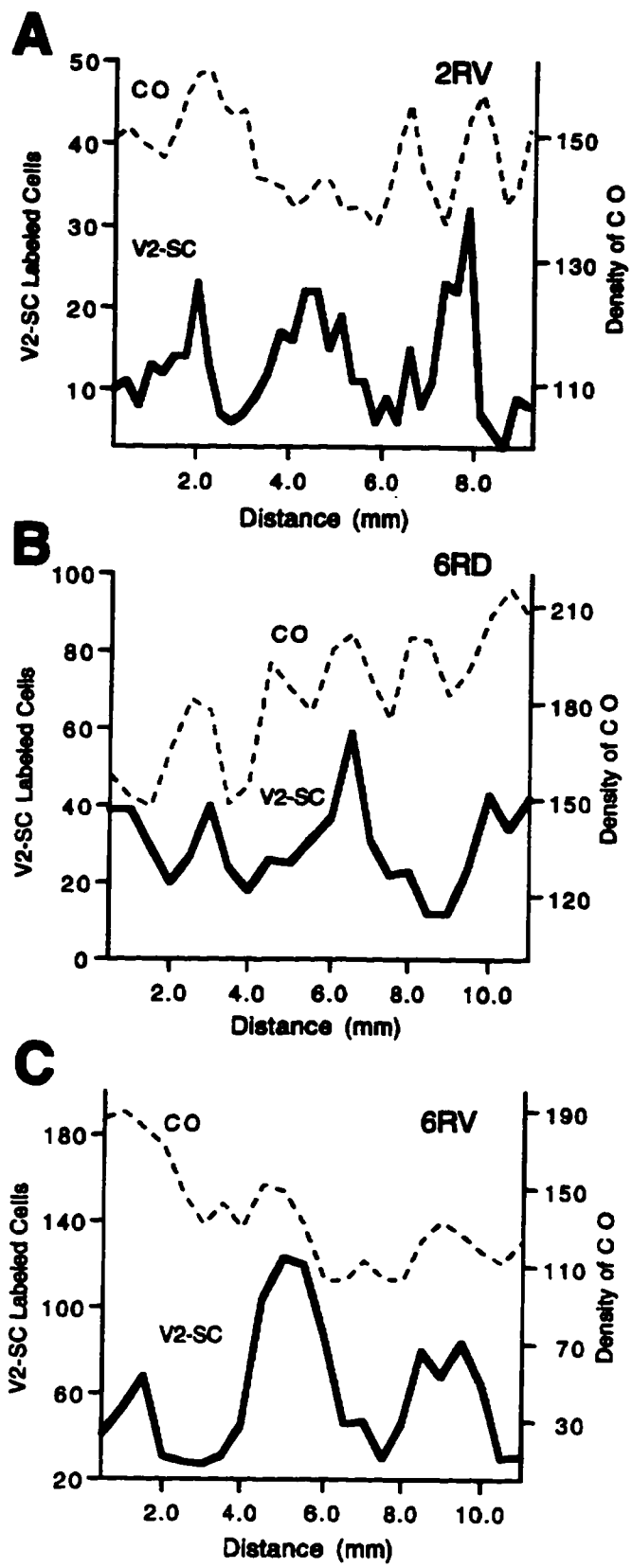
A
2RV
CO
V2-SC
V2-SC Labeled Cells
Density of C O
50
40
30
20
10
150
130
110
2.0
4.0
6.0
8.0
Distance (mm)
B
6RD
CO
V2-SC
V2-SC Labeled Cells
Density of C O
100
80
60
40
20
0
210
180
150
120
2.0
4.0
6.0
8.0
10.0
Distance (mm)
C
6RV
CO
V2-SC
V2-SC Labeled Cells
Density of C O
180
140
100
60
20
190
150
110
70
30
2.0
4.0
6.0
8.0
10.0
Distance (mm)

CHAPTER 2: THE DISTRIBUTION OF CALLOSAL CONNECTIONS CORRELATES WITH THICK AND THIN CYTOCHROME OXIDASE STRIPES IN AREA V2

In adult mammals, interhemispheric connections through the corpus callosum are not distributed uniformly across the expanse of sensory neocortex, but instead form elaborate patterns that are consistent across individuals of the same species. It is commonly thought that patterns of callosal connections bear specific spatial relationships with the underlying topographic maps of the sensory periphery. In visual cortex, it has been traditionally believed that callosal connections concentrate at the borders between adjacent visual areas where the vertical meridian of the visual field is often represented (e.g., Berlucchi et al., 1967; Van Essen and Zeki, 1978; Olavarria and Montero, 1984; Thomas and Espinoza, 1987). This idea has stimulated much research (reviewed in Kennedy et al., 1991; Innocenti, 1991) and inspired the hypothesis that visual callosal connections are concerned with establishing anatomical and functional continuity across the vertical meridian of the visual field (e.g., Hubel and Wiesel, 1967; Berlucchi et al., 1967; Choudhury et al., 1965; Blakemore et al., 1983).

However, recent studies have suggested that the distribution of callosal connections may not only reflect visual cortical topography, but also may be correlated with the modular architecture revealed in some areas with cytochrome-oxidase (CO) histochemistry. Thus, in galagos (Cusick et al., 1984, Beck and Kaas, 1994) and cats (Boyd and Matsubara, 1994) callosal connections in striate cortex form patches whose distribution has been related to the pattern of CO-dense "blobs". In area V2 of monkeys, cytochrome-oxidase histochemistry reveals a system of stripe-like subregions where densely labeled

thick and thin stripes, and pale interstripes can be recognized (Horton and Hubel, 1981; Tootell et al., 1983; 1985; Livingstone and Hubel, 1984; Horton, 1984; Hendrickson, 1985; Olavarria et al., 1989; Van Essen et al., 1990). Interestingly, in several primates callosal connections in V2 appear as "fingers" that extend anteriorly from the V1/V2 border region, resembling the arrangement of CO stripes in V2 (Van Essen et al., 1982; Cusick et al., 1984; Gould et al., 1987; Kennedy et al., 1986).

In macaque monkeys, callosal fingers in V2 have been reported to protrude 4-5 mm from the V1 border into V2 (Van Essen and Zeki, 1978; Van Essen et al., 1982), and isolated patches of callosal connections have been observed even further into V2 (Kennedy et al., 1986). Kennedy et al. (1986) reported that callosal patches in macaque V2 overlap with regions of high cytochrome oxidase activity. However, the exact correlation between callosal fingers and CO-stripes in V2 is not clear in their study because the relationship between these patterns was examined only in parasagittal sections, and not over a large tangential area. Determining the detailed relationship of callosal connections with CO-stripes in V2 is potentially important because these stripes have been associated with functional streams in visual cortex (Ungerleider and Mishkin, 1982; Mishkin et al., 1983; Livingstone and Hubel, 1987; DeYoe and Van Essen, 1988).

In the present study we took advantage of a method for physically unfolding and flattening the cortex of gyrencephalic brains (Olavarria and Van Sluyters, 1985) to directly compare the callosal and CO-staining patterns over broad regions in macaque V2. In addition, we performed spectral and coherency analyses on the distributions of labeled callosal cells and CO staining to evaluate quantitatively the degree of correlation between these distributions.

Our results showed that labeled callosal cells congregated along the V1/V2 border and in finger-like bands that protruded up to 7 mm into V2. These callosal bands were in register with thick and thin CO stripes, with relatively few labeled callosal cells found in interstripe regions. These results suggest that the distribution of callosal connections in visual cortex is dictated not only by the topography of visual areas, but also by the arrangement of cortical functional streams. Some of these data have been presented previously as an abstract (Olavarria and Lewis, 1992).

MATERIALS AND METHODS

The present experiment is based on the study of 4 hemispheres from 3 adult *Macaca fascicularis* weighing 3 - 5 kg. Surgery was performed aseptically under general anesthesia induced with ketamine hydrochloride (0.10 mg/kg i.m.) and maintained with Halothane (1.5 - 3% in oxygen). In two monkeys, we used the retrograde transport of horseradish peroxidase (HRP, Sigma Type VI) to reveal the distribution of callosal neurons in visual cortex. The corpus callosum was exposed by gently retracting the left hemisphere through a large craniotomy and durotomy. Approximately the posterior half of the corpus callosum was transected with a scalpel, and one or more pieces of polyacrylamide gel impregnated with 15% HRP (Griffin et al., 1979) were implanted with fine forceps between the cut ends. In the third monkey, callosal connections were revealed by the retrograde transport of the fluorescent tracer Nuclear Yellow (NY, Sigma Co., 5% in dH_2O). Multiple injections (total volume of about 1.0 l pressure-injected through glass micropipettes with 50-100 m internal tip diameter) of NY were delivered into the splenium of the corpus callosum and adjoining regions of the left hemisphere.

Survival periods for the retrograde transport of tracers of 2 (for HRP) or 4 (for NY) days were allowed, after which the animals were deeply anesthetized with pentobarbital sodium (0.4 mg/kg i.v.) and perfused through the heart with normal saline followed by a brief (7-8 min) perfusion (Olavarria and Van Sluyters, 1985) with either 2% glutaraldehyde (for HRP) or 2% paraformaldehyde and 0.5% glutaraldehyde (for NY) in 0.1 M phosphate buffer. Surgical procedures followed the principles of laboratory animal care (NIH publication 85-23, 1985), and protocols approved by the animal care committee at U.W. (IACUC).

Histochemical Processing

In the two monkeys in which HRP gels were directly applied to the transected callosum, the hemispheres were unfolded and flattened according to procedures described previously (Olavarria and Van Sluyters, 1985). Only three hemispheres were studied in these monkeys because one hemisphere was damaged during the flattening process. Due to intrinsic cortical curvature, it was necessary to make several cuts in the margin of the cortex so that the areas of interest would lie completely flat. The locations of these cuts were chosen so as to preserve as much as possible the continuity of V2. In the third monkey, the right occipital operculum containing portions of dorsal and ventral V2 was separated from the rest of the brain and flattened between glass slides. The flattened tissue from all three animals was left overnight at 4 deg C in 0.1 M phosphate buffer between glass slides. The glass slides were then removed and the tissue was subsequently left in fixative for about 30 min, placed in 20% sucrose in 0.1 M phosphate buffer until it sank, and then was frozen and cut tangentially at 40 m. A one in four series of sections was processed for CO histochemistry (Wong-Riley, 1979), while the remaining sections were either reacted for HRP (with tetramethyl benzidine as the chromogen, Mesulam, 1978),

or immediately mounted on glass slides for fluorescent microscopy. In some tissue blocks, portions of the flattened tissue were cut perpendicularly to the cortical surface to analyze the laminar distribution of labeled cells. The sections obtained were first processed for visualizing labeled cells and, after they had been scored, they were Nissl-stained for revealing the cortical layers.

Although our primary interest was to study the callosal pattern in V2, we also sectioned and processed blocks of tissue containing other extrastriate areas. We observed that many areas, including areas V4 and MT, also contained dense accumulations of labeled callosal cells, confirming that uptake of the tracers was not restricted to callosal axons originating from V2.

Data Acquisition

Histological sections were scored using a microscope equipped with a motorized stage (LEP) controlled by a Gateway 2000 486/33c computer, and the graphic system Neurolucida (MicroBrightField). Typically, a few tangential sections through supragranular cortex contained most of the information regarding the tangential distribution of labeled cells (e.g., see Fig. 7C). Reconstructions of the callosal patterns were prepared by superimposing all tangential sections containing labeled cells. These sections were carefully aligned with each other using blood vessels and tissue contours as landmarks.

Statistical Analysis

In order to correlate the patterns of callosal cells and CO labeling quantitatively, labeled callosal cells were counted and the intensity of CO staining was measured in areas of V2 where CO stripes were recognizable and cell labeling was dense. In order to count labeled cells, the analyzed regions in the reconstructed patterns (measuring about 10 - 14 mm parallel to the V1/V2 border) were subdivided into parallel sampling strips (0.3 mm wide each)

oriented roughly parallel to the CO stripes. Counts in these strips were used to construct distribution curves of labeled callosal cells (see solid line curve in Fig. 6D). The regions in V2 from which cell counts were obtained were scanned in digitized images of neighboring CO stained sections. The density profiles for CO staining (see dashed curve in Fig. 6D) were obtained from the digitized images by using the public domain NIH Image program (written by Wayne Rasband and available from the internet by anonymous ftp from zippy.nimh.nih.gov or on floppy disk from MTIS, 5285 Port Royal Rd., Springfield, VA 22161, part number PB93-504868).

We performed a quantitative analysis to assess the degree of correlation between the patterns of callosal neurons and CO stripes. In particular, we wished to 1) test the null hypothesis that callosal neurons were distributed randomly, and 2) assess whether fluctuations in both the callosal cell and CO density distributions were spatially aligned with each other. We used spectral analysis to address the first objective and coherency analysis to assess the spatial relationship between callosal cell and CO staining distributions. These techniques are especially suited for analyzing cyclic data series. Similar methods were used by Johnson et al. (1989) in their analysis of the correlation between callosal and association neurons in frontal and parietal cortices of macaque monkeys. In our particular application, the methods we employed take into account the periodic nature of the CO stripes and the requirement for similar periodicity in the distribution of callosal cells if the two patterns are correlated. In addition, these methods have the advantage that they do not require the delineation of the boundaries of CO stripes, which are often difficult to determine. Detailed descriptions of the techniques and software used are provided elsewhere (Gottman, 1981; Williams and Gottman, 1982).

We first obtained the spectral density function for the callosal cell distribution in order to test whether it differed significantly from that of a random

distribution (white noise). The program used (Gottman, 1981; Williams and Gottman, 1982) allowed us to identify frequencies in the distribution of labeled cells that were significant ($p < 0.05$). We then performed a cross-spectral analysis of coherence and phase to determine whether the distribution of labeled cells and CO-density profile cohered significantly ($p < 0.05$) at these frequencies. Finally, phase values not significantly different from zero ($p > 0.05$) for a particular frequency indicated that the two data series were nearly perfectly aligned at that frequency.

RESULTS

Labeled cells were observed in broad regions in both dorsal and ventral V2 in all three monkeys studied. In all cases, virtually all labeled cells were found in tangential sections cut through supragranular layers. The supragranular distribution of labeled cells was confirmed by analyzing sections cut perpendicular to the surface of the flattened cortex.

In all four hemispheres studied callosal connections in V2 formed finger-like accumulations that protruded into V2 from the V1/V2 border. Correlation of this labeling pattern with the arrangement of V2 CO stripes could not be carried out in one hemisphere due to poor labeling of the sections stained for CO. In the remaining three hemispheres, the callosal fingers were in register with CO-dense stripes. Results from these three hemispheres are illustrated in Figures 6-8.

Animals Studied with Horseradish Peroxidase

In the two monkeys whose cortices were unfolded and flattened, the tangential sections included portions of opercular striate cortex and both

banks of the lunate sulcus (for dorsal V2) or both banks of the inferior occipital sulcus (for ventral V2). In these animals we observed that callosal labeling in V2 stopped abruptly at the V1/V2 border. A few HRP-labeled cells were observed within V1, and most of them were located within 0.5 mm from the V1 border as determined in neighboring CO-stained sections. Within V2, labeling within a 0.5 mm wide strip immediately adjacent to the V1 border appeared relatively continuous (Fig. 8A), although periodic increases in cell density were often observed in this region (Figs. 6, 7A).

Further away from the V1/V2 border, the pattern of callosal labeled cells in V2 was characterized by numerous regularly spaced finger-like protrusions that extended roughly perpendicularly from the V1/V2 border. Figure 6 shows the results from a monkey that received an implant of acrylamide gel-HRP into the corpus callosum. Figure 6A shows the callosal labeling pattern reconstructed from tangential sections through ventral V2. In this case, the callosal fingers extended up to about 5 mm into V2, although less dense labeling could be observed as far as 7 mm from the V1/V2 border. The pattern of CO staining (Fig. 6B) revealed an alternation between CO-dense and CO-pale stripes oriented roughly perpendicularly to the V1/V2 border. Moreover, among the CO-dense stripes, wide stripes (T) alternated with thin stripes (t), presumably corresponding to the arrangement of thick and thin CO-stripes described previously in monkey V2 (Horton and Hubel, 1981; Tootell et al., 1983; Livingstone and Hubel, 1984; Horton, 1984; Hendrickson, 1985; Olavarria et al., 1989; Van Essen et al., 1990). The callosal and CO patterns are superimposed in Figure 6C. The area analyzed (between dashed lines in Fig. 6C) measured 13.5 mm parallel to the V1/V2 border, and contained 7 CO dense stripes (indicated with arrows in Fig. 6A-C).

Inspection of Figure 6C suggests that callosal cell clusters coincide with densely labeled CO stripes, with few cells in the interstripe regions. This

impression was borne out by our quantitative analysis. In Figure 6D, the solid line represents the distribution of labeled cells, whereas the dashed line indicates the density profile for CO staining. The spectral analysis of the distribution of labeled cells showed a frequency that was significant ($p < 0.05$), with period of approximately 2 mm. The cross-spectral analysis of coherence and phase showed that the coherence was significant ($p < 0.05$) at this frequency. Furthermore, the phase (0.01) was not significantly different from zero at this frequency ($p > 0.05$), indicating that the two data series were nearly perfectly aligned.

Similar results were obtained from dorsal V2 in the same animal (Fig. 7). Again, labeled cells formed finger-like clusters extending into V2 (Fig. 7A). Figure 7C is a photomontage showing HRP-labeled cells from one of the sections used to reconstruct the finger-like cluster marked with the arrow in Figure 7A. The longest finger-like protrusion in this case extended nearly 8 mm into V2. Figure 7B shows the distribution of callosal cells and CO staining in the area analyzed. The spectral analysis of the distribution of labeled cells showed a significant ($p < 0.05$) frequency with period of 2 mm. The cross-spectral analysis of coherence and phase showed that the coherence was significant ($p < 0.05$) at this frequency, and that the phase (0.03) was not significantly different from zero ($p > 0.05$).

Data from dorsal V2 in the second monkey studied with HRP is shown in Figure 8-B. As illustrated in Figure 8A, the density of labeled callosal cells decreased sharply at the V1/V2 border (to the left in Fig. 8A). On the V2 side, there was a region of continuous labeling near the V1/V2 border from which fingers of labeled callosal cells extended as far as 5 mm into V2. Inspection of Figure 8B suggests a good correspondence between the peaks in labeled cell density and the peaks in CO labeling density. The spectral analysis showed a

significant ($p < 0.05$) frequency with period of 1.6 mm in both labeling patterns, and a phase (0.07) not significantly different from zero ($p > 0.05$).

Animal Injected with Nuclear Yellow

The data illustrated in Figure 8C-D show that a periodic clustering of callosal connections in V2 was not dependent on the tracer and methods of applications used since similar results were obtained with injections of NY. The pattern of callosal connections (Fig. 8C) was reconstructed from sections cut tangentially to the ventral face of the separated and flattened operculum (see Methods). Because of this approach, the tangential sections did not include the V1/V2 border and opercular portions of V2, causing the finger-like clusters to appear shorter than in the previous Figures. Figure 8D shows the distribution of callosal cells and CO staining in the area analyzed. The spectral analysis of the distribution of labeled cells showed a significant ($p < 0.05$) frequency with period of approximately 2 mm. The cross-spectral analysis of coherence and phase showed that the coherence was significant ($p < 0.05$) at this frequency and that the phase (0.1) was not significantly different from zero ($p > 0.05$).

DISCUSSION

We found that callosal cells in V2 accumulate in finger-like bands that are in register with CO-dense stripes. Our results confirm and extend previous studies on the distribution of callosal connections in visual area V2 of the macaque (Winfield et al., 1975; Lund et al., 1976; Rockland and Pandya, 1979; Van Essen and Zeki, 1978; Van Essen et al., 1982; Kennedy et al., 1986), as well as on the relationship of callosal connections with the CO-architecture in V2 (Kennedy et al., 1986). In addition, our data confirm that callosal labeling in V1 is largely restricted to a narrow zone immediately adjacent to the V1/V2 border (Kennedy et al., 1986).

Relationship of Callosal Cell Pattern to CO Stripes in V2

The callosal pattern we observed was characterized by numerous regularly spaced finger-like protrusions which originated from a more continuous distribution of labeled callosal cells at the V1/V2 border. These callosal fingers extended up to about 7 mm into V2, which is about 10-13 mm wide (Olavarria et al., 1989; Van Essen et al., 1990). Similar patterns of callosal cell distribution have been described in area V2 of squirrel monkeys (Gould et al., 1987; Cusick and Kaas, 1988) and owl monkeys (Newsome and Allman, 1980; Cusick et al., 1984).

We used spectral analysis techniques to quantitatively assess the degree of correlation between the distribution of callosal cells with the CO-density profiles in V2. This approach did not require the identification of the boundaries of CO stripes, which can be difficult to delineate unambiguously. Analysis of the distribution of callosal cells revealed that increases in the number of callosal cells occurred about every 1.6 - 2 mm, which is approximately the distance between thick and thin stripes (Shipp and Zeki, 1989b; Tootell and Hamilton, 1989; Olavarria et al., 1989; Van Essen et al., 1990). Since these increases in labeled cell numbers were spatially correlated with peaks in CO density, it could be inferred that fingers of callosal connections were in register with both thick and thin stripes. This was confirmed in cases in which CO stripes could be identified by their appearance.

Functional Implications:

Functional Streams

The stripe-like subregions in V2 have been related to three parallel functional pathways emanating from V1. One pathway originates from layer 4B in V1 and projects to thick stripes in V2, and to more distant areas V3 and MT

located in parietal cortex (DeYoe and Van Essen, 1985; Shipp and Zeki, 1985; Livingstone and Hubel, 1987; Felleman et al., 1988; Shipp and Zeki, 1989a,b). A second pathway connects CO blobs in V1 with thin stripes in V2, and a third pathway connects interblobs in V1 with interstripes in V2 (Livingstone and Hubel, 1984). Thin stripes and interstripes project separately to V4 (DeYoe and Van Essen, 1985; Shipp and Zeki, 1985; Zeki and Shipp, 1989; DeYoe et al., 1988; 1994; Van Essen et al., 1990), and from here these pathways extends to inferotemporal cortex (Desimone et al., 1980; DeYoe et al., 1994).

In recent years, several views have emerged regarding the role of these pathways in vision. One of these views is that the dorsal pathway passing through thick V2 stripes is mainly involved in visual motion analysis, while the ventral pathways passing through thin and interstripes in V2 are concerned with analysis of form and color (Ungerleider and Mishkin, 1982; Mishkin et al., 1983; Maunsell and Newsome, 1987; Livingstone and Hubel, 1987; DeYoe and Van Essen, 1988; Levitt et al., 1994a). Although the relationship of V2 CO-stripes to functional streams may be more subtle or complex (DeYoe and Van Essen, 1985; Schiller et al., 1990; Merigan and Maunsell, 1990; Peterhans and von der Heydt, 1993; Levitt et al., 1994a; Ferrera et al., 1994), there is general agreement that neurons with selective responses to visual attributes, such as color and motion, tend to cluster in different CO compartments in V2. For instance, direction-selective cells have been reported to be more prominent in thick stripes whereas color-selective cells are more prominent in thin stripes and in interstripes (DeYoe and Van Essen, 1985; Hubel and Livingstone, 1987; Levitt et al., 1994a). Also, cells in thin stripes apparently lack disparity tuning, whereas thick stripes contain a high proportion of cells responsive to binocular disparity, including true binocular cells (i.e. cells which only respond to stimulation of both eyes and which could be of particular importance for depth perception) (Hubel and Wiesel, 1970; Hubel and Livingstone, 1985, 1987).

This theoretical framework suggests that the correlation between callosal connections and CO stripes we found in V2 may be functionally significant. For instance, callosal connections associated with thick stripes may participate in the generation of disparity-selectivity found in some cells in these stripes. In addition, they may contribute to the ipsilateral portion of large direction- and velocity-selective surrounds that modulate responses to moving stimuli within the classical receptive fields of cells in V2 (Allman, Miezin and McGuinnes, manuscript in preparation, cited in Allman et al., 1985). These surrounds are analogous to those described more extensively in MT (Allman et al., 1985; Tanaka et al., 1986). As suggested by Desimone et al. (1993), large suppressive surrounds in MT may be mediated at least in part by callosal connections which are widely distributed in this area (Maunsell and Van Essen, 1983), but it is also conceivable that callosal influences exerted on thick stripes of V2 may reach area MT through the thick stripe-MT ipsilateral projection (DeYoe and Van Essen, 1985; Shipp and Zeki, 1985, 1989b).

On the other hand, thin stripes have been associated with color vision on the basis of their afferent and efferent connections and cell properties (Livingstone and Hubel, 1984; DeYoe and Van Essen, 1985; Shipp and Zeki, 1985; Hubel and Livingstone, 1987; Zeki and Shipp, 1989). The role of callosal connections originating from thin stripes may be homologous to the role of callosal connections in V4 (Desimone et al., 1993), an area thought to play an important role in color vision (Zeki, 1973, 1980; Schein and Desimone, 1990). In V4, callosal connections have been implicated in the creation of wavelength selective, suppressive surrounds that extend across the vertical meridian of the visual field (Desimone et al., 1993). Desimone and colleagues have speculated that one of the roles of suppressive surrounds in V4 is to mediate long-range context effects in the visual field such as color constancy. The fact that the perceptual phenomenon of color constancy requires an intact corpus callosum in

order to span the two hemifields (Land et al., 1983) supports the idea that it involves the callosal pathway. It is possible that callosal connections of thin stripes exert similar influences in V2 at the neuronal level. In addition, callosal influences on thin stripes may be relayed to V4 through ipsilateral thin stripe-V4 connections (DeYoe and Van Essen, 1985; Shipp and Zeki, 1985; Zeki and Shipp, 1989; DeYoe et al., 1988, 1994), where this input may contribute to the callosum-mediated surround effects that have been described in V4 (Desimone et al., 1993).

Segregation and Intermixing of Functional Streams

To what extent do functional streams remain segregated throughout the visual system? Evidence that the three classes of CO stripes identify a segregation of functional pathways comes from studies showing that thick stripes project to MT, while thin and interstripes project to separate compartments in V4 (DeYoe and Van Essen, 1985; Shipp and Zeki, 1985; 1989b; DeYoe et al., 1988; 1994; Zeki and Shipp, 1989; Van Essen et al., 1990). On the other hand, cross talk between streams appears to occur at several levels including V2. Indeed, studies of intrinsic connection in V2 have shown that all three stripe classes are interconnected, although there appears to be a tendency for CO-rich stripes to connect with other CO-rich stripes, while CO-poor compartments project more equally to CO-rich and CO-poor compartments (Livingstone and Hubel, 1984; Rockland, 1985; Levitt et al., 1994b; Malach et al., 1994; Olavarria and O'Brien, unpublished observations).

Our data indicate that the pattern of interhemispheric connections in V2 differs from the pattern of *intrahemispheric* cortico-cortical connections. While interstripes maintain intrinsic connections with other interstripes and neighboring CO-rich stripes, we found that, except for a narrow region at the V1/V2 border, interstripes are not callosally connected among themselves nor do

they send many projections to contralateral CO-rich stripes. Furthermore, although V2 has been shown to send direct callosal input to more anterior extrastriate areas (Kennedy et al., 1986; Dehay et al., 1986), our data suggest that interstripes do not project callosally to other extrastriate areas involved by the callosotomy, in particular area V4, which is a major target for *ipsilateral* projections from pale interstripes (DeYoe and Van Essen, 1985; Shipp and Zeki, 1985; Zeki and Shipp, 1989; DeYoe et al., 1988). Regarding thick and thin stripes, further studies are necessary to determine to what extent their contralateral projections to V2 and other visual areas contribute to the segregation and/or mixing of cortical streams.

Callosal Pattern and Visual Topography in V2

Callosal connections may be primarily concerned with the vertical meridian of the visual field (Choudhury et al., 1965; Hubel and Wiesel, 1967; Berlucchi et al., 1967). Support for this idea comes from reports indicating that some loci in V2 located as far as 5 mm from the V1/V2 border have receptive fields on or near the VM (Van Essen and Zeki, 1978). In this context, our results would suggest that receptive fields overlapping the VM would be more prevalent in CO-rich stripes than in interstripes, due perhaps to an increase in receptive field size or scatter, but this suggestion cannot be evaluated with available mapping data from this area (Van Essen and Zeki, 1978; Gattass et al., 1981; Rosa et al., 1988).

Alternatively, callosal connections in V2 may integrate information from regions in the ipsilateral hemifield away from the vertical meridian. Support for this idea comes from the report by Kennedy et al. (1985) indicating that in area V2 of the baboon there is a strip of cortex adjacent to the V1 border subserving receptive fields in the ipsilateral hemifield. Neurons with ipsilateral receptive field centers were found as far as 6 mm from the V1/V2 border.

The exact topography of callosal influences from beyond the vertical meridian ultimately depends on the organization of callosal linkages. Callosal fibers may link non anatomically-corresponding loci that represent similar visual field coordinates, as in lateral striate cortex of rats and cats (Lewis and Olavarria, 1995; Olavarria, 1995). Alternatively, callosal fibers may connect anatomically-corresponding loci representing receptive fields located on either side of the vertical meridian. In the latter case, excitatory callosal influences could lead to the assembly of large bilateral receptive fields whose ipsilateral component would be dependent on the callosal pathway, as is the case for the majority of neurons in inferotemporal cortex (Rocha-Miranda et al., 1975). On the other hand, inhibitory callosal influences could contribute to large silent surrounds exerting suppressive modulation of classical receptive fields close to the midline, as it occurs in V4 (Desimone et al., 1993) and MT (Allman et al., 1985).

Determining the fine organization of callosal connections in V2 will thus be an important step for understanding the functional role of this pathway, and efforts towards this goal are currently underway in our laboratory (Abel et al., 1995). Moreover, since the development of specific patterns of callosal linkages may depend on the nature of the cues leading to the stabilization of juvenile connections (Olavarria and Li, 1995; Olavarria, 1995), knowing the organization of callosal linkages in macaque V2 may also help us to identify factors guiding the development of callosal connections in this extrastriate area (Dehay et al., 1988).

Figure 6: V2-CC (777RV).

A. Reconstruction of HRP-labeled callosal pattern from tangential sections through right ventral V2 in monkey 777. Dots indicate single HRP-labeled cells. Arrows indicate position of CO-dense stripes (see B); posterior is to the left, dorsal is up. The border of V1 (visible in neighboring CO-stained section shown in B) is indicated by thin line to the left. **B**. Pattern of CO staining. Arrows indicate position of CO-dense stripes. Wide stripes (T) alternate with thin stripes (t), presumably corresponding to the arrangement of thick and thin CO-stripes described previously in monkey V2 (see text for references). **C**. Superimposition of the callosal and CO patterns. **D.** Spectral and coherence analysis of callosal and CO labeling patterns. The area analyzed quantitatively (between dashed lines in Fig. 6C) measured 13.5 mm in the direction parallel to the V1/V2 border. The solid curve represents the distribution of labeled cells, while the dashed curve indicates the density profile for CO staining. Scale bar = 2.0 mm.

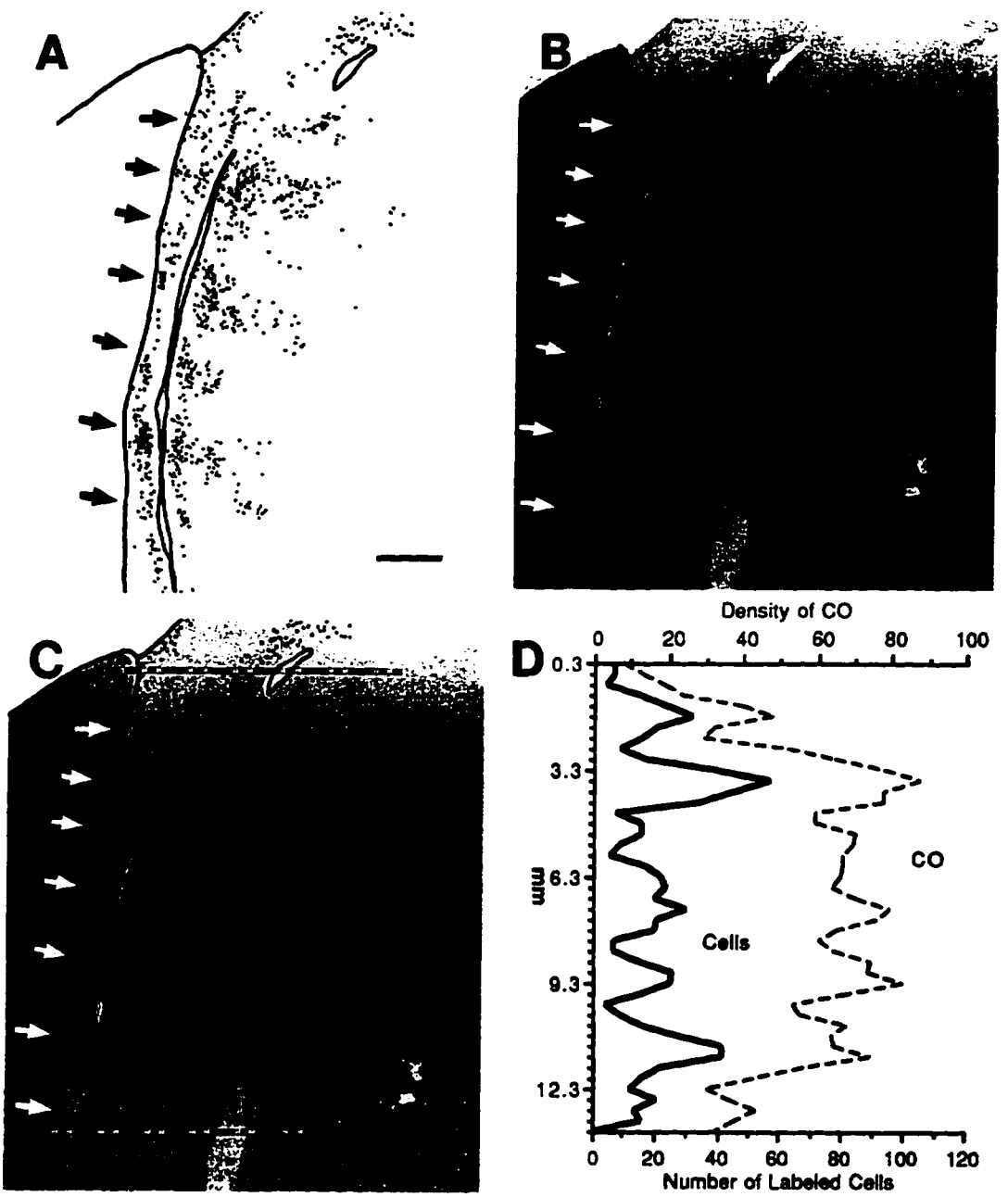
A
B
C
D
Density of CO
0
20
40
60
80
100
0.3
3.3
6.3
9.3
12.3
mm
CO
Cells
0
20
40
60
80
100
120
Number of Labeled Cells

Figure 7: V2-CC (777RD).

Data from right dorsal V2 from the same animal shown in Figure 6. **A**. Reconstruction of callosal pattern; posterior is to the left, dorsal is up. The thin line indicates a fissure in the tissue, while the dashed lines indicate area analyzed quantitatively. **B**. The solid curve represents the distribution of labeled cells, and the dashed curve indicates the density profile for CO staining. **C**. Photomontage of HRP-labeled cells from one of the sections used to reconstruct the callosal pattern shown in A. These cells belong to the finger-like cluster indicated with an arrow in A. Arrows in C indicate some retrogradely-labeled cells. Scale bar in A = 2.0 mm; in C = 0.2 mm.

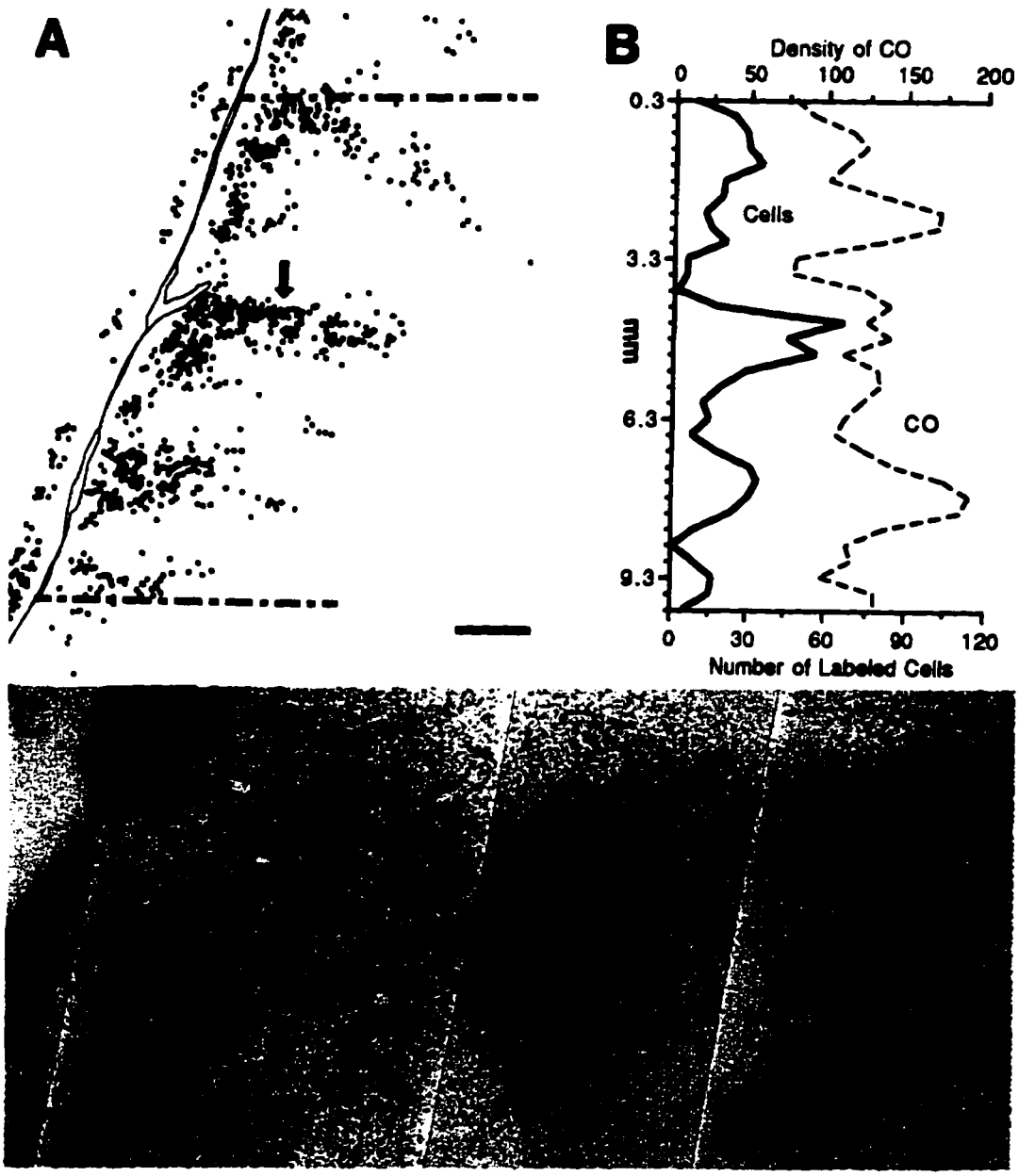
A
B
Density of CO
0
50
100
150
200
0.3
3.3
6.3
9.3
mm
Cells
CO
0
30
60
90
120
Number of Labeled Cells

Figure 8: V2-CC (428RD, 4134 RD).

A-B. Data from monkey 428 studied with HRP. **A.** Reconstruction of callosal pattern from tangential sections through dorsal V2 in the right hemisphere. The dashed lines indicate area analyzed quantitatively. Posterior is to the left, dorsal is up. **B.** The solid curve represents the distribution of labeled cells, and the dashed curve indicates the density profile for CO staining. **C-D.** Data from monkey 4134 injected with NY. **C**. Reconstruction of callosal pattern from tangential sections through right dorsal V2. The thin lines represent the borders of the tissue block, while the dashed lines indicate the area analyzed quantitatively. Posterior is to the left, dorsal is up. **D**. The solid curve represents the distribution of labeled cells, and the dashed curve indicates the density profile for CO staining. Scale bar = 2.0 mm.

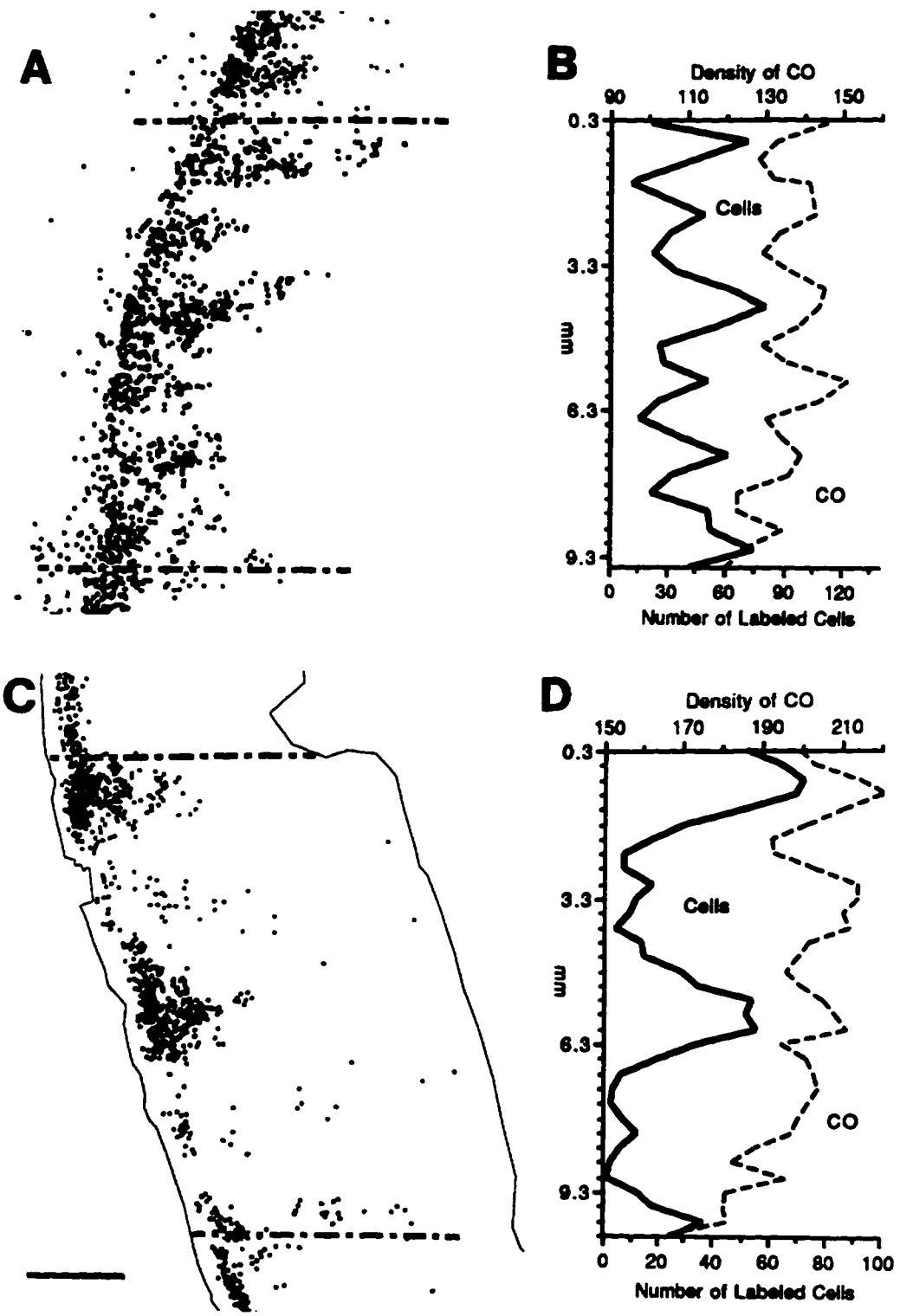
A
B
Density of CO
90
110
130
150
0.3
3.3
6.3
9.3
mm
Cells
CO
0
30
60
90
120
Number of Labeled Cells
C
D
Density of CO
150
170
190
210
0.3
3.3
6.3
9.3
mm
Cells
CO
0
20
40
60
80
100
Number of Labeled Cells

CHAPTER 3: THE ORGANIZATION OF CALLOSAL LINKAGES IN VISUAL AREA V2 OF MACAQUE MONKEY.

Interhemispheric connections are commonly thought to link cortical regions with midline representations. In visual cortex, early anatomical studies found that callosal connections accumulated along the border between visual areas (Mettler, 1935; Myers, 1962; Ebner and Myers, 1965; Myers, 1965; Cragg, 1969; Zeki, 1969, 1970). Further, physiological studies provided data that receptive fields of callosal cells overlap the representations of the vertical meridian (Choudhury et al., 1965; Whitteridge, 1965; Berlucchi et al., 1967, Hubel and Wiesel, 1967; Berlucchi and Rizzolatti, 1968; Shatz, 1977).

However, this 'vertical meridian rule' (Berlucchi, 1981) is not entirely consistent with the results from more recent studies. Owing to the use of more sensitive anatomical methods and to the increase in the number of visual areas which have been identified in visual cortex, callosal connections now appear to extend substantially *within* nearly every visual area (e.g., Van Essen et al., 1982). In fact, in some visual areas such as area MT and V4, callosal connections are found throughout much of the tangential extent of these regions (Van Essen et al., 1982; Cusick et al., 1984; Maunsell and Van Essen, 1987). These findings suggest that callosal connections are not exclusively associated with midline representations (e.g., Segraves and Rosenquist, 1982a,b; Cusick et al., 1984; Cusick et al., 1985).

Determining the functional contribution of these widespread callosal connections will in part depend upon revealing their topography. Do callosal connections randomly link portions of an area with loci in the contralateral area, or do specific patterns exist in the organization of these connections? In the rat

and cat recent studies have found that callosal connections link anatomically non-corresponding loci between the area 17/18 border regions. This pattern of callosal connections may serve to interlink overlapping representations of visual space (Lewis and Olavarria, 1995; Olavarria, 1996). On the other hand, anatomically corresponding callosal connections could provide links between visual field representations located on opposite sides of the midline. Evidence for this pattern of callosal connections has been found in medial portions of area 17 in the rat and in extrastriate cortex in the cat (Segraves and Rosenquist, 1982b; Lewis and Olavarria, 1995). There have been reports in the primate that callosal connections link anatomically corresponding loci within extrastriate cortex (Myers, 1961, 1965; Zeki, 1969; Tigges et al., 1974; 1981; Spatz and Kunz, 1984; Maunsell and Van Essen, 1983, 1987). However, the data in primates are quite limited and many regions within extrastriate cortex have not been examined.

In the present study, we examined the organization of callosal linkages in visual area V2 of macaque monkey. In macaque monkey, few callosal connections are found within area V1, although in area V2 they have been shown to be widespread (Myers, 1962; Zeki, 1970; Lund et al., 1975; Van Essen et al., 1982; Kennedy et al., 1986; Olavarria and Abel, 1996). Callosal connections accumulate in V2 at the border with V1 and within finger-like projections which extend up to 8 mm from the V1 border (Olavarria and Abel, 1996), about half way across the anterior-posterior width of V2 (Weller and Kaas, 1983; Van Essen et al., 1990; Olavarria and Van Essen, 1997). Whether callosal connections in V2 link anatomically corresponding or non-corresponding regions is not known.

Relative to other visual areas, V2 offers several advantages for this type of analysis. The organization of callosal linkages can be compared with the topography of the visual field map more readily in V2 than other extrastriate areas; receptive fields are smaller and there appears to be less scatter in the

visual field map (Van Essen and Zeki, 1978; Gattass et al., 1981; Roe and T'so, 1995). In addition, the functional organization and development of callosal connections are better understood in V2 than in other extrastriate areas (Dehay et al., 1986; Kennedy et al., 1986; Dehay et al., 1988; 1989; Chalupa et al., 1989; Olavarria and Abel, 1996). Finally, the organization of callosal linkages in other species has been examined along the V1/V2 border (Lewis and Olavarria, 1995; Olavarria, 1996) allowing for comparisons to be made with the pattern of callosal linkages along the V1/V2 border in the macaque.

In order to reveal the pattern of callosal linkages, retrogradely-transported tracers were injected into area V2 at a distance from the V1 border that varied between injection sites. The resulting distributions of labeled cells in contralateral V2 were compared between different tracers with respect to the location of their injection sites. We found that the location of labeled cells in contralateral V2 varied as a function of the location of injection sites. Labeled callosal cells were found to preferentially accumulate in anatomically corresponding locations, relative to the location of the contralateral injection site. These findings suggest that disparate representations of the visual field are linked between areas V2. Some of these data have been presented previously (Abel et al., 1995).

MATERIALS AND METHODS

Five adult monkeys (4 *Macaca fascicularis*, 1 *Macaca nemestrina*) weighing 3-6 kg, were used in this study. Surgery was performed aseptically under general anesthesia induced with ketamine (0.10 mg/kg i.m.) and maintained with Halothane (1.5-3.0%). During the surgery, a craniotomy was made over portions of the lunate, intraparietal and superior temporal sulci in one hemisphere and portions of the dura matter were retracted. A portion of the

prelunate gyrus was removed by subpial aspiration in order to visualize regions of V2 buried in the lunate sulcus.

The fluorescent tracers Bisbenzimide (10% BB in dH_2O) or Nuclear Yellow (5% NY in dH_2O) were injected into area V2 either within the dorsal surface of the operculum or the posterior bank of the lunate sulcus (see Fig. 9). Each injection site was made approximately 1.0 mm under the cortical surface and a total of about 0.2μl of tracer was injected. Some injections were found to extend into the white matter. Each tracer was injected in multiple sites at the same distance from the V1/V2 border. The total volume of each tracer injected did not exceed 1.0 μl per animal. Near the end of the surgery, unilateral intravitreal injections of horseradish peroxidase (50-60 μl of 30% HRP in saline, Sigma Type VI), were performed in each *Macaca fascicularis*, as a part of a separate experiment.

After a 3-4 day survival period, to allow for retrograde transport of tracers, animals were deeply anesthetized with pentobarbital (0.40 mg/kg i.v.) and perfused transcardially with 0.9% saline followed by a fixative solution containing 2% paraformaldehyde and 0.25% glutaraldehyde in 0.1 M phosphate buffer. All surgical procedures were performed in accordance with NIH guidelines (NIH publication 85-23) and according to protocols approved by the U.W. Animal Care Committee (IACUC).

Histochemical Processing

Brains were blocked in the coronal plane and the hemispheres were separated from the brainstems. In three animals, the hemispheres were physically unfolded and flattened according to procedures described previously (Olavarria and Van Sluyters, 1985). In the other two animals the hemispheres

were analyzed in parasagittal sections. Brainstems were analyzed in transverse sections.

Unfolded and flattened tissue was kept between glass slides for about 12 h at 4^0 C in 0.1 M phosphate buffer. The glass slides were then removed and the block of tissue was placed in 20% sucrose in fixative for approximately thirty minutes. The tissue was then transferred to a solution of 20% sucrose in phosphate buffer at $4\ ^0$C until it sank. The remaining cortical hemispheres and brainstems were kept in 20% sucrose in fixative at $4\ ^0$C until they sank. All tissue blocks were sectioned at 40-50 μm on a freezing microtome.

Sections from the flattened tissue blocks were mounted onto glass slides, air-dried, and immediately scored for labeled cells/injection sites using fluorescent microscopy. These sections were then removed from the slides and processed for cytochrome oxidase (Wong-Riley, 1979) to reveal the location of the V1/V2 border, or processed for Cat-301 immunohistochemistry to aid in the identification of CO-stripes (Hendry et al., 1988; DeYoe et al., 1990; Abel et al., 1997; Olavarria and Van Essen, 1997). In each block, a few sections were processed for cytochrome oxidase without being scored to reveal the pattern of CO stripes in tissue that had not been exposed to the fluorescent illumination. Every fourth parasagittal and transverse section (200 μm interval), was mounted onto subbed slides and scored for labeled cells/injection sites. These sections were then stained for Nissl substance. One additional series of sections from the brainstems was immunostained for the calcium binding protein calbindin-D28k (Sigma) and a second was reacted for HRP (Mesulam, 1978),

Data Analysis

Histological sections were scored using a microscope equipped with a motorized stage controlled by a Gateway 2000 486/33c computer, and the

graphic system Neurolucida (MicroBrightField). Reconstructions of the distribution of labeled cells in flattened tissue blocks were prepared by carefully superimposing all tangential sections containing labeled cells, using blood vessels, tissue contours and the V1/V2 border as landmarks. Computerized 3-dimensional reconstructions of the distribution of labeled cells in the pulvinar were prepared by aligning sections in serial order using tissue contours, differential staining for calbindin (Gutierrez et al., 1995) and blood vessels as landmarks.

In order to infer the pattern of V2 callosal linkages, deriving accurate estimates of the size of V2 injection sites was important. In the cortex, the boundaries of intense fluorescent label and diffuse fluorescent halo were plotted. Sections were inspected to determine whether pipette tracks extended into the white matter and the possible extent of fluorescent label beneath the cortex. In addition, the locations of labeled cells in ipsilateral V1, LGN, and the pulvinar nucleus were analyzed. Because of the high intensity of the fluorescent halo for injections close to the V1/V2 border, not all retrogradely-labeled cells in V1 could be plotted following these injections.

We interpreted the following as indications of tracer uptake by fibers of passage: pipette tracks that extended into the white matter, intense fluorescent label located below the cortex, labeled cells found scattered across the LGN, and large clusters of labeled cells found within the pulvinar. All of these conditions were met for the BB injections in animal mf-09. These injections resulted in callosal labeling which closely approximated the entire callosal pattern (see Fig. 10,11; Olavarria and Abel, 1996). In animal mf-13, the lateral NY injection was also found to spread diffusely into the white matter, as described below. The data from the remaining injections did not meet these criterion and considered to be largely devoid of this potential confound.

QUANTITATIVE ANALYSIS

After CO or Nissl staining, the V1/V2 border was plotted onto drawings of each section and area V2 was divided into strips 200 μm wide oriented parallel to the V1/V2 border. In parasagittal sections, strips were marked at the bottom of layer 4 and extended to the cortical surface. The number of cells found within each strip was counted and summed within corresponding strips between sections. In order to facilitate comparisons, the total number of labeled cells found within each strip was expressed as a percent of the total population of labeled cells.

RESULTS

In the hemisphere contralateral to the V2 injection sites, most labeled callosal cells were found in lower layer 3. Relatively few callosal cells were found in V1. However, when present, the number of labeled cells found was greater and their tangential distribution more widespread in lateral than in medial portions of V1. In addition to finding labeled cells in V2, callosal cells were also found within the annectant gyrus, on the posterior bank of the prelunate gyrus, in addition to extending down the posterior bank of the superior temporal sulcus. These observations are in agreement with results obtained previously in the macaque monkey (Lund et al., 1975; Van Essen et al., 1982; Kennedy et al., 1986; Olavarria and Abel, 1996).

We found that the location of labeled callosal cells in V2 varies as a function of the location of contralateral V2 injection sites. These results will be presented first from data in which two tracers were injected in the same animal at different locations within V2. Data in which one tracer was injected in different locations between animals will then be presented.

PAIRED INJECTION PARADIGM

NY and BB injections were made into animal mn-18. The data from this animal were analyzed in sections cut tangential to the unfolded and flattened cortical surface. The NY injection sites were made away from the V1 border within V2. The center of these injections was located 2 mm from the V1 border in V2. Intense fluorescent label extended medio-laterally 1 mm in diameter about the injection sites (see dark gray outlines Fig. 10A). In sections cut through lower cortical layers, both the size of the fluorescent region and intensity of the tracer were reduced, confirming that the tracer did not extend into the white matter.

In the ipsilateral hemisphere, NY-labeled cells were found in a single field within V1. This field of labeled cells extended as far as 4.5 mm from the V1 border in a fan-like pattern within V1 (see black dots Fig. 10A). The total number of NY-labeled cells in V1 approaching the V1 border was likely underestimated due to the prominence of the BB fluorescent halo. Regardless, the small size of the labeled field in V1 suggests that these injections were quite restricted. In addition, the presence of labeled cells within V1 away from the V1 border confirms that the tracer uptake zone was located away from the V1/V2 border in V2 (Zeki, 1969; Rockland and Pandya, 1979; Weller and Kaas, 1983; Perkel et al., 1986; Stepniewska and Kaas, 1996). Significant uptake within fibers of passage from these injections appeared unlikely. Few NY-labeled cells were found in the pulvinar nucleus. The largest patch of cells measured only 0.04 mm^2 in cross-sectional area and no NY-labeled cells were found in the LGN.

In the contralateral hemisphere, the proportion of NY-labeled cells that were found in V1 or near the V1/V2 border in V2 was quite low. Further away from the V1 border in V2 the number of labeled cells increased and formed three finger-like clusters oriented orthogonal to the V1 border (see black dots Fig. 10B). As illustrated in Figure 10B, the density of NY-labeled callosal cells was

maximal in regions of V2 located away from the V1 border. These data are in contrast with the overall distribution of callosal cells in V2, which are maximal near the V1/V2 border. The distribution of NY-labeled callosal cells was also quite different from the distribution of BB-labeled cells. The data from the NY injection would be consistent with an anatomically corresponding pattern of callosal connections.

BB injections were made in animal mn-18 adjacent to the V1/V2 border. The center of these injections was located on the V1/V2 border (see light gray outlines, Fig. 10A). The prominence of the fluorescent halo precluded the ability to score retrogradely-labeled cells in ipsilateral V1 along the V1/V2 border, where they would have been expected (Zeki, 1969; Rockland and Pandya, 1979; Weller and Kaas, 1983; Perkel et al., 1986; Stepniewska and Kaas, 1996). Nonetheless, no BB-labeled cells were found outside of this fluorescent halo. In sections from lower cortical layers pipette tracts from all but the most medial injection remained. However, the intensity of the label was reduced in these sections relative to those taken from superficial layers. In the pulvinar the largest patch of labeled cells measured only 0.69 mm^2. Within the LGN labeled cells were found in posterior portions regions along an arc about the medial edge of the nucleus, corresponding to representations about the vertical meridian (Malpeli and Baker, 1978; Connolly and Van Essen, 1984). These data suggest that the tracer did not spread substantially away from the injection sites.

In the contralateral hemisphere, labeled cells in V2 accumulated in a continuous medio-lateral stripe close to the V1 border, and within the three finger-like clusters which extended across V2 (see gray dots Fig. 10B). The majority of BB-labeled callosal cells accumulated near the V1 border in V2. These data would also be consistent with an anatomically corresponding pattern of callosal connections in V2.

In order to compare these data quantitatively, the number of labeled callosal cells found within V2 were counted with respect to their distance from the V1 border. The resulting distributions of labeled cells agree quite closely with the observations from tangential sections. The density of labeled BB cells peaked close to the V1 border in V2 (at 0.8 mm). whereas the density of NY-labeled cells peaked away from the V1 border in V2 (at 2.0 mm). The dip in the density of labeled cells found about 1.0 mm from the V1 border is artifactual, due to a tear in the V2 tissue block. Comparing between the distributions of labeled cells, reveals that the majority of labeled cells in V2 were found at a similar distance from the V1 border to the location of their contralateral injection sites.

The results from animals in which the cortex was sectioned parasagittally were consistent with those found in the data collected in sections cut tangential to the cortical surface. In the lateral portion of V2 in animal mf-19, two injections were made. NY was injected on the V1/V2 border and an intense fluorescent halo extended 0.2 mm within V2. BB was injected 0.4 mm from the V1 border in V2, from which a 0.4 mm diameter intense halo extended, partially overlapping the NY halo. Neither of the pipette tracks extended into the white matter, although intense fluorescent label was present below the cortex. In the pulvinar, the largest patch of NY labeled cells measured 0.08 mm^2 and the largest BB cluster was 0.98 mm^2. Because not all of the data from the brainstem could be analyzed, the amount of labeling in the LGN remains uncertain. However, the small size of labeled cell clusters in the pulvinar suggests that the amount of uptake into fibers of passage was not significant.

In contralateral V2, both NY and BB labeled cells were found within sections from lateral portions of V2. The NY injection made on the V1/V2 border, which had spread 0.2 mm from the V1 border in V2, resulted in a restricted distribution of labeled cells. NY-labeled cells in V2 extended up to only 2.2 mm from the V1 border. The peak density of labeled cells was found 0.4 mm from the

V1 border. The lateral BB injection, which extended 0.8 mm away from the V1 border in V2, resulted in a slightly more widespread distribution. BB-labeled cells were found up to 3.2 mm away from the V1 border in contralateral V2. The peak density of BB labeled cells was located 0.8 mm from the V1 border (see Fig. 12). Similar to the data from sections analyzed in unfolded and flattened corticies, these data demonstrate a predominance of labeled callosal cells in anatomically corresponding locations within V2, relative to the location of the contralateral injection sites.

SINGLE INJECTION PARADIGM

The data from single-tracer injections was consistent with the data from the double-tracer injection paradigm. Restricted injections of either NY or BB resulted in labeled callosal cells whose density peaked in anatomically corresponding locations relative to the injection sites.

In animal mf-16, two NY-injections in V2 were made close to the V1 border. These data were analyzed in sections cut tangential to the cortical surface. The center of the injection sites was located about 1mm from the V1 border and the intense fluorescent halo was about 0.6 mm in diameter. These injections were made on the surface of the dorsal operculum, and were separated medio-laterally by about 5 mm (see Fig. 13A). Both the size and intensity of the fluorescent labeled regions decreased between sections from superficial to deep cortical layers. No pipette tracks could be seen in sections from the deepest layers indicating that the tracer did not extend into the white matter. Retrogradely-labeled cells could not be scored in V1 owing to the NY halo which overlapped the adjacent V1/V2 region where labeled cells would have been expected (Zeki, 1969; Rockland and Pandya, 1979; Weller and Kaas, 1983; Perkel et al., 1986; Stepniewska and Kaas, 1996). In the pulvinar nucleus, the

largest patch of labeled cells measured 0.72 mm^2 in cross-sectional area. Fifteen NY-labeled cells were found in the LGN, near it's medial edge.

In contralateral V2, no labeled cells were found in V1. Labeled cells accumulated slightly anterior to the V1 border within V2, closely matching the location of the intense fluorescent label about the injection sites. Medially, a nearly continuous strip of labeled cells was found along the medio-lateral axis. The restricted distribution of labeled cells in the anterio-posterior plane was more pronounced in these data relative to those found in other animals. Few NY labeled callosal cells were found more than 1 mm from the V1 border in V2, and labeling was nearly absent beyond 2 mm (see Fig. 13B). Similar to the data from other animals, the majority of labeled cells were located at a distance from the V1 border in right V2 which closely matched the location of tracer spread about the injection sites in left V2.

In one animal (mf-09) two large injections of BB were made in V2 along the V1/V2 border extending into the white matter which revealed the entire callosal pattern. In addition, two small injections of NY were made away from the V1 border in V2. The center of the NY injections was located about 3 mm from the V1 border, about which an intense fluorescent halo extended about 1 mm. The reconstruction of the NY injection sites is illustrated in Figure 14A. Because the injections were not made orthogonal to the cortical surface, pipette tracts shifted slightly across sections leading to oval-shaped injection sites in the reconstruction. The possibility that some tracer spread into the white matter cannot be ruled out. In sections cut from the deepest layers, the pipette tract from the lateral injection was present. However, the size and intensity of the fluorescent labeling found about this tract was minimal.

Retrograde labeling found in ipsilateral V1 and the thalamus suggested that these injections were restricted to V2. In ipsilateral V1, two fields

of NY-labeled cells were found roughly corresponding to mirror image locations from the V2 injection sites (see black dots in Fig 14A). Labeled cells were found to be scattered over a wider portion of V1 in the lateral field, than the cells found in the medial field. Because the amount of labeled cells in V1 were similar between these fields, this difference did not seem to be due to a greater tracer uptake in the lateral V2 injection. Nonetheless, the distribution of the labeled cells within V1 agrees with previous studies which have shown a topographical organization in the pattern of V1-V2 projections (Zeki, 1969; Rockland and Pandya, 1979; Weller and Kaas, 1983; Perkel et al., 1986; Stepniewska and Kaas, 1996). Owing to the V1/V2 border region in this animal had received BB injections (data not shown), some NY labeled cells located along the V1/V2 border may not have been recovered. The largest patch of NY-labeled cells in the pulvinar measured 0.29 mm^2 in cross-sectional area, which is considerably smaller than the 1.8 mm^2 patch observed for BB-labeled cells. No NY-labeled cells were found in the LGN.

In the contralateral hemisphere a widespread pattern of BB-labeled cells was found (see gray outline in Fig. 14B). The resulting pattern of callosal fingers was found to correlate with cytochrome oxidase dense thick and thin stripes as reported previously (Olavarria and Abel, 1996). In contralateral V2, a small number of NY-labeled cells were found (see black dots, Fig. 14B). A few of these labeled cells were found in V2 within 0.2 mm of the V1/V2 border. The majority of NY- labeled cells was found near the end of the callosal fingers revealed with BB. Because the overall callosal pattern in V2 can be characterized by a negative exponential function (PL Abel, BJ O'Brien, JF Olavarria, unpublished observations), the random probability of finding any cell located away from the V1 border is extremely low. For this reason, finding proportionately more labeled cells located away from the V1 border in a small sample further supports the notion that the pattern of callosal linkages is not diffuse.

The quantification of the data from the BB injections in animal mf-16 and the NY injections in mf-09 provide further evidence for an anatomically corresponding pattern of callosal connections in V2. As shown in Figure 15, the peaks in the distributions of labeled cells within each animal closely corresponded to the location of the contralateral injection sites. In addition, these distributions were quite dissimilar between the tracer-injections made in different locations in V2, between animals.

Finally, we present additional data from two animals in which the data were analyzed in the parasagittal plane. In the medial portion of V2 in animal mf-19, a BB injection was made 0.4 mm from the V1 border about which an intense fluorescent halo extended 0.8 mm (Fig. 16A). In animal mf-13, a NY injection was centered 1.2 mm from the V1 border, about which an intense fluorescent halo extended 0.6 mm. Neither the pipette tracks, nor intense fluorescent label was found in the white matter underlying these injections. Similar to the data presented previously, the distributions of V2 labeled cells from both injections peaked at a distance from the V1 border which corresponded to the location of the contralateral injection sites (see Fig. 16B).

DISCUSSION

The results indicate that the pattern of callosal linkages in V2 is not diffuse. We found that the location of labeled cells in contralateral V2 varied as a function of the location of our injection sites. Injection sites located away from the V1 border in V2 resulted in accumulations of labeled callosal cells that were located away from the V1 border in contralateral V2 (Fig. 11B, 12B, 15B, 16B). V2 injection sites placed close to the V1 border, resulted in accumulations of labeled cells that were located close to the V1 border in contralateral V2 (Fig. 11A, 12A, 15A, 16A). These findings are consistent with the idea that callosal

connections in V2 preferentially link anatomically corresponding regions between the hemispheres.

Our results confirm and extend the results from previous anatomical studies. Myers (1961, 1965) reported that small lesions made within "juxtastriate" cortex produce degeneration in homologous regions in the opposite hemisphere. Subsequent studies in V2 using degeneration staining (Zeki, 1969; Tigges et al., 1974) or horseradish peroxidase (Tigges et al., 1981; Spatz and Kunz, 1984) techniques reported similar observations. However, because the extent of callosal connections in V2 had not been appreciated, previous studies were not aimed at systematically addressing this issue throughout the width of the callosal region in V2. As a result, the data from these experiments include only the strip of V2 located on the dorsal operculum which contain callosal connections. Moreover, much of the previous data were obtained from relatively insensitive methods (degeneration staining) or an approach which was not well suited to examine this issue (large injection sites).

Methodological Considerations

Before discussing the potential importance of these results, the accuracy of our method for revealing the organization of callosal linkages should be considered. Our choice of NY and BB for the retrograde tracers was advantageous for several reasons. Distinct from other fluorescent tracers NY and BB require similar survival periods and they exhibit similar transport properties (Kuypers et al., 1979; Bentivoglio et al., 1980a; 1980b). In addition, these tracers are as effective as horseradish peroxidase in characterizing the overall distribution of callosal connections in V2 (Olavarria and Abel, 1996; PL Abel, BJ O'Brien, JF Olavarria, unpublished observations).

Nonetheless, these tracers can be picked up by damaged fibers (Sawchenko and Swanson, 1981; Talyor et al., 1983; Olavarria and Abel, 1996; however see Illert et al., 1982). This raises the possibility that some of the retrogradely labeled cells we found may have resulted from leakage of the tracers into fibers which terminate outside of the injection sites. For example, V2 callosal projections have been shown to extend to the prelunate gyrus (Kennedy et al., 1986). By aspirating this gyrus, in order to reach buried portions of V2, our approach could have resulted in inadvertent update of tracers by callosal cells projecting from V2 to V4.

Although this possibility cannot be ruled out, we do not believe that the pattern of callosal linkages observed in V2 could have resulted from this potential confound. The spread of two different tracers into damaged axons would not likely have resulted in finding anatomically separate labeled fields in contralateral V2. In addition, tracer injections made in V2 away from the V1 border would be the most accessible to damaged V2-V4 callosal fibers. Indeed, it is the results from these injections that revealed the most dramatic restriction of labeled callosal fields to anatomically corresponding regions of area V2 (e.g., Fig. 10). Moreover, when the prelunate gyrus was injected in a separate experiments, equivalent results were not obtained (PL Abel, BJ O'Brien, JF Olavarria, unpublished observations).

Callosal Connections and Visual Topography in V2

The data from early anatomical studies suggested that callosal connections are restricted to the borders between visual areas. In the macaque monkey, degenerating callosal fibers were found to be largely restricted in their tangential extent to within 2 mm of the area 17/18 border (Mettler, 1935; Myers, 1962, 1965; Zeki, 1969, 1970, Van Essen and Zeki, 1978). Because this border region was found to represent the vertical meridian (Talbot and Marshell, 1941;

Daniel and Whitteridge, 1961), these data supported the idea that only midline representations are relayed through callosal connections. Further support for this notion was provided by the experiments of Zeki and colleagues. In their studies, callosal labeling was found to accumulate in the same regions in which receptive fields were found to be located about the vertical meridian (Zeki and Sandman, 1976; Van Essen and Zeki, 1978).

However using more sensitive anatomical methods, callosal connections have now been shown to be widely distributed within V2. Callosal connections accumulate at the border with V1 as well as within finger-like projections which extend up to 8 mm from the V1 border (Van Essen et al., 1982; Kennedy et al., 1986; Olavarria and Abel, 1996; present results), about half of the anterior-posterior width of V2 (Weller and Kaas, 1983; Van Essen et al., 1990; Olavarria and Van Essen, 1997). Although representations of the vertical meridian have been found in V2 as far as 5mm from the V1 border (Van Essen and Zeki, 1978), midline representations are not commonly thought to extend within bands projecting across V2. Thus, the distribution of callosal connections within V2 may not be consistent with the vertical meridian rule.

Based on the results of previous mapping studies, an orthogonal progression from the V1/V2 border across V2 would be expected to cross cortical representations of the visual field along an isoeccentricity line moving from the vertical to the horizontal meridians (Gattass et al., 1981; Roe and T'so, 1995). Accordingly, callosal cells located on the V1/V2 border likely respond to stimuli located about the midline. Callosal cells located away from the V1 border would be expected to respond to visual stimuli that are located away from the vertical meridian (see Fig. 17). Nonetheless, the relationship between the V2 map described in previous studies and the distribution of V2 callosal connections might not be this simple. Recent work suggests that multiple interleaved maps exist within each stripe-like compartment in V2 orthogonal to the V1 border (Roe

and Ts'o, 1995). Whether multiple representations of the midline extend across V2 associated with the distribution of callosal connections remains to be examined.

The possibility that callosal connections contain representations of the visual field located away from the midline is consistent with our data. Localized tracer-injections made in V2 away from the V1 border which resulted in labeled cells in contralateral V2, also resulted in labeled fields in V1 located away from the V1 border (Fig. 10,14). Labeled cells in V1 were found beyond the regions where the vertical meridian is represented (Talbot and Marshell, 1941; Daniel and Whitteridge, 1961; Van Essen et al., 1984). Whether labeled cells may have also been located along the representation of the vertical meridian in V1 could not be determined because of the presence of intense fluorescent labeling from the second tracers injected on top of the V1/V2 border. Nonetheless, these data demonstrate that callosal connections are found in regions of V2 which receive input from V1 cells whose visual fields are located off the vertical meridian. By extension, callosal cells in these regions would be expected to contain representations of visual space located away from the midline.

According to this idea, our findings suggest that V2 callosal connections link non-retinotopically corresponding sites. Portions of V2 located along the V1/V2 border containing representations of the vertical meridian would be interlinked between the hemispheres. In addition this region would also receive input from contralateral representations located away from the vertical meridian. Anterior portions of V2 located away from the V1 border containing representations away from the vertical meridian would be also interlinked. The vertical meridian rule could still be supported in this model, if the visual fields of the callosal cells always include the midline, independent of the location of their receptive field centers. Support for this idea has come from studies in the cat

(Sanides and Albus, 1980; Antonini et al., 1983), however cells with unusually large receptive fields have not been reported in previous physiological studies of V2 in Macaque (e.g., Gattass et al., 1981; Roe and Ts'o, 1995).

FUNCTIONAL IMPLICATIONS

If V2 callosal connections serve to link representations of the visual field located away from the midline, then stimuli within the *ipsilateral* visual field relayed through callosal connections would be expected to effect the responses of V2 cells. Consistent with this idea, ipsilateral visual fields have been found within V2 (e.g., Van Essen and Zeki, 1978; PL Abel, BJ O'Brien, JF Olavarria, unpublished observations). In addition, the suggestion has been made that a continuous representation of the ipsilateral field exists along the V1/V2 border (Kennedy et al., 1985), overlapping the callosal-dense region in V2. The idea that callosal connections can drive visual field responses of cells is supported by earlier studies in the cat. In this species, callosal connections within the area 17/18 region have been reported to mediate visual field responses following optic tract section (Choudhury et al., 1965; Whitteridge, 1965), in addition to mediating binocular responses in the split chiasm preparation (Berlucchi and Rizolatti, 1968; Lepore and Guillemot, 1982). Collectively, these data support the idea that V2 callosal connections located along the V1 border in the macaque are important in mediating ipsilateral representations.

On the other hand, ipsilateral visual fields could also be accounted for by the naso-temporal overlap in the retino-fugal projections (Stone et al., 1973; Bunt et al., 1977; Leventhal et al., 1988; Fukuda et al., 1989; Chalupa and Lia, 1991). Responses to stimuli within the ipsilateral visual field have been found in the LGN (Malpeli and Baker, 1978) and adjacent to the V1/V2 border within V1 (Van Essen et al., 1984). In fact, the ipsilateral visual fields observed by Van Essen and Zeki (1978) in V2 were found *after* the callosum had been sectioned.

The possibility that callosal connections mediate ipsilateral visual fields away from the V1 border in V2 appears even less probable. Callosal connections have been found to lie in spatial register with CO-dense stripes (mn-09, present study; Olavarria and Abel, 1996). However, previous studies have not reported that receptive fields in these regions preferentially include the vertical meridian or extend into the ipsilateral field (Hubel and Livingstone, 1987; Perterhans and von der Heydt, 1993, Levitt et al., 1994; Munk et al., 1995; Yoshioka and Dow, 1996; Gegenfurtner et al., 1996). Moreover, a recent analysis of the visual field representation within different V2 compartments failed to reveal a difference between the amount of receptive field scatter, receptive field size, or cortical magnification factor between different V2 compartments (Roe and Ts'o, 1995).

Perhaps a more likely role of callosal linkages in V2 is to mediate 'silent' surround regions. Accordingly, stimuli presented within portions of the ipsilateral visual field would modulate the responses of cells to stimuli presented within their contralateral receptive fields. The presentation of visual stimuli outside of the classical receptive field (CRF) of cells has been shown to effect the response properties of cells to stimuli within their CRF (e.g., Rizzolatti and Camarda, 1977; Hammond and MacKay, 1981; Allman et al., 1985; Desimone et al., 1985; Tanaka et al., 1986; Knierim and Van Essen, 1992; Zipser et al., 1996). Recently, Desimone and his colleagues (1993) demonstrated a role of callosal connections in mediating ipsilateral portions of surround effects in area V4. In their study, the presentation of stimuli within the ipsilateral visual field was found to reduce the response of cells to stimuli located within the CRF. These inhibitory effects were found for stimuli presented out to 16^0 within the ipsilateral field in the intact animals. However, following a callosotomy, these effects were found only for stimuli presented up to 4^0 away from the vertical meridian. The presence of inhibitory surround effects has been reported in V2 (Allman et al., 1985),

although the extent to which these extend into the ipsilateral visual field has not been examined.

Although the nature by which the callosal connections contribute to the response properties of cells in V2 remain to be resolved, the observation of callosal linkages between anatomically corresponding loci in V2 supports the notion that these connections are involved in midline stereopsis (Blakemore, 1969; Mitchell and Blakemore, 1970). Disparity-selective cells likely contribute to fine stereopsis (Barlow et al., 1967; Nikara et al., 1968; Hubel and Wiesel, 1970; Joshua and Bishop, 1970; Bishop and Henry, 1971; Poggio and Fisher, 1977; Hubel and Livingstone, 1987). Callosal linkages between anatomically corresponding regions of V2 along the V1 border could provide the interactions needed to generate cells with disparate representations located about the vertical meridian. Our results suggest that callosal projections link anatomically corresponding regions, possibly providing the necessary connections needed for generating these types of responses. Nonetheless, owing to the naso-temporal overlap in the retinofugal projections (see above), callosal connections may not be required to link these fields. In fact, callosal connections have been proposed not to play a role in fine stereopsis (Bishop and Henry, 1971). In line with this idea, lesions of the corpus callosum have been reported not to effect stereoacuity in macaque monkey (Cowey and Wilkinson, 1991).

On the other hand, callosal connections might play a role in coarse stereopsis about the midline (Bishop and Henry, 1971). In human observers, qualitative depth perception and the initiation of vergence eye movements has been shown to be possible for crossed and uncrossed stimuli presented up to 10' disparate about the vertical meridian (Westheimer and Tanzman, 1956; Westheimer and Mitchell, 1969). However, under the same testing parameters, these abilities were found to be absent in a subject whose callosal connections had been severed (Westheimer and Mitchell, 1969; Mitchell and Blakemore,

1970). Moreover in a subject with a sectioned optic chiasm, Blakemore (1970) found that depth perception was not possible for stimuli presented behind the fixation point (falling on the 'blind' nasal retinae). However, judgements of depth could be made for stimuli presented in front of the fixation point (falling on the temporal retinae). Due to the optic chiasm section, the representations of these stimuli would be in different hemispheres and presumably the callosal connections would be required to mediate this perception.

In the intact brain, images located on the vertical meridian though off the horopter are relayed to opposite sides of retinae. When the projected image on the retina falls outside the region of naso-temporal overlap, each retina will relay this input to different hemispheres. As described above, input from portions of the visual field lying symmetrically opposed to the vertical meridian would be expected to reach anatomically corresponding regions between areas V2. Thus our finding that V2 callosal connections preferentially link anatomically corresponding regions away from the V1 border in V2 could provide a substrate for linking disparate images extending outside the range of the naso-temporal overlap. In addition, callosal connections within other visual areas may also be involved.

Comparison with Other Species

Two connectivity patterns have been discussed in other species. On one hand, callosal connections have been shown to link anatomically corresponding regions. For example, employing anatomical tracing and physiological recording techniques, Segraves and Rosenquist (1982b) found evidence for anatomically corresponding callosal linkages in extrastriate cortex in the cat. Localized injections made in different areas of cortex were found to result in labeling which preferentially accumulated in anatomically corresponding locations in the contralateral hemisphere. In addition, mapping data revealed that

this pattern of callosal connectivity likely links representations of the visual field symmetrically opposed to the vertical meridian, including representations which are located away from the vertical meridian (however see Antonini et al., 1983). In medial portions of area 17 in the rat representing peripheral visual fields, callosal connections located within infragranular layers have also been shown to be linked within corresponding regions in the contralateral hemisphere (Lewis and Olavarria, 1995). A predominance of anatomically corresponding callosal connections has also been reported for the infragranular callosal cells within area 17 in tree shrew (Kretz and Rager, 1990).

On the other hand, callosal connections have also been shown to provide links between non-corresponding regions. Recent work from our laboratory suggests that callosal connections located along the lateral area 17/18 border region in both rat and cat preferentially link anatomically *non-corresponding* loci. Callosal cells located *on* the area 17/18 border were labeled following restricted tracer injections made *within* area 17 away from the 17/18 border, in the opposite hemisphere. Conversely, callosal cells located *within* area 17 were labeled following restricted tracer injections made *on* the contralateral area 17/18 border (Lewis and Olavarria, 1995; Olavarria, 1996). Similar patterns of connection have been reported previously for Siamese cats (Shatz, 1977). The presence of non-corresponding callosal connections has also be found in the tree shrew (Pritzel et al., 1988; Kretz and Rager, 1990).

Collectively, these data suggest that callosal connections link anatomically corresponding regions within most of striate and extrastriate cortex, whereas the area 17/18 border region appears to represent a unique callosal region with anatomically non-corresponding connections. Based on cytoarchitectural distinctions the V1/V2 border region has been described as a separate cortical area, area OBγ in primates (von Economo, 1929; OBg of von

Bonin, 1942). Area OBγ was characterized as a narrow region (~1mm in width) located between striate and parastriate cortex that contains an accumulation of large pyramidal cells at the bottom of layer 3. Previous studies suggested that these cells send projections through the callosum. In both humans lacking callosal connections (Shumura et al., 1975) and monkeys studied after sectioning the callosum (Glickstein and Whitteridge, 1976) these large layer 3 cells in OBγ were reported to be largely absent. In the cat, this region has been called the 'transition zone' (Payne, 1990), which has been shown to be linked to non-corresponding contralateral regions (Olavarria, 1996). These data, combined with the suggestion that this region represents the ipsilateral visual field (e.g., Kennedy et al., 1985, Payne, 1990; Siwek and Payne, 1991), raises the intriguing possibility that additional distinctions might be also be found between area OBγ and other visual areas, across species.

Figure 9: Experimental approach.

Parasagittal section through the posterior pole of the cortex illustrating the experimental approach. Portions of the prelunate sulcus were removed in order to inject anatomical tracers down the bank of the lunate sulcus under visual guidance. Two hypothetical injections are illustrated. A nuclear yellow (NY) injection close to the V1/V2 border, and a second bisbenzimide (BB) injection made away from the V1 border in V2. Posterior is to the right, dorsal is to the top of the page.

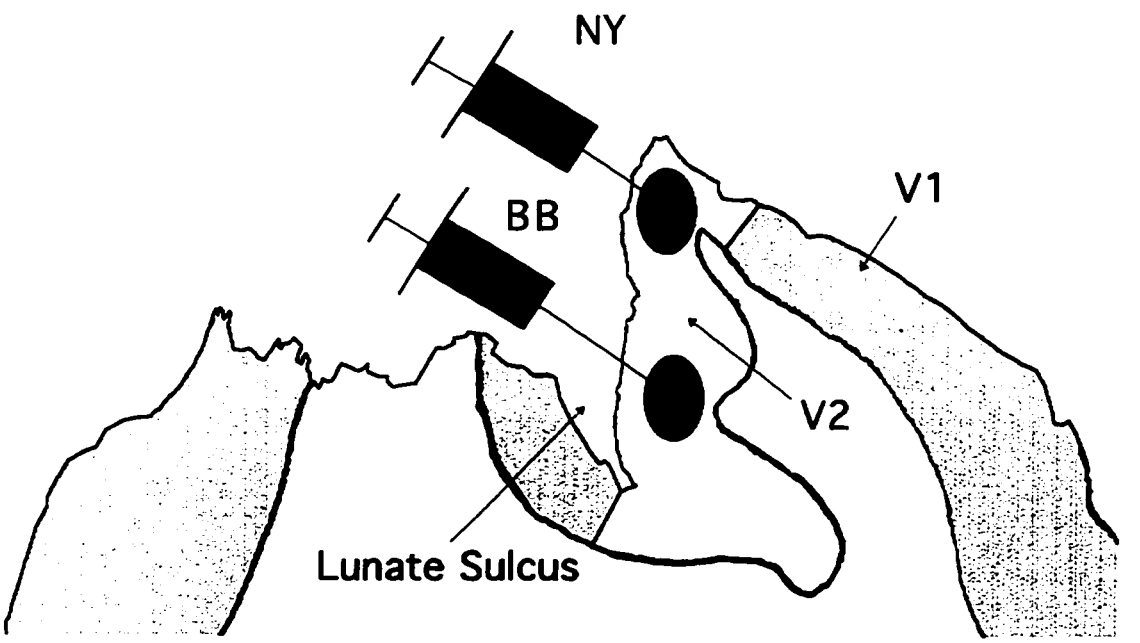
NY
BB
V1
V2
Lunate Sulcus

Figure 10: Data from animal mf-18 (BB, NY).

A. Reconstruction of NY (black/dark grays) and BB (dark/light grays) injection sites from tangential sections through dorsal V2 in the left hemisphere and distribution of retrogradely-labeled NY cells within V1 (black dots). Black line separates area V1 from area V2 as determined in CO-stained sections. Dark ovals represents the tissue damaged by the pipette track, surrounding gray region represents the extent of intense fluorescent label, lighter gray surround represents the diffuse fluorescent halo. Posterior is to the right, dorsal is up. **B.** Reconstruction of the NY-labeled (black dots) and BB-labeled (gray dots) cells from tangential sections through dorsal V2 in the right hemisphere. Black line separates area V1 from area V2 as determined in CO-stained sections. Gray outlines represent tears in the tissue as a result of the flattening procedure. Posterior is to the left, dorsal is up.

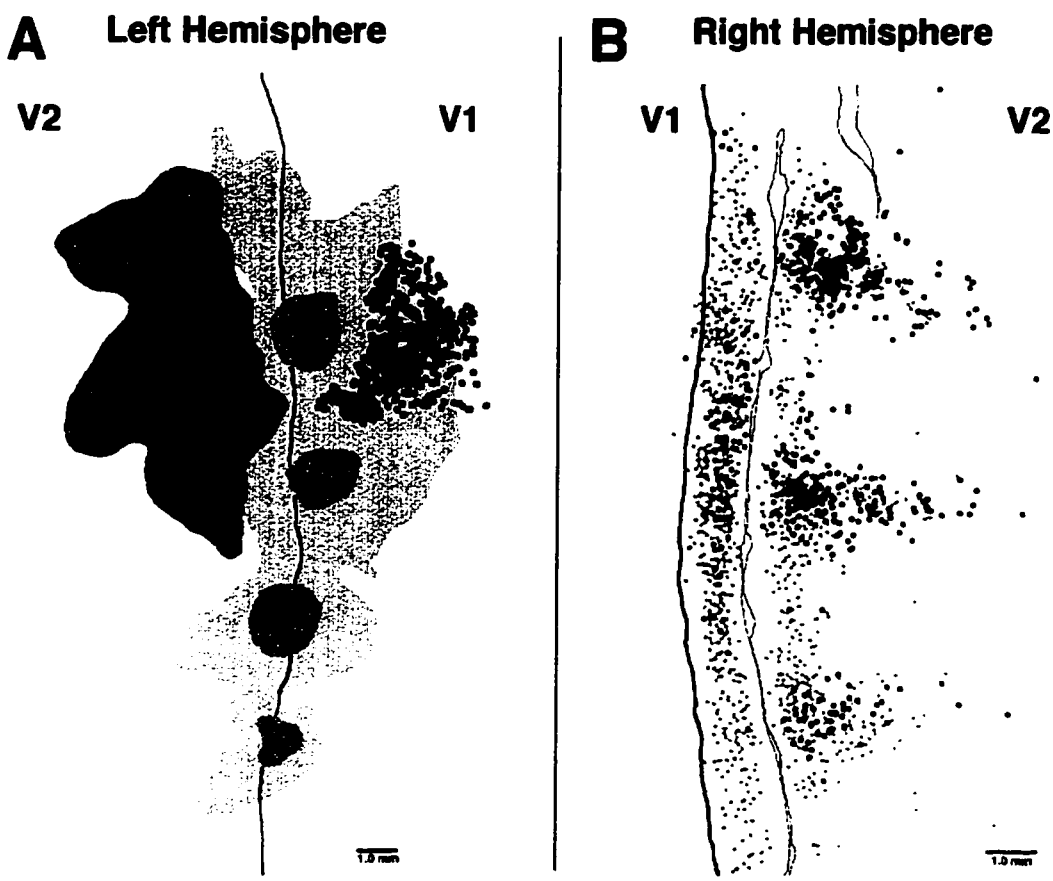
A
Left Hemisphere
V2
V1
B
Right Hemisphere
V1
V2

Figure 11: Quantified data from mn-18.

A. Distribution of BB-labeled callosal cells found across V2. Each datum on this curve represents the percent of the total number of labeled cells found within successive 200 μm strips oriented parallel to the V1 border. Black region underneath the curve represents the region of V2 damaged by the pipette track; the gray region represents the extent of the intense fluorescent halo. **B**. Percent of NY-labeled callosal cells found across V2.

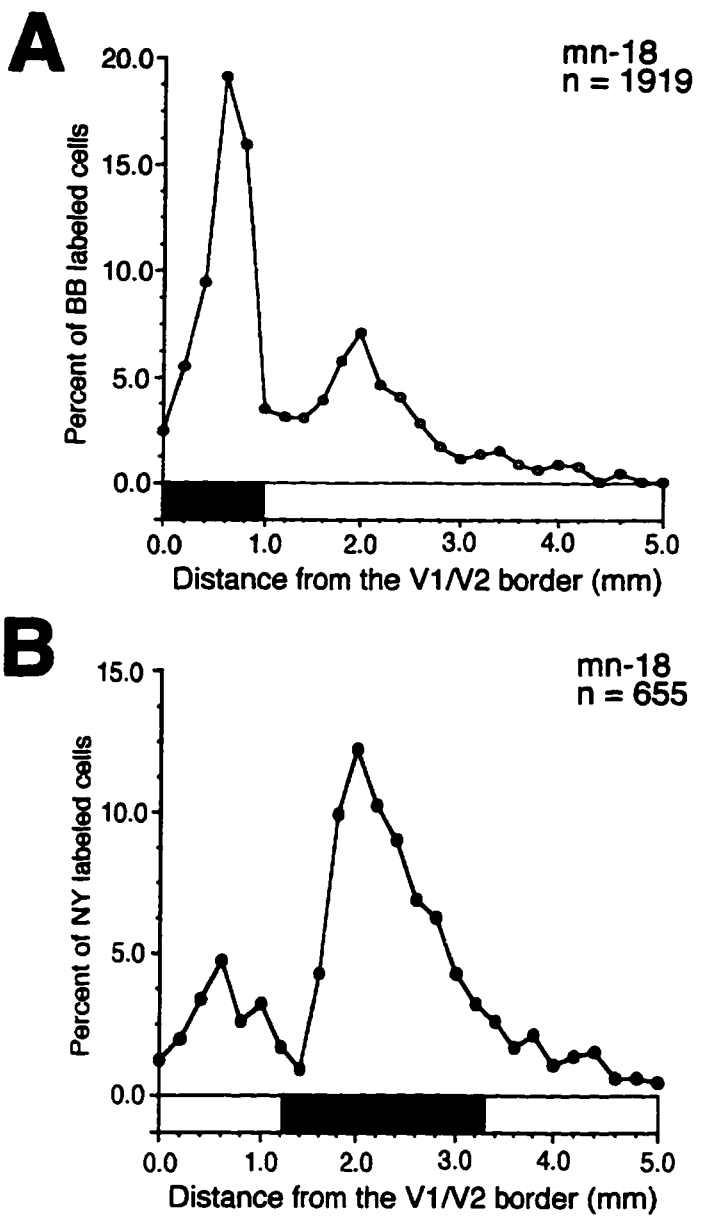
A
mn-18
n = 1919
20.0
15.0
10.0
5.0
0.0
Percent of BB labeled cells
0.0
1.0
2.0
3.0
4.0
5.0
Distance from the V1/V2 border (mm)
B
mn-18
n = 655
15.0
10.0
5.0
0.0
Percent of NY labeled cells
0.0
1.0
2.0
3.0
4.0
5.0
Distance from the V1/V2 border (mm)

Figure 12: Data from animal mf-19l (BB, NY).

Distribution of callosal cells found across V2 in animal mf-19 resulting from two injections in contralateral V2 analyzed in parasagittal sections. **A**. Percent of NY-labeled cells found across lateral portions of V2. **B**. Percent of BB-labeled cells found across lateral portions of V2. Same conventions as Figure 11.

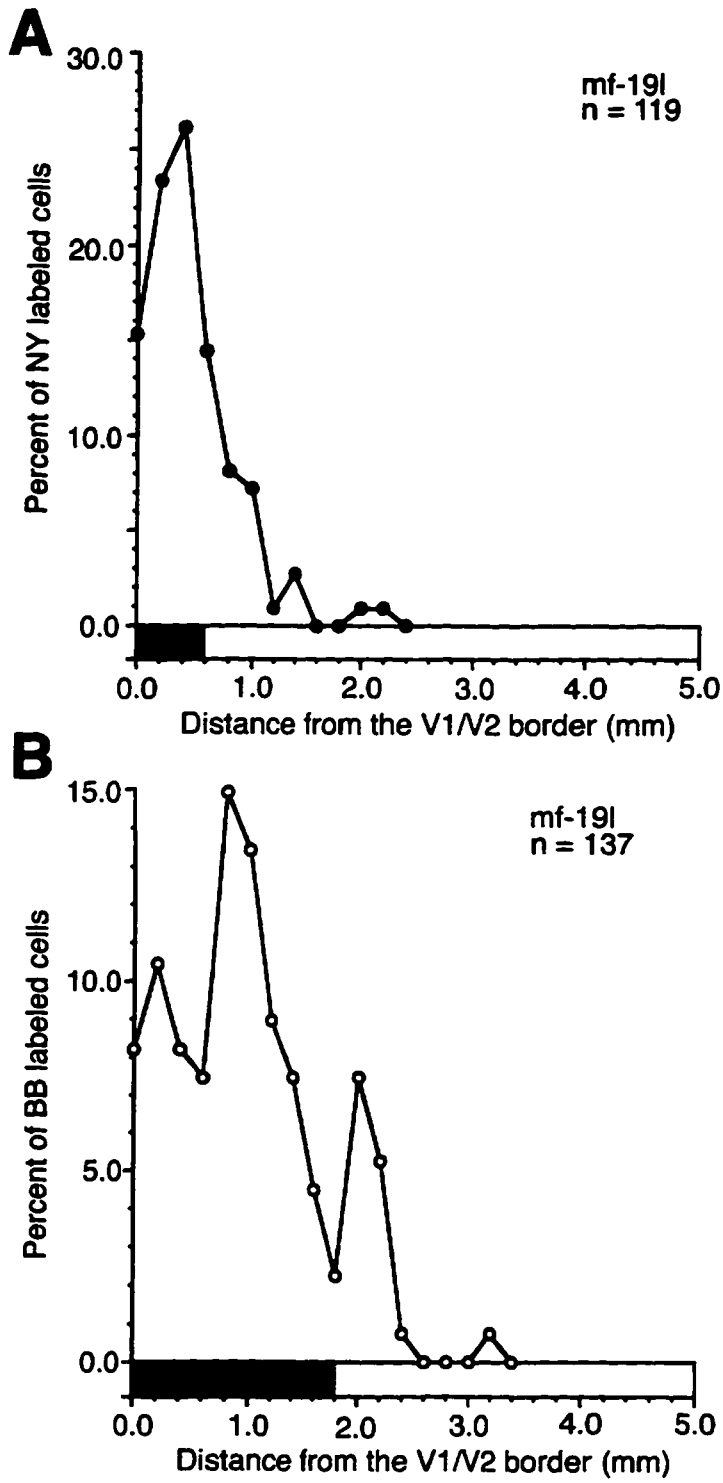
A
30.0
20.0
10.0
0.0
Percent of NY labeled cells
mf-19l
n = 119
0.0
1.0
2.0
3.0
4.0
5.0
Distance from the V1/V2 border (mm)
B
15.0
10.0
5.0
0.0
Percent of BB labeled cells
mf-19l
n = 137
0.0
1.0
2.0
3.0
4.0
5.0
Distance from the V1/V2 border (mm)

Figure 13: Data from animal mf-16 (NY).

A. Reconstruction of NY injection sites from tangential sections through dorsal V2 in the left hemisphere. The distribution of retrogradely-labeled cells within V1 could not be differentiated from the fluorescent halo. **B**. Reconstruction of the NY-labeled cells from tangential sections through dorsal V2 in the right hemisphere. Black line separates area V1 from area V2 as determined in CO-stained sections. Black dots represent the NY-labeled callosal cells. Conventions as in Figure 10.

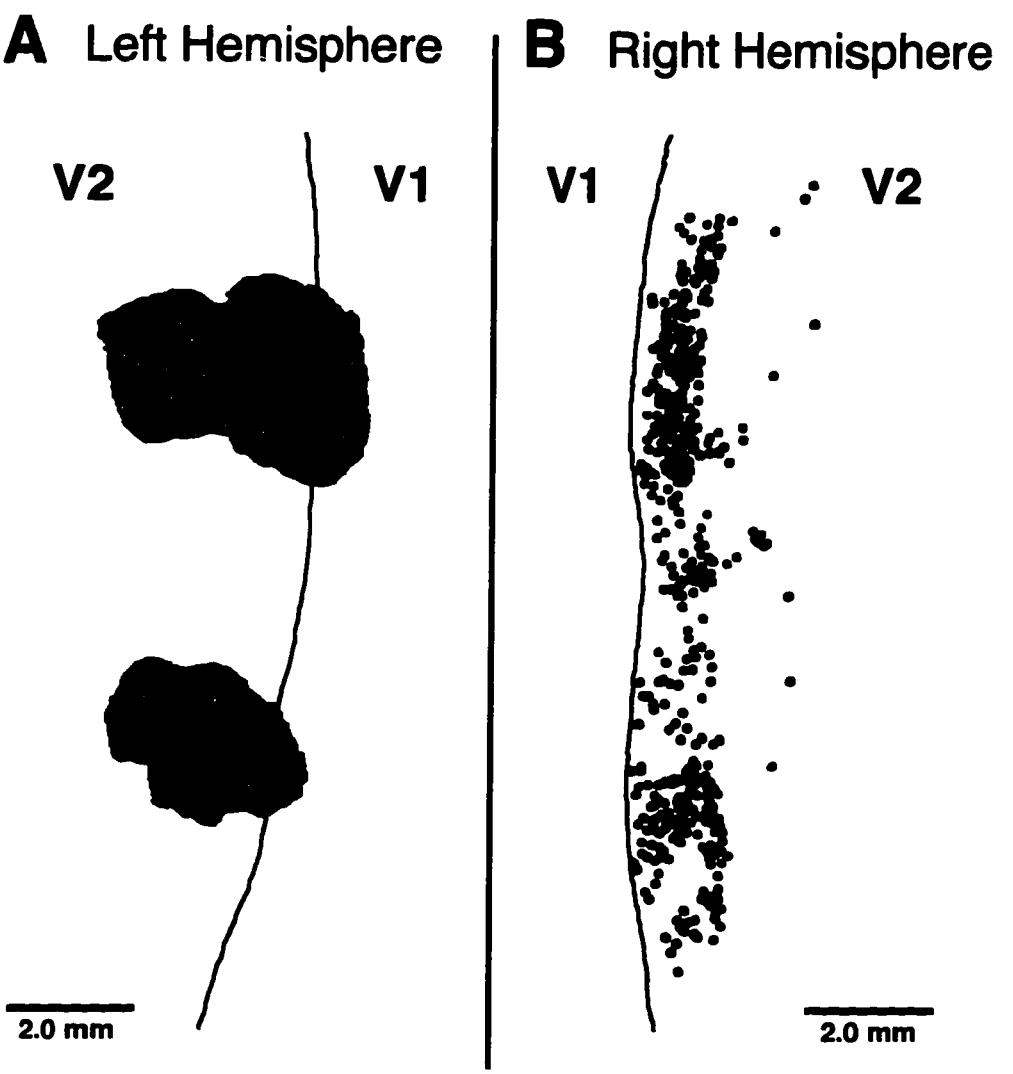
A Left Hemisphere
V2
V1
2.0 mm
B Right Hemisphere
V1
V2
2.0 mm

Figure 14: Data from animal mf-09.

A. Reconstruction of NY injection sites from tangential sections through dorsal V2 in the left hemisphere and distribution of retrogradely-labeled cells within V1 (black dots). The thick line separates area V1 from area V2 as determined in CO-stained sections. The cut through the middle of the operculum is represented by the contours at the bottom right corner. **B**. Reconstruction of the NY-labeled cells from tangential sections through dorsal V2 in the right hemisphere. Thick line separates area V1 from area V2 as determined in CO-stained sections. Gray outline represents the overall distribution of callosal cells labeled with BB from two large injections in the left hemisphere (not shown). Black dots represent the NY-labeled cells. Conventions as in Figure 10.

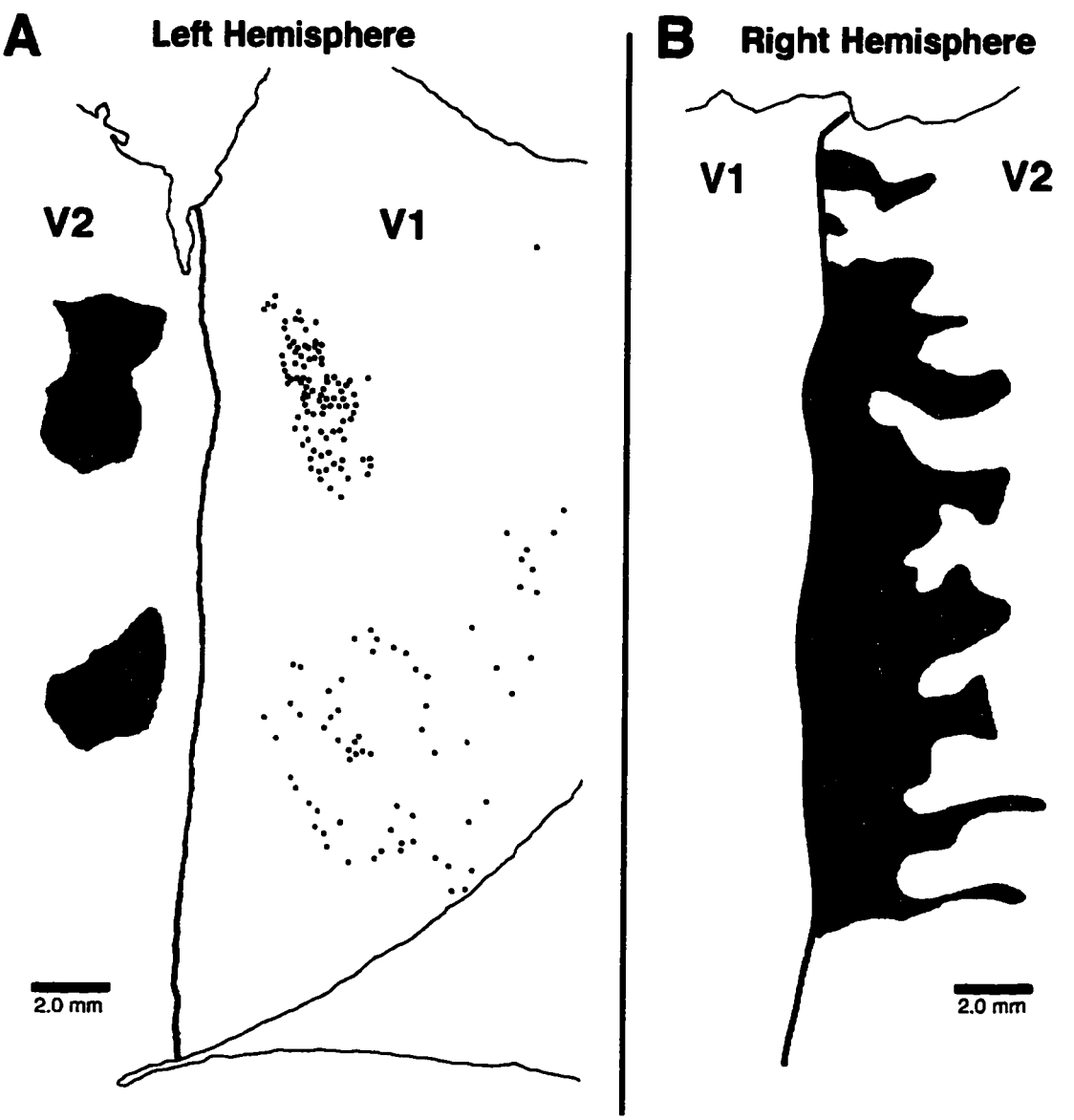
A
Left Hemisphere
V2
V1
2.0 mm
B
Right Hemisphere
V1
V2
2.0 mm

Figure 15: Quantified data from mf-16, mf-09

Distribution of callosal cells found across V2 in animal mf-16 and mf-09. **A.** Percent of NY-labeled cells found across V2 in animal mf-16 **B.** Percent of NY-labeled cells found across V2 in animal mf-09. Conventions as in Figure 11.

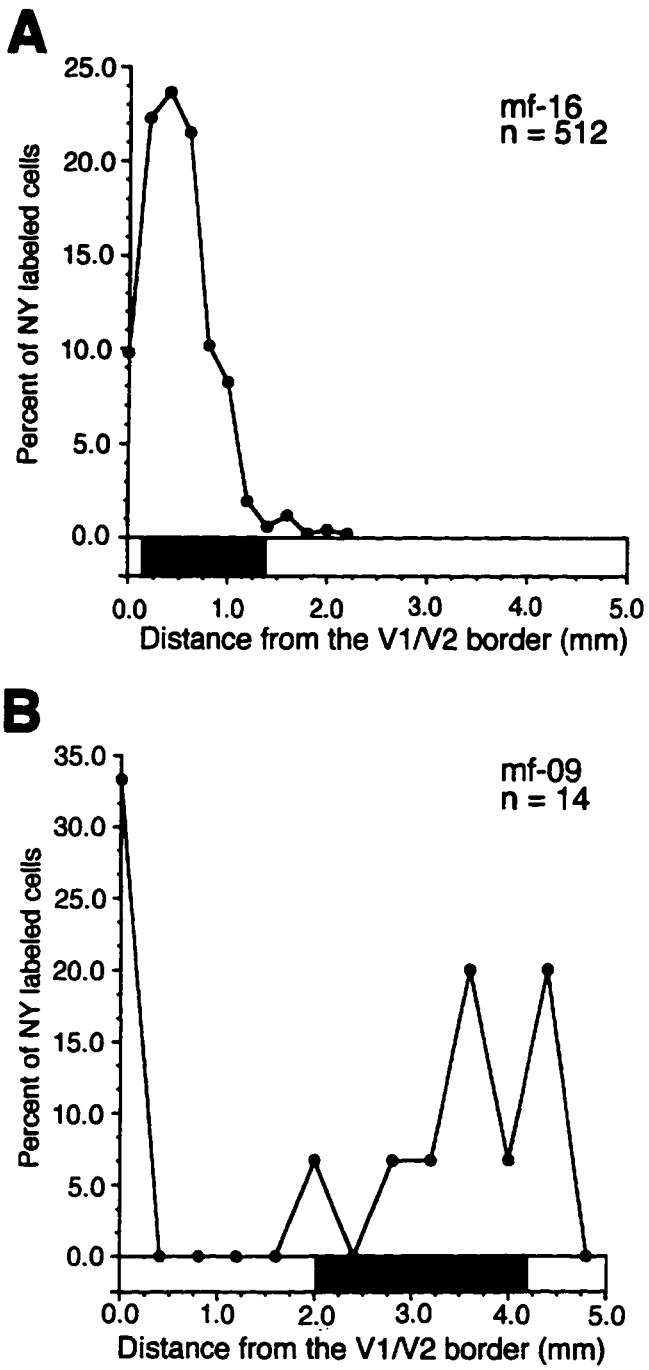
A
mf-16
n = 512
Percent of NY labeled cells
25.0
20.0
15.0
10.0
5.0
0.0
0.0
1.0
2.0
3.0
4.0
5.0
Distance from the V1/V2 border (mm)
B
mf-09
n = 14
Percent of NY labeled cells
35.0
30.0
25.0
20.0
15.0
10.0
5.0
0.0
0.0
1.0
2.0
3.0
4.0
5.0
Distance from the V1/V2 border (mm)

Figure 16: Data from animal mf-13m, mf-19m

Distribution of callosal cells found across V2 in animal mf-13 and mf-19 analyzed in parasagittal sections. **A**. BB-labeled cells found within medial portions of V2 following an injection in medial portions of contralateral V2 in animal mf-19 **B**. NY-labeled cells found within medial portions of V2 following an injection in medial portions of contralateral V2 in animal mf-13. Conventions as in Figure 11.

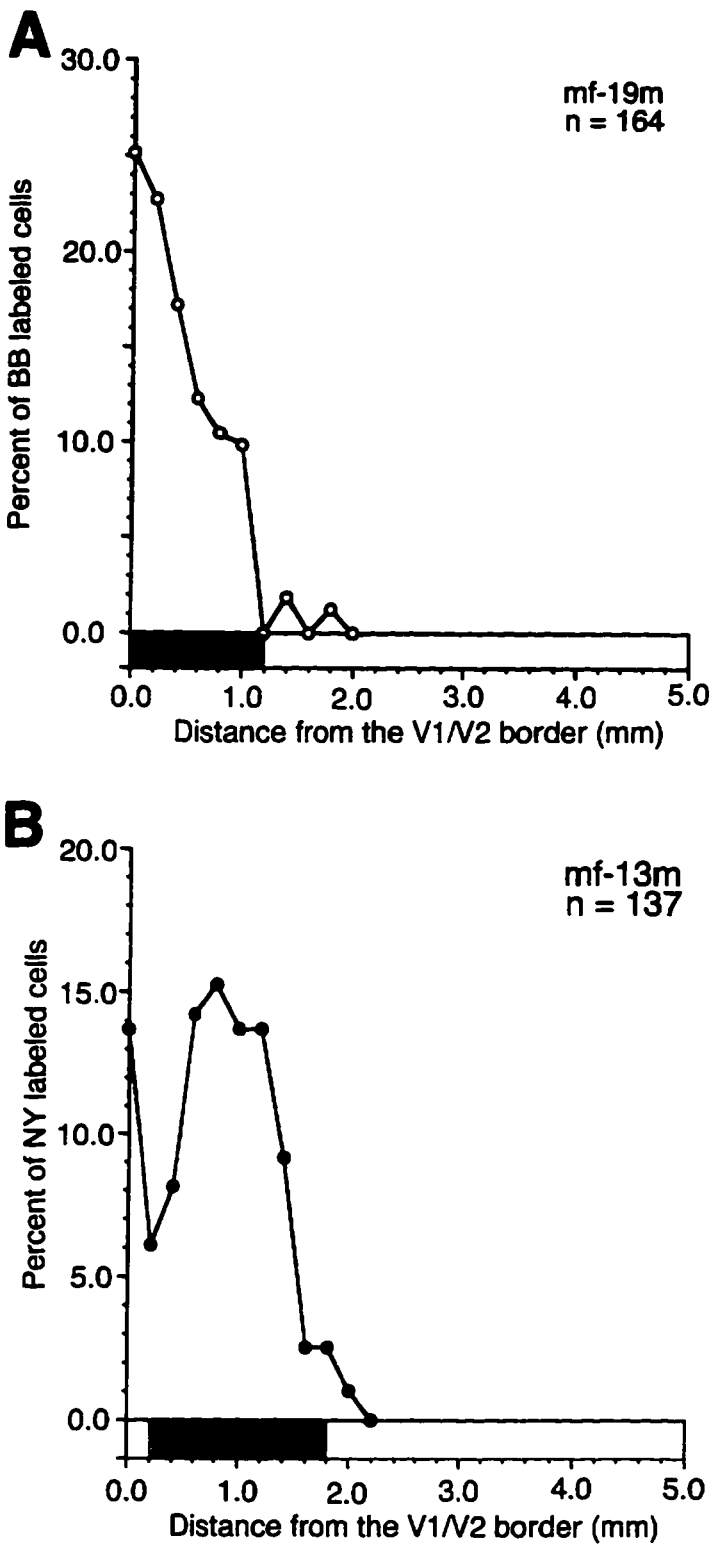
A
30.0
20.0
10.0
0.0
Percent of BB labeled cells
mf-19m
n = 164
0.0
1.0
2.0
3.0
4.0
5.0
Distance from the V1/V2 border (mm)
B
20.0
15.0
10.0
5.0
0.0
Percent of NY labeled cells
mf-13m
n = 137
0.0
1.0
2.0
3.0
4.0
5.0
Distance from the V1/V2 border (mm)

Figure 17: CC and visual field map in V2.

Relationship between the visual field map and callosal connections within area V2. **Left**. Unfolded and flattened representation of visual area V2. Gray region represents the overall pattern of callosal connections within V2. The representation of the visual field as described in previously studies has been superimposed onto this representation and are illustrated in B. Posterior is to the left. The top and bottom edges represent the most medial portions of V2. **Right**. Visual field represented within right V2. Gray regions represent the potential extent of the visual field represented in V2 which overlap callosal connections.

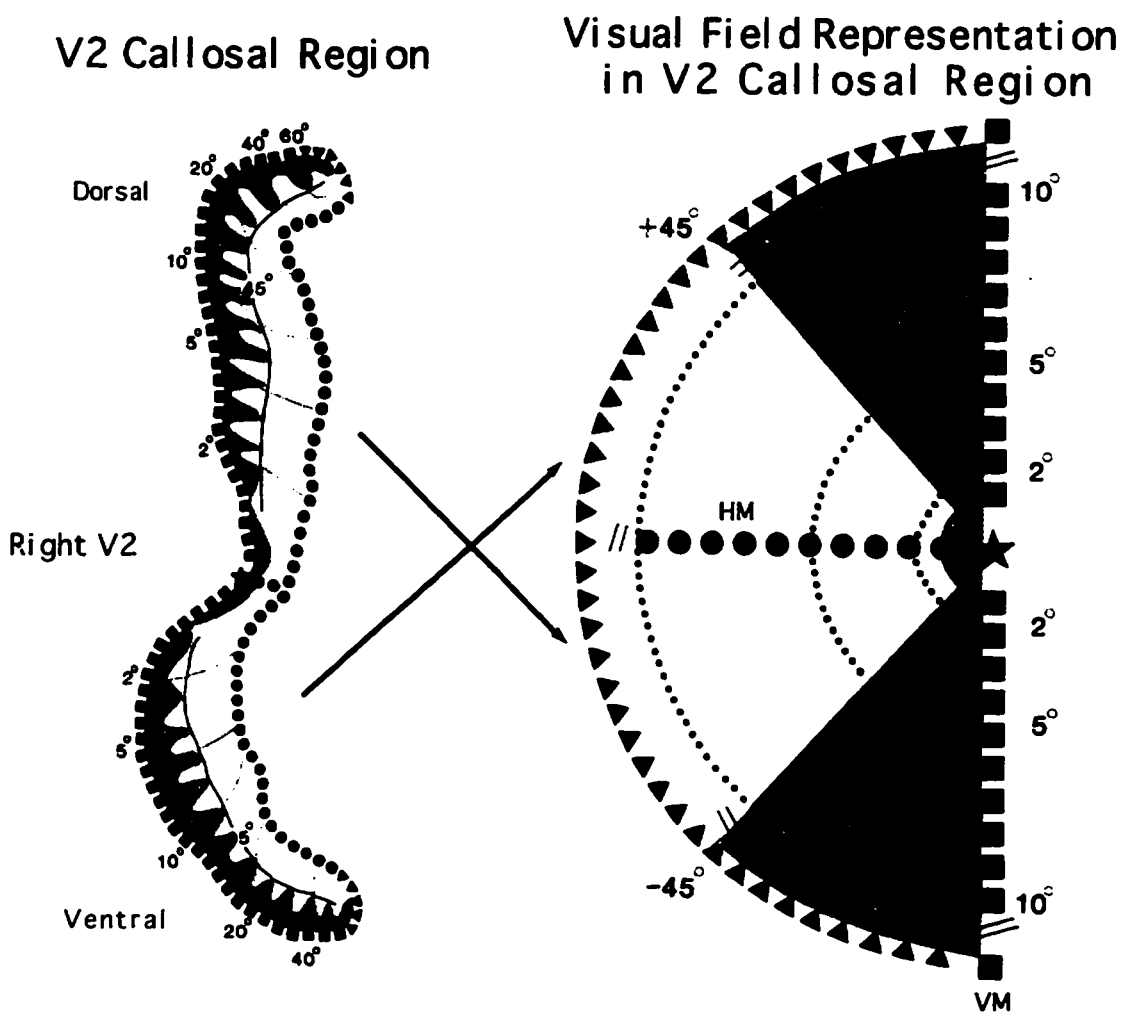
V2 Callosal Region
Visual Field Representation
in V2 Callosal Region
Dorsal
Right V2
Ventral
40°
60°
20°
10°
5°
2°
2°
5°
10°
20°
40°
+45°
-45°
HM
VM
10°
5°
2°
2°
5°
10°

CONCLUSION

In the first two experiments, the distributions of cortico-tectal and callosal projection neurons were compared to the pattern of CO stripes in area V2 of macaque monkey. The results indicate that the tangential distributions of these cells bare a relationship to the modular organization within V2. Tracer injections made into the superior colliculus resulted in band-like accumulations of labeled cells across the tangential extent of V2. These bands were found to lie in spatial register with alternate CO-dense stripes. Based on their physical appearance and the predominance of Cat-301 immunopositive cells, these stripes were identified as thick stripes. Retrogradely-labeled callosal cells were also found to be distributed non-uniformly across the tangential extent of V2. Labeled cells accumulated along the V1/V2 border and within finger-like clusters extending up to 8 mm across V2. These callosal fingers were found to lie in spatial register with CO-dense thick and thin stripe regions. Both of these observations were supported by quantitative analyses.

These findings extend previous data on the organization of anatomical connections in area V2. Previous studies have shown that many cortico-cortical connections are largely segregated within different CO stripe-like compartments within V2. Our data extend this notion to the cortico-subcortical and interhemispheric pathways. In addition, our data suggest that not all cortico-cortical pathways are reflected in interhemispheric connections. Callosal connections tended to avoid the CO-pale stripes within V2, which are known to send ipsilateral projections within V2 as well as projections to modules within area V4. Finally, our data support the idea that these stripe-like compartments are related to functionally separate pathways. The cortico-tectal pathway has been associated preferentially with the broad-band pathway, our results

demonstrate that cortico-tectal projection neurons predominate in CO-dense thick stripe regions in V2.

In the final chapter we examined the topography of V2 callosal connections. Based on previous data on the visual field map in V2, callosal connections could link representations of the visual field located away from the vertical meridian. We examined whether the pattern of V2 callosal linkages supports this idea. We found that the organization of callosal linkages is not random. Labeled callosal cells were found to accumulate in anatomically corresponding regions of V2, relative to the locations of the contralateral injection sites. These data support the hypothesis that V2 callosal connections mediate interactions between visual field representations located away from the vertical meridian

BIBLIOGRAPHY

FOR CHAPTER 1

Abel, P.L., B.J. O'Brien, B. Lia, and J.F. Olavarria (1994) The distribution of cortico-collicular projection neurons correlates with thick cytochrome oxidase stripes in visual area V2 of macaque monkey. Soc. Neurosci. Abstr. *20*:710.6.

Baizer, J.S., R. Desimone, and L.G. Ungerleider (1993) Comparison of subcortical connections of inferior temporal and posterior parietal cortex in monkeys. Vis. Neurosci. *10*:59-72.

Benevento, L.A., and J.H. Fallon (1975) The ascending projections of the superior colliculus in the rhesus monkey (*Macaca mulatta*). J. Comp. Neurol. *160*:339-362.

Benevento, L.A., and M. Rezak (1976) The cortical projections of the inferior pulvinar and adjacent lateral pulvinar in the rhesus monkey (*Macaca mulatta*): an autoradiographic study. Brain Res. *108*:1-24.

Benevento, L.A., and G.P. Standage (1983) The organization of projections of the retinorecipient and nonretinorecipient nuclei of the pretectal complex and layers of the superior colliculus to the lateral pulvinar and medial pulvinar in the macaque monkey. J. Comp. Neurol. *217*:307-336.

Bruce, C.J., R. Desimone, and C.G. Gross (1986) Both striate cortex and superior colliculus contribute to the visual properties of neurons in superior temporal polysensory area of macaque monkey. J. Neurophys. *55*:1057-1075.

Bullier, J., and L.G. Nowak (1995) Parallel versus serial processing: new vistas on the distributed organization of the visual system. Curr. Opin. Neurobiol. *5*:497-503.

Casagrande, V.A., and J.H. Kaas (1994) The afferent, intrinsic, and efferent connections of primary visual cortex in primates. In A. Peters and K. Rockland (eds): Cerebral Cortex, vol. 10. New York: Plenum Press, pp. 201-259.

Curcio, C.A., and J.K. Harting (1978) Organization of pulvinar afferents to area 18 in the squirrel monkey: evidence for stripes. Brain Res. *143*:155-161.

Cusick, C.G. (1988) Anatomical organization of the superior colliculus in monkeys: corticotectal pathways for visual and visuomotor functions. Prog. Brain Res. *75*:1-15.

Desimone, R., R.J. Fleming, and C.G. Gross (1980) Prestriate afferents to inferior temporal cortex: An HRP study. Brain Res. *184*:41-55.

DeYoe, E.A., D.J. Felleman, D.C. Van Essen, and E. McClendon (1994) Multiple processing streams in occipitotemporal visual cortex. Nature *371*:151-154.

DeYoe, E.A., S. Hockfield, H. Garren, and D.C. Van Essen (1990) Antibody labeling of functional subdivisions in visual cortex: Cat-301 immunoreactivity in striate and extrastriate cortex of macaque monkey. Vis. Neurosci. *5*:67-81.

DeYoe, E.A., and D.C. Van Essen (1985) Segregation of efferent connections and receptive field properties in visual area V2 of the macaque. Nature *317*:58-61.

DeYoe, E.A., and D.C. Van Essen (1988) Concurrent processing streams in monkey visual cortex. Trends Neurosci. *11*:219-226.

Felleman D.J., E.A. DeYoe, J. Knierim, J. Olavarria, and D.C. Van Essen (1988) Compartmental organization of projections from V2 to extrastriate visual areas V3, V3A, and V4t in macaque monkeys. Invest. Ophthal. Vis. Sci., ARVO Abstr. Suppl. *29*:115.

Felleman, D.J., and D.C. Van Essen (1991) Distributed hierarchical processing in the primate cerebral cortex. Cerebral Cortex *1*:1-47.

Ferrera, V.P., T.A. Nealey, and J.H.R. Maunsell (1994) Responses in macaque visual area V4 following inactivation of the parvocellular and magnocellular LGN pathways. J. Neurosci. *14*:2080-2088.

Fitzpatrick, D., W.M. Usrey, B.R. Schofield, and G. Einstein (1994) The sublaminar organization of corticogeniculate neurons in layer 6 of macaque striate cortex. Vis. Neurosci. *11*:307-315.

Fries, W. (1984) Cortical projections to the superior colliculus in the macaque monkey: a retrograde study using horseradish peroxidase. J. Comp. Neurol. *230*:55-76.

Fries, W., K. Keizer, and H.G.J.M. Kuypers (1985) Large layer VI cells in macaque striate cortex (Meynert cells) project to both the superior colliculus and prestriate Visual area V5. Exp. Brain Res. *58*:613-616.

Fries, W. (1986) Distribution of Meynert cells in primate striate cortex: spatial relationships with cytochrome oxidase blobs. Naturwissenschaften *73*:S557.

Gattass, R., C.G. Gross, and J.H. Sandell (1981) Visual topography of V2 in the macaque. J. Comp. Neurol. *201*:519-539.

Gegenfurtner, K.R., D.C. Kiper, and S.B. Fenstemaker (1996) Processing of color, form and motion in macaque area V2. Vis. Neurosci. *13*:161-172.

Girard, P., P.-A. Salin, and J. Bullier (1991) Visual activity in macaque area V4 depends upon area 17 input. NeuroReport *2*:81-84.

Gottman, J.M. (1981) Time Series Analysis. A comprehensive introduction for social scientists. Cambridge: University Press.

Graham, J., C.-S. Lin, and J.H. Kaas (1979) Subcortical projections of six visual cortical areas in the owl monkey *Aotus trivirgatus*. J. Comp. Neurol. *187*:557-580.

Gross, C.G. (1991) Contribution of striate cortex and the superior colliculus to visual function in area MT, the superior temporal polysensory area and the inferior temporal cortex. Neuropsychologia *29*:497-515.

Harting, J.K., M.F. Huerta, A.J. Frankfurter, N.L. Strominger, and G.J. Royce (1980) Ascending pathways from monkey superior colliculus: an autoradiographic analysis. J. Comp. Neurol. *192*: 853-882.

Hendry, S.H.C., E.G. Jones, S. Hockfield, and R.D.G. McKay (1988) Neuronal populations stained with the monoclonal antibody Cat-301 in the mammalian cerebral cortex and thalamus. J. Neurosci. *8*:518-542.

Horton, J.C. (1984) Cytochrome oxidase patches: a new cytoarchitectonic feature of monkey visual cortex. Phil. Trans. R. Soc. Lond. B *304*:199-253.

Horton, J.C., and D.H. Hubel (1981) Regular patchy distribution of cytochrome oxidase staining in primary visual cortex of macaque monkey. Nature *292*:762-764.

Hubel, D.H., and M.S. Livingstone (1987) Segregation of form, color and stereopsis in primate area 18. J. Neurosci. *7*:3378-3415.

Hubener, M., and J. Bolz (1992) Relationships between dendritic morphology and cytochrome oxidase compartments in monkey striate cortex. J. Comp. Neurol. *324*:67-80.

Kennedy, H., C. Dehay, and J. Bullier (1986) Organization of the callosal connections of visual areas V1 and V2 in the macaque monkey. J. Comp. Neurol. *247*:398-415.

Kuypers, H.G.J.M., and D.G. Lawrence (1967) Cortical projections to the red nucleus and the brain stem in the rhesus monkey. Brain Res. *4*:151-188.

Lachica, E.A., P. Beck, and V.A. Casagrande (1992) Parallel pathways in macaque monkey striate cortex: anatomically defined columns in layer III. Proc. Natl. Acad. Sci. USA *89*:3566-3570.

Levitt, J.B., D.C. Kiper, and J.A. Movshon (1994a) Receptive fields and functional architecture of macaque V2. J. Neurophys. *71*:2517-2542.

Levitt, J.B., T. Yoshioka, and J.S. Lund (1994b) Intrinsic cortical connections in macaque visual area V2: evidence for interaction between different functional streams. J. Comp. Neurol. *342*:551-570.

Levitt, J.B., T. Yoshioka, and J.S. Lund (1995) Connections between the pulvinar complex and cytochrome oxidase-defined compartments in visual area V2 of macaque monkey. Exp. Brain Res. *104*:419-430.

Lia, B., and J.F. Olavarria (1996) The distribution of corticotectal projection neurons correlates with the interblob compartment in macaque striate cortex. Vis. Neurosci. *13*:461-466.

Livingstone, M.S., and D.H. Hubel (1982) Thalamic inputs to cytochrome oxidase-rich regions in monkey visual cortex. Proc. Natl. Acad. Sci. USA *79*:6098-6101.

Livingstone, M.S., and D.H. Hubel (1983) Specificity of cortico-cortical connections in monkey visual system. Nature *304*:531-534.

Livingstone, M.S., and D.H. Hubel (1984) Anatomy and physiology of a color system in the primate visual cortex. J. Neurosci. *4*:309-356.

Livingstone, M.S., and D.H. Hubel (1987a) Connections between layer 4B of area 17 and the thick cytochrome oxidase stripes of area 18 in the squirrel monkey. J. Neurosci. *7*:3371-3377.

Livingstone, M.S., and D.H. Hubel (1987b) Psychophysical evidence for separate channels for the perception of form, color, movement, and depth. J. Neurosci. *7*:3416-3468.

Livingstone, M.S., and D.H. Hubel (1988) Segregation of form, color, movement, and depth: Anatomy, physiology, and perception. Science *240*:740-749.

Lui, F., K.M. Gregory, R.H.I. Blanks, and R.A. Giolli (1995) Projections from visual areas of the cerebral cortex to pretectal nuclear complex, terminal accessory optic nuclei, and superior colliculus in macaque monkey. J. Comp. Neurol. *363*:439-460.

Lund, J.S., A.E. Hendrickson, M.P. Ogren, and E.A. Tobin (1981) Anatomical organization of primate visual cortex area VII. J. Comp. Neurol. *202*:19-45.

Lund, R.D. (1972) Synaptic patterns in the superficial layers of the superior colliculus of the monkey, *Macaca mulatta*. Exp. Brain Res. *15*:194-211.

Lynch, J.C., A.M. Graybiel, and L.J. Lobeck (1985) The differential projection of two cytoarchitectonic subregions of the inferior parietal lobule of macaque upon the deep layers of the superior colliculus. J. Comp. Neurol. *235*:241-254.

Malach, R. (1992) Dendritic sampling across processing streams in monkey striate cortex. J. Comp. Neurol. *315*:303-312.

Malach, R., R.B.H. Tootell, and D. Malonek (1994) Relationship between orientation domains, cytochrome oxidase stripes, and intrinsic horizontal connections in squirrel monkey area V2. Cerebral Cortex *4*:151-165.

Malpeli, J.G., and P.H. Schiller (1981) Response properties of single cells in monkey striate cortex during reversible inactivation of individual lateral geniculate laminae. J. Neurophys. *46*:1102-1119.

Martin, K.A.C. (1988) From enzymes to visual perception: a bridge gone too far? Trends Neurosci. *11*:380-387.

Maunsell, J.H.R. (1992) Functional visual streams. Curr. Opin. Neurobiol. *2*:506-510.

Maunsell, J.H.R., and W.T. Newsome (1987) Visual processing in monkey extrastriate cortex. Ann. Rev. Neurosci. *10*:363-341.

Maunsell, J.H.R., and D.C. Van Essen (1983) The connections of the middle temporal visual area (MT) and their relationship to a cortical hierarchy in the macaque monkey. J. Neurosci. *12*:2563-2586.

Merigan, W.H., and J.H.R. Maunsell (1990) Macaque vision after magnocellular lateral geniculate lesions. Vis. Neurosci. *5*:347-352.

Merigan, W.H., and J.H.R. Maunsell (1993) How parallel are the primate visual pathways? Ann. Rev. Neurosci. *16*:369-402.

Mesulam, M.M. (1978) Tetramethyl benzidine for horseradish peroxidase neurohistochemistry: a non-carcinogenic blue reaction product with superior sensitivity for visualizing neural afferents and efferents. J. Histochem. Cytochem. *26*:106-117.

Mishkin, M., L.G. Ungerleider, and K.A. Macko (1983) Object vision and spatial vision: two cortical pathways. Trends Neurosci. *6*:414-417.

Nakamura, H., R. Gattass, R. Desimone, and L.G. Ungerleider (1993) The modular organization of projections from areas V1 and V2 to areas V4 and TEO in macaques. J. Neurosci. *13*:3681-3691.

Nealey, T.A., and J.H.R. Maunsell (1994) Magnocellular and parvocellular contributions to the responses of neurons in macaque striate cortex. J. Neurosci. *14*:2069-2079.

Ogren, M.P., and A.E. Hendrickson (1977) The distribution of pulvinar terminals in visual areas 17 and 18 of the monkey. Brain Res. *137*: 343-350.

Olavarria, J., and P.L. Abel (1996) The distribution of callosal connections correlates with the pattern of cytochrome oxidase stripes in visual area V2 of macaque monkeys. Cerebral Cortex *In press*.

Olavarria, J., E.A. DeYoe, and D.C. Van Essen (1989) Pattern of cytochrome oxidase staining in the unfolded and flattened V2 of macaque monkey. Invest. Ophthal. Vis. Sci., ARVO Abstr. Suppl. *30*:298.

Olavarria, J., and R.C. Van Sluyters (1985) Unfolding and flattening the cortex of gyrencephalic brains. J. Neurosci. Meth. *15*:191-202.

Partlow, G.D., M. Colonnier, and J. Szabo (1977) Thalamic projections of the superior colliculus in the rhesus monkey, *Macaca mulatta*. A light and electron microscopic study. J. Comp. Neurol. *171*:285-318.

Payne, B.R., and A. Peters (1989) Cytochrome oxidase patches and Meynert cells in monkey visual cortex. Neurosci. *28*:353-363.

Peterhans, E., and R. von der Heydt (1993) Functional organization of area V2 in the alert macaque. Euro. J. Neurosci. *5*:509-524.

Rockland, K.S. (1985) A reticular pattern of intrinsic connections in primate area V2 (area 18). J. Comp. Neurol. *235*:467-478.

Roe, A., and D.Y. T'so (1995) Visual topography in primate V2: multiple representation across functional stripes. J. Neurosci. *15*:3689-3715.

Sawatari, A., and E.M. Callaway (1996) Convergence of magno- and parvocellular pathways in layer 4B of macaque primary visual cortex. Nature *380*:442-446.

Schiller, P.H. (1981) Input and output specificity of striate cortex. In O. Pompeiano, and C.A. Marsan (eds): Brain Mechanisms and Perceptual Awareness. New York: Raven Press, pp. 21-36.

Schiller, P.H., N.K. Logothetis, and E.R. Charles (1990) Role of the color-opponent and broad band channels in vision. Vis. Neurosci. *5*:321-346.

Schiller, P.H., J.G. Malpeli, and S.J. Schein (1979) Composition of the geniculostriate input to superior colliculus of the rhesus monkey. J. Neurophys. *42*:1124-1133.

Schiller, P.H., M. Stryker, M. Cynader, and N. Berman (1974) Response characteristics of single cells in the monkey superior colliculus following ablation or cooling of the visual cortex. J. Neurophys. *37*:181-194.

Shipp, S., and S. Zeki (1985) Segregation of pathways leading from area V2 to areas V4 and V5 of macaque monkey visual cortex. Nature *315*:322-325.

Shipp S., and S. Zeki (1989a) The organization of connections between areas V5 and V1 in macaque monkey visual cortex. Euro. J. Neurosci. *1*:309-332.

Shipp, S., and S. Zeki (1989b) The organization of connections between areas V5 and V2 in macaque monkey visual cortex. Euro. J. Neurosci. *1*:333-354.

Tigges, J., and M. Tigges (1981) Distribution of retinofugal and corticofugal axon terminals in the superior colliculus of the squirrel monkey. Invest. Ophthal. Vis. Sci. *20*:149-158.

Tootell, R.B.H., M.S. Silverman, R.L. DeValois, and G.H. Jacobs (1983) Functional organization of the second visual area in primates. Science *220*:737-739.

Tootell R.B.H., and S.L. Hamilton (1989) Functional anatomy of the second visual area (V2) in the macaque. J. Neurosci. *9*:2620-2644.

Ungerleider, L.G., and M. Mishkin (1982) Two cortical systems. In D.J. Ingle, M.A. Goodale, and R.J.W. Mansfield (eds): Analysis of Visual Behavior Cambridge: MIT, pp. 549-585.

Valverde, F. (1978) The organization of area 18 in the monkey: a Golgi study. Anat. Embryol. *154*:305-334.

Van Essen, D.C., C.H. Andersen, and D.J. Felleman (1992) Information processing in the primate visual system: an integrated systems perspective. Science *255*:419-423.

Van Essen, D.C., D.J. Felleman, E.A. DeYoe, J. Olavarria, and J. Knierim (1990) Modular and hierarchical organization of extrastriate visual cortex in the macaque monkey. Cold Spring Harbor Symp. Quant. Biol. *55*:679-696.

Van Essen, D.C., W.T. Newsome, and J.L. Bixby (1982) The pattern of interhemispheric connections and its relationship to extrastriate visual areas in the macaque monkey. J. Neurosci. *2*:265-283.

Williams, E.A., and J.M. Gottman (1982) A user's guide to the Gottman-Williams time-series analysis computer programs for social scientists. Cambridge: University Press.

Wilson, M.E., and M.J. Toyne (1970) Retino-tectal and cortico-tectal projections in *Macaca mulatta*. Brain Res. *24*:395-406.

Wong-Riley, M. (1979) Changes in the visual system of monocularly sutured or enucleated cats demonstrable with cytochrome oxidase histochemistry. Brain Res. *171*:11-28.

Wong-Riley, M.T.T., and E.W. Carroll (1984) Quantitative light and electron microscopic analysis of cytochrome oxidase-rich zones in VII prestriate cortex of squirrel monkey. J. Comp. Neurol. *222*:18-37.

Yoshioka, T., J.B. Levitt, and J.S. Lund (1994) Independence and merger of thalamocortical channels within macaque monkey visual cortex: anatomy of interlaminar projections. Vis. Neurosci. *11*:467-489.

Zeki, S., and S. Shipp (1988) The functional logic of cortical connections. Nature *335*:311-317.

Zeki, S., and S. Shipp (1989) Modular connections between areas V2 and V4 of macaque monkey visual cortex. Euro. J. Neurosci. *1*:494-506.

FOR CHAPTER 2

Abel PL, O'Brien BJ, Olavarria JF (1995) Callosal connections interlink anatomically corresponding regions in visual area V2 of macaque monkey. Soc Neurosci Abstr (in press).

Allman J., Miezin F, McGuiness E. (1985) Direction- and velocity-specific responses from beyond the classical receptive field in the middle temporal visual area (MT). Perception 14:105-126.

Beck PD, Kaas JH (1994) Interhemispheric connections in neonatal owl monkeys (*Aotus trivirgatus*) and galagos (*Galago crassicaudatus*). Brain Res 651:57-75.

Berlucchi G., M.S. Gazzaniga, and G. Rizzolatti (1967) Microelectrode analysis of transfer of visual information by the corpus callosum. Arch Ital Biol *105*:583-596.

Blakemore C, Diao Y, Pu M, Wang Y, Xiao Y (1983) Possible functions of the interhemispheric connexions between visual cortical areas in the cat. J Physiol (Lond) 337:334-349.

Boyd J, Matsubara J (1994) Tangential organization of callosal connectivity in the cat's visual cortex. J Comp Neurol 347:197-210.

Choudhury BP, Whitteridge D, Wilson ME (1965) The function of the callosal connections of the visual cortex. Quart J Exp Physiol 50:214-219.

Cusick CG, Gould HJ, Kaas JH (1984) Interhemispheric connections of visual cortex of owl monkeys (*Aotus trivirgatus*), marmosets (*Callithrix jacchus*), and galagos *(Galago crassicaudatus*). J Comp Neurol 230:311-336.

Cusick CG, Kaas JH (1988) Cortical connections of area 18 and dorsolateral visual cortex in squirrel monkeys. Vis Neurosci 1:211-237.

Dehay C, Kennedy H, Bullier J (1986) Callosal connectivity of areas V1 and V2 in the newborn monkey. J Comp Neurol 254:20-33.

Dehay C, Kennedy H, Bullier J, Berland M (1988) Absence of interhemispheric connections of area 17 during development in the monkey. Nature 331:348-350.

Desimone R, Fleming J, Gross CG (1980) Prestriate afferents to inferior temporal cortex: An HRP study. Brain Res 184:41-55.

Desimone R, Moran J, Schein SJ, Mishkin M (1993) A role for the corpus callosum in visual area V4 of the macaque. Vis Neurosci 10:159-171.

DeYoe EA, Van Essen DC (1985) Segregation of efferent connections and receptive field properties in visual area V2 of the macaque. Nature 317:58-61.

DeYoe EA, Van Essen DC (1988) Concurrent processing streams in monkey visual cortex. Trends Neurosci 11:219-226.

DeYoe EA, Felleman DJ, Knierim JJ, Olavarria J, Van Essen DC (1988) Heterogeneous subregions of macaque visual area V4 receive selective projections from V2 thin stripes and interstripe regions. Invest Ophthal Vis Sci, ARVO abstr Suppl 29:215.

DeYoe EA, Felleman DJ, Van Essen DC, McClendon E (1994) Multiple processing streams in occipitotemporal visual cortex. Nature 371:151-154.

Felleman DJ, DeYoe EA, Knierim J, Olavarria J, Van Essen DC (1988) Compartmental organization of projections from V2 to extrastriate visual areas V3, V3A, and V4t in macaque monkeys. Invest Ophthal Vis Sci, ARVO Abstr Suppl. 29:115.

Ferrera VP, Nealey TA, Maunsell JHR (1994) Responses in macaque visual area V4 following inactivation of the parvocellular and magnocellular LGN pathways. J Neurosci 14:2080-2088.

Gattass R, Gross CG, Sandell JH (1981) Visual topography of V2 in the macaque. J Comp Neurol 201:519-539.

Gottman, JM (1981) Time-series analysis. A comprehensive introduction for social scientists. Cambridge:University Press.

Gould HJ III, Weber JT, Rieck RW (1987) Interhemispheric connections in the visual cortex of the squirrel monkey (*Saimiri sciureus*). J Comp Neurol 256:14-28.

Griffin G, Watkins LR, Mayer DJ (1979) HRP pellets and slow-release gels: Two new techniques for greater localization and sensitivity. Brain Res 168:595-601.

Hendrickson AE (1985) Dots, stripes and columns in monkey visual cortex. Trends Neurosci 8:406-410.

Horton JC, Hubel DH (1981) Regular patchy distribution of cytochrome oxidase staining in primary visual cortex of macaque monkey. Nature 292:762-764.

Horton JC (1984) Cytochrome oxidase patches: a new cytoarchitectonic feature of monkey visual cortex. Phil Trans R Soc Lond B 304:199-253.

Hubel DH, Wiesel TN (1967) Cortical and callosal connections concerned with the vertical meridian of visual fields in the cat. J Neurophysiol 30:1561-1573.

Hubel DH, Wiesel TN (1970) Cells sensitive to binocular depth in area 18 of the macaque monkey cortex. Nature 225: 41-42.

Hubel DH, Livingstone MS (1985) Complex-unoriented cells in a subregion of primate area 18. Nature 315:325-327.

Hubel DH, Livingstone MS (1987) Segregation of form, color, and stereopsis in primate area 18. J Neurosci 7:3378-3415.

Innocenti GM (1991) The development of projections from cerebral cortex. Prog in Sensory Physiol 12:65-114.

Johnson PB, Angelucchi A, Ziparo RM, Minciacchi D, Bentivoglio M, Caminiti R (1989) Segregation and overlap of callosal and association neurons in frontal and parietal cortices of primates: a spectral and coherency analysis. J Neurosci 9:2313-2326.

Kennedy H, Martin KAC, Orban GA, Whitteridge D (1985) Receptive field properties of neurons in visual area 1 and visual area 2 in the baboon. Neurosci 14:405-415.

Kennedy H, Dehay C, Bullier J (1986) Organization of the callosal connections of visual areas V1 and V2 in the macaque monkey. J Comp Neurol 247:398-415.

Kennedy H, Meissirel C, Dehay C (1991) Callosal pathways and their compliancy to general rules governing the organization of cortical connectivity. In:

Neuroanatomy of the visual pathways and their development (Dreher B, Robinson S, eds), pp 324-359. New York: Macmillan.

Land EH, Hubel DH, Livingstone MS, Perry SH, Burns MM (1983) Colour-generating interactions across the corpus callosum. Nature 303:616-618.

Levitt JB, Kiper DC, Movshon JA (1994a) Receptive fields and functional architecture of macaque V2. J Neurophysiol 71:2517-2542.

Levitt JB, Yoshioka T, Lund JS (1994b) Intrinsic cortical connections in macaque visual area V2: evidence for interaction between different functional streams. J Comp Neurol 342:551-570.

Lewis J W, Olavarria JF (1995) Two rules for callosal connectivity in striate cortex of the rat. J Comp Neurol 361:119-137.

Livingstone MS, Hubel DH (1984) Anatomy of a color system in the primate visual system. J Neurosci 4:309-356.

Livingstone MS, Hubel DH (1987) Connections between layer 4B of area 17 and the thick cytochrome oxidase stripes of area 18 in the squirrel monkey. J Neurosci 7:3371-3377.

Lund JS, Lund RD, Hendrickson AE, Bunt AH, Fuchs AF (1976) The origin of efferent pathways from the primary visual cortex, area 17, of the macaque monkey as shown by retrograde transport of horseradish peroxidase. J Comp Neurol 164:287-304.

Malach R, Tootell RBH, Malonek D (1994) Relationship between orientation domains, cytochrome oxidase stripes, and intrinsic horizontal connections in squirrel monkey area V2. Cerebral Cortex 4:151-165.

Maunsell JHR, Newsome WT (1987) Visual processing in monkey extrastriate cortex. Ann Rev Neurosci 10:363-341.

Maunsell JHR, Van Essen DC (1983) Functional properties of neurons in middle temporal visual area (MT) of macaque monkey. I. Selectivity for stimulus direction, velocity and orientation. J Neurophysiol 49:1127-1147.

Merigan WH, Maunsell JHR (1990) Macaque vision after magnocellular lateral geniculate lesions. Visual Neurosci 5:347-352.

Mesulam MM (1978) Tetramethyl benzidine for horseradish peroxidase neurohistochemistry: a non-carcinogenic blue reaction product with superior sensitivity for visualizing neural afferents and efferents. J Histochem Cytochem 26:106-117.

Mishkin M, Ungerleider LG, Macko KA (1983) Object vision and spatial vision: Two cortical pathways. Trends Neurosci 6:414-417.

Newsome WT, Allman JM (1980) Interhemispheric connections of visual cortex in the owl monkey, *Aotus trivirgatus*, and the bushbaby, *Galago senegalensis*. J Comp Neurol 194:209-233.

Olavarria J, Montero VM (1984) Relation of callosal and striate-extrastriate cortical connections in the rat: Morphological definition of extrastriate visual areas. Exp Brain Res 54:240-252.

Olavarria J, Van Sluyters RC (1985) Unfolding and flattening the cortex of gyrencephalic brains. J Neurosci Meth 15:191-202.

Olavarria J, DeYoe EA, Van Essen DC (1989) Pattern of cytochrome oxidase staining in the unfolded and flattened V2 of the macaque monkey. Invest Ophthal Vis Sci, ARVO abstr Suppl 30:298.

Olavarria JF, Lewis JW (1992) The distribution of callosal cells correlates with dense cytochrome oxidase stripes in V2 of the macaque monkey. Soc Neurosci Abstr 18:293.

Olavarria JF (1995) Non mirror-symmetric patterns of callosal linkages in areas 17 and 18 in cat visual cortex. J Comp Neurol (in press).

Olavarria JF, Li Ch -P (1995) Effects of neonatal enucleation on the organization of callosal linkages in striate cortex of the rat. J Comp Neurol 361:138-151.

Peterhans E, von der Heydt R (1993) Functional organization of area V2 in the alert macaque. Eur J Neurosci 5:509-524.

Rocha-Miranda CE, Bender DB, Gross CG, Mishkin M (1975) Visual activation of neurons in inferotemporal cortex depends on striate cortex and forebrain commissures. J Neurophysiol 38:475-491.

Rockland KS, Pandya DN (1979) Laminar origins and terminations of cortical connections of the occipital lobe in the rhesus monkey. Brain Res 179:3-20.

Rockland KS (1985) A reticular pattern of intrinsic connections in primate area V2 (area 18). J Comp Neurol 235:467-478.

Rosa MGP, Sousa APB, Gattass R (1988) Representation of the visual field in the second visual area in the Cebus monkey. J Comp Neurol 275:326-345.

Schein S, Desimone R (1990) Spectral properties of V4 neurons in the macaque. J Neurosci 10:3369-3389.

Schiller PH, Logothetis NK, Charles ER (1990) Role of the color-opponent and broad band channels in vision. Visual Neurosci 5:321-346.

Shipp S, Zeki SM (1985) Segregation of pathways leading from area V2 to areas V4 and V5 of macaque monkey visual cortex. Nature 315:322-325.

Shipp S, Zeki S (1989a) The organization of connections between areas V5 and V1 in macaque monkey visual cortex. Eur J Neurosci 1: 309-332

Shipp S, Zeki S (1989b) The organization of connections between areas V5 and V2 in macaque monkey visual cortex. Eur J Neurosci 1:333-354.

Tanaka K, Hikosaka K, Saito H, Yukie M, Fukada Y, Iwai E (1986) Analysis of local and wide-field movements in the superior temporal visual area of the macaque monkey. J Neurosci 6:134-144.

Thomas HC, Espinoza SG (1987) Relationship between interhemispheric cortical connections and visual areas in hooded rats. Brain Res 417:214-224.

Tootell RBH, Silverman MS, DeValois RL, Jacobs GH (1983) Functional organization of the second cortical area of primates. Science 220:737-739.

Tootell RBH, Hamilton SL, Silverman MS (1985) Topography of cytochrome oxidase activity in owl monkey cortex. J Neurosci 5:2786-2800.

Tootell RBH, Hamilton SL (1989) Functional anatomy of the second visual area (V2) in the macaque. J Neurosci 9:2620-2644.

Ungerleider LG, Mishkin M (1982) Two cortical visual systems. In: Analysis of visual behavior (Ingle DJ, Goodale MA, Mansfield RLW, eds), pp 549-585. Cambridge, MA:MIT.

Van Essen DC, Zeki SM (1978) The topographic organization of rhesus monkey prestriate cortex. J Physiol (Lond) 277:193-226.

Van Essen DC, Newsome WTN, Bixby JL (1982) The pattern of interhemispheric connections and its relationship to extrastriate visual areas in the macaque monkey. J Neurosci 2:265-283.

Van Essen DC, Felleman DJ, DeYoe EA, Olavarria J, Knierim J (1990) Modular and hierarchical organization of extrastriate visual cortex in primates. Cold Spring Harbor Symp Quant Biol 55:679-696.

Williams EA, Gottman JM (1982) A user's guide to the Gottman-Williams time-series analysis computer programs for social scientists. Cambridge: University Press.

Winfield DA, Gatter KC, Powel TPS (1975) Certain connections of the visual cortex of the monkey shown by the use of horseradish peroxidase. Brain Res 92:456-461.

Wong-Riley M (1979) Changes in the visual system of monocularly sutured or enucleated cats demonstrable with cytochrome oxidase histochemistry. Brain Res 171:11-28.

Zeki SM (1973) Colour coding in rhesus monkey prestriate cortex. Brain Res 53:422-427.

Zeki SM (1980) The representation of colours in the cerebral cortex. Nature 284:412-418.

Zeki S, Shipp S (1989) Modular connections between areas V2 and V4 of macaque monkey visual cortex. Eur J Neurosci 1:494-506.

FOR CHAPTER 3

Abel PL, O'Brien BJ, Olavarria JF (1995) Callosal connections interlink anatomically corresponding regions in visual area V2 of macaque monkey. *Soc. Neurosci. Abstr* **21**:903.

Abel PL , O'Brien BJ, Lia B, Olavarria JF (1997) Distribution of neurons projecting to the superior colliculus correlates with thick cytochrome oxidase stripes in macaque visual area V2. *J Comp Neurol* **377**: 313-323.

Allman J, Miezin F, McGuinness E (1985) Stimulus specific responses from beyond the classical receptive field: Neurophysiological mechanisms for local-global comparisons in visual neurons. *Ann Rev Neurosci* **8**:407-430.

Allman and Kaas (1974) The organization of the second visual area (VII) in the owl monkey: a second transformation of the visual hemifield. *Brain Res* **76**:247-265.

Antonini A, Berlucchi G, Lepore F (1983) Physiological organization of callosal connections of a visual lateral suprasylvian cortical area in the cat. *J Neurophysiol* **49**:902-921.

Antonini A, Di Stefano M, Minciacchi D, Tassinari G (1985) Interhemispheric influences on area 19 of the cat. *J Neurophysiol* **49**:902-921.

Barlow HB, Blakemore C, Pettigrew JD (1967) The neural mechanism of binocular depth discrimination. *J Physiol* **193**:327-342.

Bentivoglio M, Kuypers HGJM, Catsman-Berrevoets CE (1980a) Retrograde neuronal labeling by means of Bisbenzimide and Nuclear Yellow (Hoechst 769121). Measures to prevent diffusion of the tracers out of retrogradely laeled neurons. *Neurosci Lett* **18**:19-24.

Bentivoglio M, Kuypers HGJM, Catsman-Berrevoets CE, Loewe H, Dann O (1980b) Two new fluorescent retrograde neuronal tracers which are transported over long distances. *Neurosci Lett* **18**:25-30.

Berlucchi G, MS Gazzaniga, and G Rizzolatti (1967) Microelectrode analysis of transfer of visual information by the corpus callosum. *Arch. Ital. Biol.* **105**:583-596.

Berlucchi G, G Rizzolatti (1968) Binocularly driven neurons in visual cortex of split chiasm cats. *Science* **159**:308-310.

Berlucchi G (1981) Recent advances in the analysis of the neural substrates of interhemispheric communication. In O. Pompeiano and CA Marsan (eds): Brain Mechanisms and Perceptual Awareness. New York: Raven Press, pp 133-152.

Bishop PO, and Henry GH (1971) Spatial vision. *Ann Rev Psych* **22**:119-161.

Blakemore C (1969) Binocular depth discrimination and the naso temporal division. *J Physiol* **205**:471-497.

Blakemore C (1970) Binocular depth perception and the optic chiasm. *Vision Res* **10**:43-47.

Blakemore C, Diao Y, Pu M, Wang Y, Xiao Y (1983) Possible functions of the interhemispheric connexions between visual cortical areas in the cat. *J Physiol (Lond)* **337**:334-349.

Bunt AH, Minkler DS, Johanson, GW (1977) Demonstration of bilateral projection of the central retina of the monkey with horseradish peroxidase neuronography. *J Comp Neurol* **171**:619-630.

Chalupa LM, Killackey HP, Snider CJ, Lia B (1989) Callosal projection neurons in area 17 of the fetal rhesus monkey. *Devel Brain Res* **46**:303-308.

Chalupa LM, Lia B (1991) The nasotemporal division of retinal ganglion cells with crossed and uncrossed projections in the fetal rhesus monkey. *J Neurosci* **11**:191-202.

Choudhury BP, Whitteridge D, Wilson ME (1965) The function of the callosal connections of the visual cortex. *Quart J exp Physiol* **50**:214-219.

Connolly M, Van Essen DC (1984) The representation of the visual field in parviclular and magnocellular layers of the lateral geniculate nucleus in the macaque monkey. *J Comp Neurol* **226**:544-564.

Cowey A, Wilkinson F (1991) The role of the corpus callosum and extrastriate visual areas in stereoacuity in macaque monkeys. *Neuropsychologia* **29**:465-479.

Cragg BG (1969) The topography of afferent projections in the circumstriate visual cortex of the monkey studied by the Nauta method. *Vision Res* **9**:733-747.

Cusick CG, Gould HJ, Kaas JH (1984) Interhemispheric connections of visual cortex of owl monkeys (*Aotus trivirgatus*), marmosets (*Callithrix jacchus*), and galagos *(Galago crassicaudatus*). *J Comp Neurol.* **230**:311-336.

Cusick CG, MacAvoy, Kaas JH (1985) Interhemispheric connections of cortical sensory areas in tree shrews. *J Comp Neurol* **235**:111-128.

Cusick, CG, and JH Kaas (1988) Cortical connections of area 18 and dorsolateral visual cortex in squirrel monkeys. *Vis Neurosci.* **1**:211-237.

Daniel PM, Whitteridge D (1961) The representation of the visual field of the cerebral cortex in monkeys. *J Physiol* **159**:203-221

Desimone R, Moran J, Schein SJ, Mishkin M (1993) A role for the corpus callosum in visual area V4 of the macaque. *Vis Neurosci* **10**:159-171.

Dehay C, Kennedy H, Bullier J (1986) Callosal connectivity of areas V1 and V2 in the newborn monkey. *J Comp Neurol* **254**:20-33.

Dehay C, Kennedy H, Bullier J, Berland M (1988) Absence of interhemispheric connections of area 17 during development in the monkey. *Nature* **331**:348-350.

Dehay C, Horsburgh G, Berland M, Killackey H, Kennedy H (1989) Maturation and connectivity of the visual cortex in monkey is altered by prenatal removal of retinal input. *Nature* **337**:265-267.

Desimone R, Schein SJ, Moran J, Ungerleider LG(1985) Contour, color and shape analysis beyond the striate cortex. *Vision Res* **25**:441-452.

Desimone R, Moran J, Schein SJ, Mishkin M (1993) A role for the corpus callosum in visual area V4 of the macaque. Vis Neurosci 10:159-171.

DeYoe, E.A., S. Hockfield, H. Garren, and D.C. Van Essen (1990) Antibody labeling of functional subdivisions in visual cortex: Cat-301 immunoreactivity in striate and extrastriate cortex of macaque monkey. Vis. Neurosci. *5*:67-81.

Ebner FF, Myers RE (1965) Distribution of corpus callosum and anterior commissure in the cat and the raccoon *J. Comp. Neurol.* **124**:353-365.

Fukuda Y, Sawai H, Watanabe M, Wakakuwa K, Morigiwa K (1989) Nasotemporal overlap of crossed and uncrossed retinal ganglion cell

projections in the Japanese monkey (*Macaca fuscata*). *J Neurosci* **9**:2353-2373.

Gattass R, Gross CG, Sandell JH (1981) Visual topography of V2 in the macaque. *J Comp Neurol* **201**:519-539.

Gegenfurtner, K.R., D.C. Kiper, and S.B. Fenstemaker (1996) Processing of color, form and motion in macaque area V2. Vis. Neurosci. *13*:161-172.

Glickstein M, Whitteridge D (1976) Degeneration of layer III pyramidal cells in area 18 following destruction of callosal input. *Brain Res* **104**:148-151.

Gutierrez C, Yaun A, Cusick CG (1995) Neurochemical subdivisions of the inferior pulvinar in macaque monkeys. *J Comp Neurol* **363**:545-562.

Hammond P, MacKay DM (1981) Modulatory influences of moving textured backgrounds on responsiveness of simple cells in feline striate cortex. *J Physiol* **319**:431-442

Hedreen J, Yin TCT (1981) Homotopic and heterotopic callosal afferents of caudal inferior parietal lobule in *Macaca mullata*. *J Comp Neurol* **197**:605-621.

Hendry, S.H.C., E.G. Jones, S. Hockfield, and R.D.G. McKay (1988) Neuronal populations stained with the monoclonal antibody Cat-301 in the mammalian cerebral cortex and thalamus. J. Neurosci. *8*:518-542.

Hubel DH, Wiesel TN (1967) Cortical and callosal connections concerned with the vertical meridian of visual fields in the cat. *J Neurophysiol* **30:**1561-1573.

Hubel DH, Wiesel TN (1970) Cells sensitive to binocular depth in area 18 of the macaque monkey cortex. *Nature* **225**: 41-42.

Hubel, D.H., and M.S. Livingstone (1987) Segregation of form, color and stereopsis in primate area 18. J. Neurosci. 7:3378-3415.

Illert M, Fritz N, Aschoff A, Hollander H (1982) Fluorescent compunds as retrograde tracers compared with horseradish peroxidase (HRP). II. A parametric study in the peripheral motor system of the cat. *J Neurosci Meth* **6**:199-218.

Joshua DE, Bishop PO (1970) Binocular single vision and depth discrimination. Receptive field disparaties for cetral and peripheral vision and binocular interaction on peripheral single units in cat striate cortex. *Exp Brain Res* **10**:389-416.

Kennedy H, Martin KAC, Orban GA, Whitteridge D (1985) Receptive field properties of neurons in visual area I and visual area II in the baboon. *Neuroscience* **14**:405-415.

Kennedy H, Dehay C, Bullier J (1986) Organization of the callosal connections of visual areasV1 and V2 in the macaque monkey. *J Comp Neurol* **247**:398-415.

Kennedy, H., C. Meissirel, and C. Dehay (1991) Callosal pathways and their compliancy to general rules governing the organization of cortical connectivity. In B. Dreher and S. Robinson (eds): Neuroanatomy of the Visual Pathways and Their Development. New York: Macmillan, pp 324-359.

Knierim JJ, Van Essen DC (1992) Neuronal responses to static texture patterns in area V1 of the alert macaque monkey. *J Neurophys* **67**;961-980.

Kretz R, Rager G (1990) Reciprocal heterotopic callosal connections between the two striate areas in Tupaia. *Exp Brain Res* **82**:271-278.

Kretz R, Rager G (1992) Postnatal development of area 17 callosal connections in *Tupaia*. *J Comp Neurol* **326**:217-228.

Kuypers HGJM, Bentivoglio M, Van der kooy D, Catsman-Berrevoets (1979) Retrograde transport of Bisbenzimide and propidium iodid through axons to their parent cell bodies. *Neurosci Lett* **12**:1-7.

Land, EH, Hubel, DH, Livingstone, MS, Perry, SH and Burns, MM (1983) Colour-generating interactions across the corpus callosum. *Nature* **303**:616-618.

Lepore F, Guillemot J-P (1982) Visual receptive fields properties of cells innervated through the corpus callosum in the cat. *Exp. Brain Res.* **46**:413-424.

Leventhal AG, Ault SJ, Vitek DJ (1988) The nasotemporal division in primate retina: The neual basis of macular sparing and splitting. *Science* **240**:66-67.

Levitt JB, Kiper DC, Movshon JA (1994) Receptive fields and functional architecture of macaque V2. *J. Neurophysiol.* **71**:2517-2542.

Lewis JW, and Olavarria JF (1995) Two rules for callosal connectivity in striate cortex of the rat. *J. Comp. Neurol.* **361**:119-137.

Lund JS, Lund RD, Hendrickson AE, Bunt AH and Fuchs AF (1975) The origin of efferent pathways from primary visual cortex, area 17, of the macaque monkey as shown by retrograde transport of horseradish peroxidase. *J Comp Neurol.* **164**:287-304.

Malpeli JG, Baker FH (1978) The representation of the visual field in the lateral geniculate nucleus of *Macaca mulatta*. *J Comp Neuol* **161**:569-594.

Marzi CA, Antonini A, Di Stefano M, Legg CR (1980) Callosum-dependent binocular interactions in the lateral suprasylvian area of siamese cats which lack binocular neurons in areas 17 and 18. *Brain Res.* **197**:230-235.

Maunsell JHR, Van Essen DC (1983) The connections of the middle temporal visual area (MT) and their relationship to a cortical hierarchy in the macaque monkey. *J Neurosci* **3**:2563-2586.

Maunsell JHR, Van Essen DC (1987) Topographic organization of the middle temporal visual area in the macaque monkey: representational biases and the relationship to callosal connections and myeloarchitectonic boundaries. *J. Comp. Neurol.* **266**:535-555.

Mesulam MM (1978) Tetramethyl benzidine for horseradish peroxidase neurohistochemistry: a non-carcinogenic blue reaction product with superior sensitivity for visualizing neural afferents and efferents. *J Histochem Cytochem* **26**:106-117.

Mettler FA (1935) Coticofugal fiber connections of the cortex of macac mullatta. The occipital region. *J Comp Neurol* **61**:221-256.

Mitchell DE, Blakemore C (1970) Binocular depth perception and the corpus callosum. *Vision Res* **10**:49-54.

Munk MHJ, Nowak LG, Girard P, Chounlamountri N, Bullier J (1995) Visual latencies in cytochrome oxidase bands of macaque area V2. *Proc Natl Acad Sci* **92**:988-992.

Myers RE (1961) Contralateral projections of juxta-striate parts of cortical area 18 in the monkey. *Anat Rec* **139**:259.

Myers RE (1962) Commissural connections between occipital lobes of the monkey. *J Comp Neurol* **118**:1-16.

Myers RE (1965) The neocortical commissures and interhemisoheric transmission of information In EG Ettliner (Ed) *Functions of Corpus Callosum* Little Brown & Co., Boston 1-17.

Nikara T, Bishop PO, Pettigrew JD (1968) Analysis of retinal correspondence by studying receptive fields of binocular single units in cat striate cortex. *Exp Brain Res* **6**:353-372.

Olavarria JF (1995) The effect of visual deprivation on the number of callosal cells in the cat is less pronounced in extrastriate cortex than in the 17/18 border region. *Neurosci Let.*

Olavarria JF (1996) Non mirror symmetric pattern of callosal linkages in areas 17 and 18 in cat visual cortex. *J. Comp. Neurol.* **366**:643-655.

Olavarria J, DeYoe EA, Van Essen DC (1989) Pattern of cytochrome oxidase staining in the unfolded and flattened V2 of the macaque monkey. *Invest Ohthal Vis Sci, ARVO abstr Suppl* **30**:298.

Olavarria J, Montero VM (1984) Relation of callosal and striate-extrastriate cortical connections in the rat: morphological definition of extrastriate visual areas. *Exp Brain Res* **54**:240-252.

Olavarria J, Van Sluyters RC (1985) Unfolding and flattening the cortex of gyrencephalic brains. *J Neurosci Meth* **15**:191-202.

Olavarria JF, Li, Ch-P (1995) Effects of neonatal enucleation on the organization of callosal linkages in striate cortex of the rat. *J Comp Neurol* **361**:138-151.

Olavarria J, Van Sluyters RC (1995) The overall pattern of callosal connections in visual cortex of normal and enucleated cats. *J Comp Neurol* **363**:161-173.

Olavarria JF, Abel PL (1996) The distribution of callosal connections correlates with the pattern of cytochrome oxidase stripes in visual area V2 of macaque monkeys. *Cerebral Cortex* **6**:631-639.

Payne BR (1990) The representation of the ipsilateral visual field in the transition zone between areas 17 and 18 of the cat's cerebral cortex. *Vis Neurosci* **4**:445-474.

Payne BR (1991) Visual-field map in the transcallosal sending zone of area 17 in the cat. *Vis Neurosci* **7**:201-219.

Payne BR and Siwek DF (1991) Visual-field map in the callosal recipient zone at the border between areas 17 and 18 in the cat. *Vis Neurosci* **7**"221-236.

Perkel DJ, Bullier J, Kennedy H (1986) Topography of afferent connectivity of area 17 in the macaque monkey: a double-labelling study. *J. Comp. Neurol.* **253**:374-402.

Peterhans, E., and R. von der Heydt (1993) Functional organization of area V2 in the alert macaque. Euro. J. Neurosci. *5*:509-524.

Poggio GF, Fischer B (1977) Binocular interaction and depth sensitivity of striate and prestriate cortical neurons of the behaving rhesus monkey. *J Neurophys* **40**:1392-1405.

Pritzel M, Kretz R, Rager G (1988) Callosal projections between areas 17 in the adult tree shrew (*Tupaia belangeri*). *Exp Brain Res* **72**:481-493.

Rizzolatti G, Camarda R (1977) Influence of the presentation of remote visual stimuli on visual responses of cat area 17 and lateral suprasylvian area. *Exp Brain Res* **29**: 107-122.

Rockland KS, Pandya DN (1979) Laminar origins and terminations of cortical connections of the occipital lobe in the rhesus monkey. *Brain Res* **179**:3-20.

Roe, AW, Ts'o, DY (1995) Visual topography in primate V2: multiple representations across functional stripes. *J Neurosci* **15**:3689-3715.

Rosa MGP, Sousa APB, Gattass R (1988) Representation of the visual field in the second visual area in the Cebus monkey. *J Comp Neurol* **275**:326-345.

Sanides D (1978) The reinotopic distribution of visual callosal projections in the suprasylvian visual areas compared to the classical visual areas (17, 18, 19) in the cat. *Exp Brain Res* **33**:435-443.

Sanides D, Albus K (1980) The distribution of interhemispheric projections in area 18 of the cat: coincidence with discontinuities of the representation of the visual field in the second visual area (V2). *Exp Brain Res* **38**:237-240.

Sawchenko PE, Swanson LW (1981) A method for tracing biochemically defined pathways in the central nervous system using combined fluorescence retrograde transport and immunohistochemical techniques. *Brain Res* **210**:31-51.

Segraves MA, Rosenquist AC (1982a) The distribution of the cells of origin of callosal projections in cat visual cortex. *J Neurosci* **2**:1079-1089.

Segraves MA, and Rosenquist, AC (1982b) The afferent and efferent callosal connections of retinotopically defined areas in cat cortex. *J Neurosci* **2**:1090-1107

Shatz C (1977) Abnormal interhemispheric connections in the visual system of Boston siamese cats: A physiological study. *J Comp Neurol* **171**:229-246.

Shoumura K, Ando T, Kato K (1975) Structural organization of 'callosal' OBg in human corpus callosum agenesis. *Brain Res* **93**:241-252.

Spatz WB, B Kunz (1984) Area 17 of anthropoid primates does participate in visual callosal connecitons. *Neurosci Lett* **48**: 49-53.

Spatz WB, Tigges J (1972) Experimental-anatomical studies on the "middle temporal visual areas (MT)" in primates. I. Efferent corticocortical connections in the marmoset *Callithrix jacchus*. *J Comp Neurol* **146**:451-464.

Stepniewska I, Kaas JH (1996) Topographic patterns of V2 cortical connections in macaque monkeys. *J Comp Neurol* **371**:129-152.

Stone J, Leicester J, Sherman SM (1973) The naso-temporal division of the monkey's retina. *J Comp Neurol* **150**:333-348.

Talbot SA, Marshall WH (1941) Physioogical studies on neural mechanisms of visual localization and discrimination. *Amer J Ophthal* **24**:1255-1264.

Tanaka K, Hikosaka K, Saito H, Yukie M, Fukada Y, Iwai E (1986) Analysis of local and wide-field movements in the superior temporal visual area of the macaque monkey. *J Neurosci* **6**: 134-144.

Taylor DCM, Pierau Fr-K, Schmid H (1982) The use of fluorescent tracers in the peripheral sensory nervous system. *J Neurosci Meth* **8**:211-224.

Tigges J, Spatz WB, Tigges M (1974) Efferent cortico-cortcial fiber connections of area 18 in the squirrel monkey (*Saimiri*). *J Comp Neurol* **158**:219-236.

Tigges J, Tigges M, Anschel S, Cross NA, Letbetter WD, McBride RL (1981) Areal and laminar distribution of neurons interconnecting the central visual cortical areas 17, 18, 19, and MT in squirrel monkey (*Saimiri*). *J Comp Neurol* **202**:539-560.

Tootell RBH, Hamilton SL (1989) Functional anatomy of the second visual area (V2) in the macaque. *J. Neurosci* **9**:2620-2644.

Tootell RBH, Silverman MS, De Valois RL, Jacobs GH (1983) Functional organization of the second cortical area of primates. *Science* **220**:737-739.

Tootell RBH, Switkes E, Silverman MS, Hamilton SL (1988) Functional Anatomy of macaque striate cortex. II.Retinotopic organization. *J. Neurosci* **8**:1531-1568.

Van Essen DC (1985) Functional organization of primate visual cortex. In: *Cerebral cortex* (Peters A, Jones EG, eds), pp 259-329. New York:Plenum.

Van Essen DC, Felleman DJ, DeYoe EA, Olavarria J, Knierim J (1990) Modular and hierarchical organization of extrastriate visual cortex in the macaque monkey. *Cold Spring Harbor Symp Quant Biol* **55**: 679-695.

Van Essen DC, Newsome WTN, Bixby JL (1982) The pattern of interhemispheric connections and its relationship to extrastriate visual areas in the macaque monkey. *J Neurosci* **2**:265--283.

Van Essen DC, Newsome WT, Maunsell JHR (1984) The visual field representation in striate cortex of the macaque monkey: Asymmetries, anisotropies, and individual variability. *Vision Res* **24**:429-448.

Van Essen DC, Newsome WT, Maunsell JHR, Bixby JL (1986) The projections from striate cortex (V1) to areas V2 and V3 in the macaque monkey:

Asymmetries, areal boundaries, and patchy connections. *J Comp Neurol* **244**:451-480.

Van Essen DC, Zeki SM (1978) The topographic organization of rhesus monkey prestriate cortex. *J Physiol (Lond)* **277**:193-226.

von Economo C (1929) The Occipital Lobe. In: *The cytoarchitectonics of the human cerebral cortex* S. Parker (transl.), pp98-109. London:Oxford University Press.

von Bonin G (1942) The striate area of primates. *J Comp Neurol* **77**:405-429.

Wagor E, Lin CS, Kaas, JH (1975) Some cortical projections of the dorsomedial visual area (DM) of association cortex in the owl monkey, *Aotus trivirgatus*. *J Comp Neurol* **163**:227-250.

Weller RE, Kaas JH (1983) Retinotopic patterns of connections of area 17 with visual areas V-II and MT in macaque monkeys. *J Comp Neurol* **220**:253-279.

Westheimer g, Mitchell DE (1969) The stimulus for convergence and divergence eye movements. *Vision Res* **9**:749-755.

Westheimer, G, Tanzman, IJ (1956) Qualtitative depth localization with diplopic images. *J Opt Soc Am* **46**:116-117.

Whitteridge, D (1965) Area 18 and the vertical meridian of the visual field. In EG Ettliner (Ed) *Functions of Corpus Callosum* Little Brown & Co., Boston 115-120.

Wong-Riley M (1979) Changes in the visual system of monocularly sutured or enucleated cats demonstrable with cytochrome oxidase histochemistry. *Brain Res* **171**:11-28.

Yoshioka T, Dow BM (1996) Color, orientation and cytochrome oxidase reactivity in areas V1, V2 and V4 of macaque monkey visual cortex. *Beh Brain Res* **76**:71-88.

Zeki, SM (1969) Representation of central visual fields in prestriate cortex of monkey. *Brain Research* **14**:271-291.

Zeki, SM (1970) Interhemispheric connections of prestriate cortex in monkey. *Brain Res* **19**:63-75.

Zeki, SM (1971) Cortical projections from two prestriate areas in the monkey. *Brain Res* **34**:19-35.

Zeki SM (1977) Simultaneous anatomical demonstration of the representation of the vertical and horizontal meridian in areas V2 and V3 of rhesus monkey visual cortex. *Proc R Soc Lond B* **195**:517-523.

Zeki S M, Sandeman DR (1976) Combined anatomical and elctrophysiological studies on the boundary between the second and third visual areas of rhesus monkey cortex. *Proc R Soc Lond B* **194**:555-662.

Zisper K, Lamme VAF, Schiller PH (1996) Contextual modulation in primary visual cortex. *J Neurosci* **16**:7376-7389.

VITA

Paul Lawrence Abel

University of Washington

1997

Education

University of Washington, Seattle.	Ph.D. Psychology, expected June 1997.
Cold Spring Harbor Laboratory, NY	Summer course on visual system, 1995.
University of California, Los Angeles.	B.S. Psychobiology. 1989-1992.
University of Edinburgh, Scotland	Scottish History & Literature, 1991.
University of London, England	English History & Literature, 1991.
University of Colorado, Boulder	Molecular Biology, 1988-1989.
Mesa College, San Diego	Biology, 1987-1989.

Publications

O'Brien BJ, Abel PL, Olavarria JF (1997) A morphological anomaly of the dorsal lateral geniculate nucleus in *Macaca fascicularis*. *Cell Tiss Res* **289**:11-16

Abel PL, O'Brien BJ, Lia B, Olavarria JF (1997) Distribution of neurons projecting to the superior colliculus correlates with thick cytochrome oxidase stripes in macaque visual area V2. *J Comp Neurol* **377**:313-323.

Olavarria JF, Abel PL (1996) The distribution of callosal connections correlates with the pattern of cytochrome oxidase stripes in visual area V2 of macaque monkey. *Cerebral Cortex* **6**:631-639.

Abel PL, Olavarria JF (1996) The callosal pattern in striate cortex is more patchy in monocularly enucleated albino than pigmented rats. *Neurosci Lett* **204**:169-172.

Breed MD, Abel P, Bleuze TJ, Denton SE (1990) Thievery, home ranges, and nestmate recognition in *Ectatomma ruidum*. *Oecologia* **84**:117-121.

Abel PL, O'Brien BJ, Olavarria JF (1995) Callosal connections interlink anatomically corresponding regions in visual area V2 of macaque monkey. *Soc Neurosci Abstr* **25**:359.4.

O'Brien BJ, Abel PL, Olavarria JF (1995) Pulvino-cortico connections of area V2 in monkeys *Soc Neurosci Abstr* **25**:266.14

Abel, PL, O'Brien BJ, Lia B, Olavarria JF (1994) The distribution of cortico-collicular projection neurons correlates with thick cytochrome oxidase stripes in visual area V2 of macaque monkey. *Soc Neurosci Abstr* **20**:710.6.

Fitts DA, Abel PL, Lane JR, Olavarria JF (1994) Horseradish peroxidase leakage through the blood brain barrier after electrolytic lesion of the subfornical organ. *Soc Neurosci Abstr* **20**:338.2.